

UNIVERSITÄTSKLINIKUM HAMBURG-EPPENDORF

Bernhard Nocht Institute for Tropical Medicine
Department of Molecular Biology and Immunology
Protozoa Immunology Group
PD Dr. Thomas Jacobs

Role of the PD-1/PD-L inhibitory pathway during experimental infection by *Trypanosoma cruzi* Tulahuen strain

Dissertation

to obtain the doctoral degree (PhD)
at the Medical Faculty of the University of Hamburg

submitted by:

Yanina Helga Arana Policarpo

Hamburg 2018

Angenommen von der Medizinischen Fakultät am: 19.12.2018

Veröffentlicht mit Genehmigung der Medizinischen Fakultät der Universität Hamburg

Prüfungsausschuss, der/die Vorsitzende: PD Dr. Thomas Jacobs

Prüfungsausschuss, 2. Gutachter/in: Prof. Dr. Eva Tolosa

Hamburg, den 07.01.2019

A mi amada madre...

Table of contents

1. Introduction	1
1.1. The immune system	1
1.1.1. The innate immune system	1
1.1.2. The adaptive immune system	2
1.2. Inhibitory pathways	4
1.2.1. BTLA:HVEM	5
1.2.2. PD-1:PD-L1/PD-L2	6
1.2.3. LAG-3:MHC class II	7
1.2.4. TIM-3:Gal-9	7
1.2.5. 2B4:CD48	8
1.3. <i>Trypanosoma cruzi</i> and Chagas disease	8
1.3.1. Chagas disease (Human american trypanosomiasis)	9
1.3.2. Chagas disease – Clinical evolution	10
1.3.3. Life cycle of <i>Trypanosoma cruzi</i>	12
1.3.4. The immune response against <i>Trypanosoma cruzi</i> and pathology	13
1.4. Aim	15
2. Materials	16
2.1. Biological material	16
2.1.1. Cell lines	16
2.1.2. Laboratory animals	16
2.2. Material for cell biology	16
2.2.1. Reagents for cell biology	16
2.2.2. Antibodies and fluorescent dyes	16
2.2.3. Buffers and cell culture media for cell biology	17
2.2.4. Kits for cell biology	17
2.3. Materials for antibody blocking	18
2.4. Materials for molecular biology	18
2.4.1. Kits for molecular biology	18
3. Methods	19
3.1. Cell biology	19
3.1.1. Cultivation of adherent cells	19
3.1.2. Generation of bone-marrow derived dendritic cells (BM-DCs)	19
3.1.3. Isolation of spleen cells	19
3.1.4. Flow cytometry	20
3.1.5. Cytometric beads assay-LEGENDplex™	20
3.2. Experimental infection model	21
3.3. <i>In vivo</i> blocking assays	21
3.4. Molecular biology	21
3.4.1. Organ sampling	21
3.4.2. Isolation of DNA	21
3.4.3. Quantification of DNA	22
3.4.4. Standards for qPCR	22
3.4.5. Quantitative Real Time PCR (qRT-PCR)	22
3.5. Statistical analysis	23
4. Results	24

4.1. Evaluation of PD-L1 expression on <i>Trypanosoma cruzi</i> Tulahuen strain <i>in vitro</i> infection model.....	24
4.2. Development of mouse model of experimental <i>T. cruzi</i> Th strain infection.....	25
4.3. Modulation of PD-1, PD-L1 and PD-L2 expression during <i>T. cruzi</i> Th infection <i>in vivo</i>	27
4.4. PD-1/PD-L axis and its effects in the adaptive immune response against <i>T. cruzi</i> Th infection.....	33
4.5. <i>T. cruzi</i> Th infection in PD-L1 knockout mice.....	34
4.6. Effect of PD-L1 deficiency on immune response against <i>T. cruzi</i> Th infection <i>in vivo</i>	36
4.7. Evaluation of the <i>ex vivo</i> cytokine profile upon interruption of PD-1/PD-L1 signaling by a cytometric beads assay.....	40
4.8. Evaluation of other co-inhibitory receptors upon interruption of PD-1/PD-L1 signaling.....	40
4.9. Effect of PD-1 blockade during the <i>T. cruzi</i> Th infection <i>in vivo</i>	42
4.10. Evaluation of the <i>ex vivo</i> cytokine profile upon PD-1 blockade by a cytometric beads assay.....	46
4.11. Effect of combined blockade of PD-1 and TIM-3 by monoclonal antibodies during the <i>T. cruzi</i> Th infection <i>in vivo</i>	48
4.12. Evaluation of the <i>ex vivo</i> cytokine profile upon combined blockade of PD-1 and TIM-3 by a cytometric beads assay.....	51
4.13. Evaluation of interruption of PD-1/PD-L1 signaling on the parasite load analyzed by qRT-PCR.....	52
5. Discussion.....	55
5.1. <i>T. cruzi</i> Tulahuen strain infection induces expression of PD-L1 on BM-DCs.....	55
5.2. Mouse model of <i>T. cruzi</i> Tulahuen experimental infection.....	55
5.3. <i>T. cruzi</i> Th infection modulates the PD-1, PD-L1 and PD-L2 expression on immune cells <i>in vivo</i>	56
5.4. PD-1 expression might not be associated with exhausted T cell function during <i>T. cruzi</i> Th infection.....	57
5.5. PD-L1 deficiency does not improve the resistance to the infection neither T cell effector functions but increases IL-10 expression by CTL at the early chronic phase.....	58
5.6. Blockade of PD-1 by monoclonal antibodies does not improve the resistance to the infection neither T cell effector functions in the course of <i>T. cruzi</i> Th infection <i>in vivo</i>	60
5.7. Combined blockade of PD-1 and TIM-3 does not improve the resistance to the infection neither T cell effector functions in the course of <i>T. cruzi</i> Th infection <i>in vivo</i>	61
5.8. PD-1/PD-L1 pathway plays a role in the resistance to <i>T. cruzi</i> Th infection.....	62
6. Abstract.....	64
7. Zusammenfassung.....	65
8. References.....	67
9. Abbreviations.....	71
10. List of figures.....	74
11. List of tables.....	76
12. Acknowledgments.....	77
13. Curriculum vitae.....	79

14. Eidesstattliche Versicherung.....	81
--	-----------

1. Introduction

1.1. The immune system

Eukaryotes are constantly exposed to the threat of microbial species including viruses, bacteria, and parasites. In mammals, the protection against invading pathogens is mediated by two different immune systems: the evolutionarily conserved innate immune system, which is essential for the first line of host defense, and the acquired immune system, which is critical for immunological memory (1).

1.1.1. The innate immune system

Innate immunity coevolved with microbes to protect all multicellular organisms from infections. Some components of the mammalian innate immune system are remarkably similar to components in plants and insects, suggesting that these appeared in common ancestors long ago in evolution. Most of the mechanisms of innate immune defense appeared very early in evolution, after the development of complex multicellular organisms, about 750 million years ago (1, 2). In mammals, innate immunity uses a variety of induced effector mechanisms to clear an infection or, failing that, keep it in check until the pathogen can be recognized by the adaptive immune system. Different mechanisms work at different stages of infection: epithelial barriers impair microbial entry into the host, resident and recruited phagocytes in sub epithelial and other tissues provide protection if the barriers are breached, and a system of plasma proteins known as the complement system and, circulating phagocytes provide protection if microbes reach the blood stream (1-4). Innate immunity discriminates self and non-self by a limited number of molecules called pattern recognition receptors (PRRs) that respond to evolutionarily conserved molecular signatures of microbes, parasites and viruses, known as pathogen-associated molecular patterns (PAMPs) that are often essential for their survival. Many cell types, including hematopoietic and non-hematopoietic cells, express PRRs and respond to PAMPs presence by engaging downstream signaling pathways. Among the different classes of PRRs are the C-type lectins and scavenger receptors, which mainly participate in the uptake of microbes into phagocytes and dendritic cells (DCs) through the process of phagocytosis. Other important class of PRRs

is the Toll-like receptors (TLRs) whose activation triggers intracellular signaling pathways leading to the expression of a variety of genes involved in inflammatory responses and enhance killing of microbes (1, 2, 5). TLRs link innate and adaptive immunity by up-regulating the ability of accessory cells to generate immune responses mediated by T and B lymphocytes (3).

Phagocytes constitute the first line of microbial defense and they function by sensing the presence of different types of infectious agents through PRRs and high-affinity receptors for certain opsonins, including antibody molecules, complement proteins, and plasma lectins. After recognition, microbes are internalized into phagosomes, which fuse with lysosomes to form phagolysosomes, where the microbes are killed by reactive oxygen and nitrogen species and proteolytic enzymes. Peptides generated from microbial proteins are presented to T lymphocytes to initiate adaptive immune response. In addition to killing phagocytosed microbes, activated macrophages produce cytokines such as tumor necrosis factor alpha (TNF- α), Interleukin-1 (IL-1) and Interleukin-6 (IL-6) and chemokines that enhance the inflammatory reactions to microbes and bring in more leukocytes (neutrophils, macrophages and NK T lymphocytes) and plasma proteins to the site of infection (1, 2, 6). Innate phase of immunity is rapidly supplemented by an adaptive response characterized by the activities of pathogen-specific B and T cells. The key cellular players in translating innate information into adaptive immunity are the members of the DC family. DCs recognize pathogen infection via PRRs, undergo a profound phenotypic and functional transformation (DC activation) to become immunogenic antigen-presenting cells (APCs) and instruct acquired immune cells by presenting antigens as well as by expression of co-stimulatory molecules and cytokines (1, 2, 4, 5).

1.1.2. The adaptive immune system

An adaptive immune response is induced when an infection overwhelms innate defense mechanisms. Lymphocytes are the key components of adapted immunity as they focus immune defense in an antigen-specific manner using highly specific antigen receptors. An adaptive immune response involves the selection and amplification of clones of lymphocytes bearing receptors that recognize the foreigner antigen. There are two types of lymphocytes: B lymphocytes (B cells), and T lymphocytes (T cells). Both B and T lymphocytes develop from bone marrow stem cells and mature in the generative

INTRODUCTION

lymphoid organs (bone marrow and thymus for B and T cells respectively). Once they have completed maturation, both types of lymphocyte enter to the bloodstream as mature naive lymphocytes. They circulate through the peripheral lymphoid (lymph nodes, spleen, and mucosal lymphoid tissues), in which an adaptive immune response is initiated if a lymphocyte meets its corresponding antigen. Each lymphocyte carries cell-surface receptors of a single antigen specificity that are generated by the random recombination of variable receptor gene segments during the early stages of the development. B-cell receptor (BCR) is called immunoglobulin and is made both as a membrane-bound receptor and as secreted antibody. T-cell receptor (TCR), in contrast, is made only as cell-surface receptor. During B lymphocyte maturation, immature B cells that express high-affinity antigen receptors specific for self-antigens present in the bone marrow are induced to edit their receptor genes or these cells are eliminated. On the other hand, during T lymphocyte maturation, immature T cells undergo proliferation, rearrangement of TCR genes, and surface expression of CD3, TCR, CD4, and CD8 molecules that after a positive selection results in the matching of TCRs that recognize major histocompatibility complex (MHC) class I with CD8 expression and TCRs that recognize MHC class II with CD4 expression. Three signals are required for T-cell activation. The first signal, which gives specificity to the immune response, is provided by the interaction of antigenic peptide-MHC complex with the T cell receptor (TCR). The second, antigen-independent co-stimulatory signal is delivered to T cell by APCs to promote T cell clonal expansion, cytokine production, and effector function. Finally, cytokines that control differentiation into different types of effector cells deliver the third signal. In order to provide a mechanism for turning off T cell activation, co-inhibitory receptors (immune checkpoints) are induced by TCR stimulation and costimulation and subsequently transduce feedback signals that dampen the ascending co-stimulatory signals. Therefore, the net outcome of TCR stimulation is modified by both co-stimulatory and co-inhibitory receptors. Both sets of receptors are expressed by all T cell subsets, thereby helping to shape the overall immune response (7-11).

There are two types of adaptive immune response: Humoral immunity, mediated by B lymphocytes and cell-mediated immunity, conducted by T lymphocytes. Activation of naive B cells is triggered by antigen and usually requires helper T cells (T_H) such as the T follicular helper (T_{FH}). After antigen binds to BCR, B lymphocyte proliferates and differentiates into plasma cell that is the effector form of B lymphocyte and produce

antibodies (immunoglobulins) which are the secreted form of the BCR. Antibodies cause the destruction of extracellular microorganisms and prevent the spread of intracellular infections. On the other hand, after activation, CD8 T cells all differentiate into cytotoxic T cells (CTLs) that kill cells that are infected with intracellular pathogens, especially viruses. In contrast with CD8 T cells, CD4 T cells differentiate into several subsets of effector T cells called helper T cells (T_H) (T_{H1} , T_{H2} , T_{H17} , T_{H22}) which provide essential additional signals that influence the behavior and activity of other cells; and regulatory T cells (Tregs) which suppress the activity of other lymphocytes. During the course of an immune response, some of B and T cells activated by antigen differentiate into memory cells, the lymphocytes that are responsible for the long-lasting immunity that can follow exposure to disease or vaccination (1, 2, 4).

1.2. Inhibitory pathways

In chronic infections and cancer, T cells are exposed to persistent antigen and /or inflammation that leading to an altered deterioration state of their function termed “exhaustion”. Exhausted T cells are functionally characterized by a loss of IL-2 production, reduced proliferative and cytotoxic capacity, an impaired production of pro-inflammatory cytokines and, altered expression and use of key transcription factors. However the major hallmark of T-cell exhaustion is the sustained upregulation and co-expression of multiple checkpoints (9, 12-14). Exhausted T cells were first identified in the context of chronic viral infection in mice by lymphocytic choriomeningitis virus (LCMV); however T cells with a similar phenotype were later identified in humans during viral infections such as human immunodeficiency virus (HIV) and hepatitis C virus (HCV), as well as in the tumor microenvironment (9, 14). Recently, T-cell exhaustion and increased expression of immune checkpoints on T cells has been observed in mice and humans infected with parasites such as *Schistosoma*, *Leishmania*, *Plasmodium* and *Toxoplasma* (9). Exhausted T cells are not inert. These cells retain suboptimal but crucial functions that limit ongoing pathogen replication or tumor progression. Several studies have suggested that blockade of immune checkpoints overexpressed in the context of chronic infection may lead to a reversion of T cell-dysfunction and reinvigorated immune responses (9, 14).

Several families of inhibitory receptors (immune checkpoints) and their ligands have been found to be important in negatively regulating responses of T cells and other

leukocytes during persisting infection. These include the immunoglobulin (Ig)-superfamily with molecules often related to CD28, and receptors and ligands in the tumor necrosis factor (TNF) receptor superfamily (Fig. 1) (12). Nowadays, there is evidence that parasites enhance the expression of immune checkpoints and their ligands to limit host-protective antigen-specific immune responses, suggesting that their blockade would have the potential to enhance antiparasitic immune response (9).

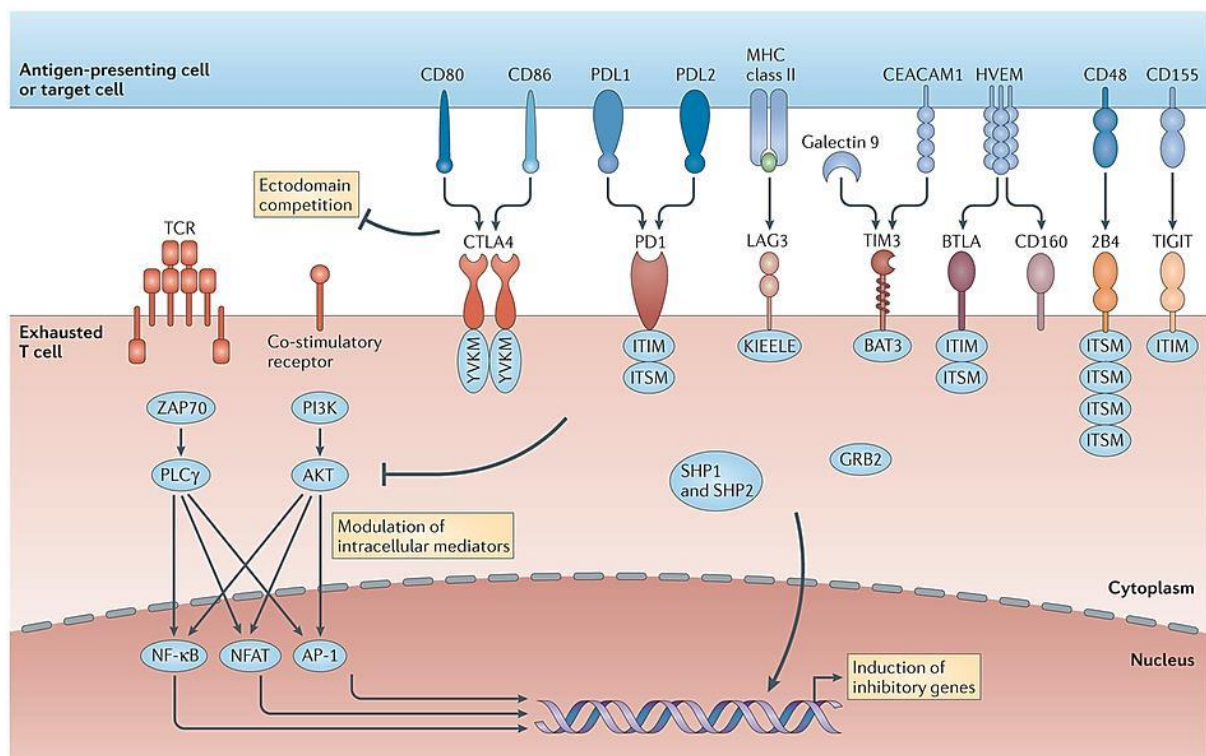


Fig. 1: Molecular pathways of inhibitory receptors associated with T cell exhaustion. Ligand and receptor pairs for inhibitory pathways are depicted, showing the intracellular domains of receptors that contribute to T cell exhaustion. The molecular mechanisms of inhibitory receptor signalling are also illustrated. Cytotoxic T lymphocyte antigen 4 (**CTLA-4**), programmed cell death protein 1 (**PD-1**), lymphocyte activation gene 3 protein (**LAG3**), T cell immunoglobulin and mucin domain-containing protein 3 (**TIM3**), B and T lymphocyte attenuator (**BTLA**), **CD160**, **2B4**, and T cell immunoreceptor with immunoglobulin and ITIM domains (**TIGIT**). Source: Wherry et al., 2015 (14).

1.2.1. BTLA:HVEM

B- and T-cell lymphocyte attenuator (BTLA) is a member of the Ig superfamily (IgSF) receptors, sharing a homology with PD-1 and CTLA-4. BTLA contains a single C-type Ig domain and two immunoreceptor tyrosine-based inhibitory motifs (ITIM) in the cytoplasmic tail. BTLA is constitutively expressed on most hematopoietic cells, including

T cells (especially T_H1), B cells, NK cells, DCs, and endothelial cells with the highest levels present on B cells. The relatively low levels of BTLA on naive CD4 T cells increase substantially after activation. Tregs express little BTLA, whereas anergic CD4 T cells have the highest expression. Human herpesvirus entry mediator (HVEM) is a member of the tumor necrosis factor superfamily (TNFSF) receptors and is the known ligand of BTLA. The BTLA-HVEM interaction is the first demonstration of crosstalk between IgSF and TNFSF receptors. HVEM is widely expressed, and T cells, B cells and DCs, and all other types of cells within the lymphoid tissue can express HVEM. Its expression on naive T cells is high and decreases at an early activation stage, but is upregulated at the late activation stage (15-17). Crosslinking of BTLA with HVEM results in the phosphorylation of ITIM motif in the cytoplasmic region of BTLA followed by subsequent recruitment of phosphatases SHP-1 and SHP-2, and Akt suppression, this response reduces TCR signaling and eventually diminishes T cell activation (9, 16-19). HVEM not only binds to BTLA but also to CD160, lymphotoxin α (LT α), and LIGHT [lymphotoxin-like, exhibits inducible expression, and competes with herpes simplex virus glycoprotein D (gD) for binding to HVEM, a receptor expressed by T lymphocytes] (9, 16, 17). The binding of HVEM to CD160 and BTLA on T cells delivers a co-inhibitory signal to T-cell activation, while the binding of HVEM to LT α and LIGHT stimulates host immune responses. Thus, HVEM serves as a bimolecular switch to regulate the host immune response depending on which ligand it engages (15).

1.2.2. PD-1:PD-L1/PD-L2

Programmed cell death 1 (PD-1 or CD279) was originally identified as an inducible T-cell surface receptor during programmed cell death. PD-1 shares structural similarity with CD28, as a member of the IgSF receptors, with an extracellular single immunoglobulin domain and two intracellular tyrosine kinase motifs: an ITIM as well as an immunoreceptor tyrosine-based switch motif (ITSM) (10, 16). PD-1 can be expressed on T cells, B cells, NK T cells, activated monocytes, and DCs. Naive T cells, in particular, do not express PD-1 but can do so following activation (9, 10, 12, 16, 17). There are two surface molecules reported as ligands of PD-1: programmed cell death ligand 1 (PD-L1, CD274, or B7-H1) and programmed cell death ligand 2 (PD-L2, CD273, or B7-DC). PD-L1 and PD-L2 are both structurally similar to B7 ligands, consisting of both IgV- and IgC-like extracellular domains and a short intracellular domain. PD-L1 is broadly expressed on

both hematopoietic and non-hematopoietic cells. PD-L1 is constitutively expressed in mouse T and B cells, DCs, macrophages, NK cells, and bone marrow-derived mast cells, and its levels increase after activation. The expression of PD-L2 is restricted to hematopoietic cells. PD-L2 is inducibly expressed on professional APCs such as DCs, macrophages, and bone marrow-derived mast cells (9, 10, 12, 16, 17). In addition, subsequent studies have shown that PD-L1 also binds to B7-1 ligand leading to bidirectional inhibitory responses in T cells (9, 16, 20). Upon binding to its ligands, ITSM in the cytoplasmic domain of PD-1 is phosphorylated and recruits the phosphatases SHP-1 and SHP-2. These phosphatases act inhibiting PI3K and the subsequent phosphorylation and activation of protein kinase B (Akt), reducing the TCR signal and leading to diminished T-cell activation and cytokine production (9, 10, 14, 16, 17). Signaling through PD-1:PD-L1/PD-L2 exerts inhibitory effects in multiple ways: inhibition of cytokine production including IFN- γ , TNF- α and IL-2; blockade of T cell differentiation and proliferation; and inhibition of cell survival through suppression of Bcl-xL with greater inhibition at low levels of TCR stimulation (10, 16). The PD-1 inhibitory pathway is known to regulate immune responses to self-antigens (10, 21). PD-1 mainly exerts its inhibitory effect on T cells in the periphery where T cells encounter PD-1 ligands (9, 16, 17). Several studies have confirmed the importance of PD-1 in settings of persisting viral, bacterial, and parasitic infections including prominent roles in HCV, HBV, *Mycobacterium tuberculosis*, malaria, and many others (9, 10, 12, 16).

1.2.3. LAG-3:MHC class II

Lymphocyte activation gene 3 protein (LAG-3) is a homolog of CD4 likely arising from a gene duplication, and the two molecules share considerable structural similarity. LAG-3 binds to MHC class II with higher affinity than CD4⁺, thereby compromising CD4⁺ T-cell activation (9, 12). However, LAG-3 expression is also associated with impairment of CD8⁺ and NK-cell function, suggesting that there may be additional LAG-3 ligands (9). LAG-3 expression often is found on exhausted T cells in HBV, HCV, and HIV (12).

1.2.4. TIM-3:Gal-9

T-cell immunoglobulin-3 (TIM-3) is a large transmembrane inhibitory receptor that contains an N-terminal Ig domain as well as a mucin domain that is highly glycosylated

(12). It was identified as a molecule expressed in IFN- γ -producing CD4 T helper type 1 (T_H1) and in CD8 cytotoxic T cells, but not naive T cells. TIM-3 can also be expressed by NK cells, and myeloid cells, such as DCs and monocytes. Its counter-receptor, Galectin-9, is a soluble S-type lectin, widely expressed on immune and non-immune cells and up-regulated upon IFN- γ stimulation. Galectin-9 binds to IgV domain of TIM-3, inducing phosphorylation of interleukin inducible T-cell kinase (ITK), leading to apoptosis (9, 16). Binding of TIM-3 to high mobility group box 1, a marker of immunogenic cell death that triggers innate cell responses by binding to pattern recognition receptors, prevent innate cell activation (9). TIM-3 also binds in *cis* to carcinoembryonic antigen cell adhesion molecule 1 (CEACAM1) and this molecule facilitates the suppressive function of TIM-3 (12). Multiple reports have shown that TIM-3 blockade results in abrogation of peripheral tolerance (16). Lastly, TIM-3 is reported to be expressed by “exhausted” T cells in chronic viral infections in mice, HCV, HBC and HIV in humans, playing a central role in the impairment of effector activities (12, 16).

1.2.5. 2B4:CD48

2B4 (CD244) is a member of the CD2 subset of the IgSF receptors. In mice, 2B4 is found on all NK cells, activated CD8⁺ T cells (12, 22), subsets of $\gamma\delta^+$ T cells, monocytes, mast cells, as well as on a subset of memory -like CD8⁺ T cells. In humans, is expressed on NK cells and $\gamma\delta^+$ T cells, ~50% of CD8⁺ T cells, and on subsets of basophils, monocytes, and eosinophils. In addition, T cells have been shown to acquire 2B4 expression under certain activating conditions. 2B4 expression is also upregulated on antigen-specific CD8 T cells in chronic HBV, EBV, and HIV, as well as in mouse models of chronic infection (12), and has been found on a large proportion of effector/memory CD4⁺ T cell in CMV-infected individuals (22). In both mice and humans, 2B4 binds to CD48, which is broadly expressed on hematopoietic cells (12, 22). At least in the mouse, 2B4 does not appear to bind any other molecule than CD48. CD48 expression is upregulated upon viral infection and by stimulation of IFN- $\alpha\beta$ and IFN- γ (22). 2B4 contains four cytoplasmic ITSM motifs. 2B4-CD48 interactions might deliver negative signals via 2B4 directly, however, this direct signaling by 2B4 can be either co-stimulatory or inhibitory depending on which ITSM is phosphorylated (12).

1.3. *Trypanosoma cruzi* and Chagas disease

One hallmark of most parasitic infections is that the great majority of individuals are able to trigger innate immunity and elicit an activated T-cell response during the acute infection, leading to the control of the parasite and establishment of a chronic infection. Interestingly, while many individuals develop severe forms of parasitic diseases once infection progresses to the chronic phase, most patients develop relatively mild forms, allowing for host-parasite coexistence. One such example is observed upon human infection with the protozoan parasite *Trypanosoma cruzi* (*T. cruzi*), which leads to Chagas disease (23).

1.3.1. Chagas disease (Human American trypanosomiasis)

Chagas disease, also called Human American trypanosomiasis, was named after the Brazilian medical doctor Carlos Chagas, who discovered the disease in 1909 during a campaign to fight malaria in Brazil. Carlos Chagas identified, associated with diseased individuals living in poor dwellings, a triatomine blood-sucking insect. He found in the intestine of the bug flagellated parasites, which he named *Trypanosoma cruzi* (*T. cruzi*). He also found *T. cruzi* parasites in the blood of sick people, and soon correlated the parasitemia (level of parasites in the blood) with some symptoms of the disease, such as fever, anemia, lymphadenopathy, splenomegaly and a cardiac form of the disease (24).

Recent molecular studies suggest that the ancestor of *T. cruzi* may have been introduced to South America approximately 7–10 million years ago and the oldest record of human infection dates from 9,000 years ago (25). *T. cruzi* is responsible for the infection of ~ 20 million individuals worldwide. The World Health Organization (WHO) estimates that about 100 million people are at risk of becoming infected, with 56,000 new cases per year for all forms of transmission, causing 12,000 deaths per year (Fig. 2) (26, 27). In endemic zones, the contact with feces from infected hematophagous vectors belongs to Triatominae subfamily is the main route of transmission, however other mechanisms has been described such as blood transfusion, organs transplantation, congenital, laboratory accidents and recently reported, oral transmission through food and drink contaminated with infected vector feces (24, 27). Chagas disease is being transmitted beyond its endemic presence in Latin America. Usually through vector migration occurring through population movement, travel, and trade, Chagas disease has spread to areas where it is not endemic, including high-income countries such as Australia, Canada, Europe, Japan, and the United State; thus, transmission by blood and

organ transplantation are becoming a new threat for *T. cruzi* infection as well as the presence of native vectors that may support the transmission of infection in these non-endemic regions. The pathogenesis of Chagas disease remains largely unknown, and there are still no effective vaccines to prevent chronic infection (13, 20, 24, 28). Two nitroaromatic heterocyclic compounds, nifurtimox and benznidazole are available as treatment for *T. cruzi* infection; however, they present several limitations because of their toxicity and side effects related to gastrointestinal and neurologic involvement (29).

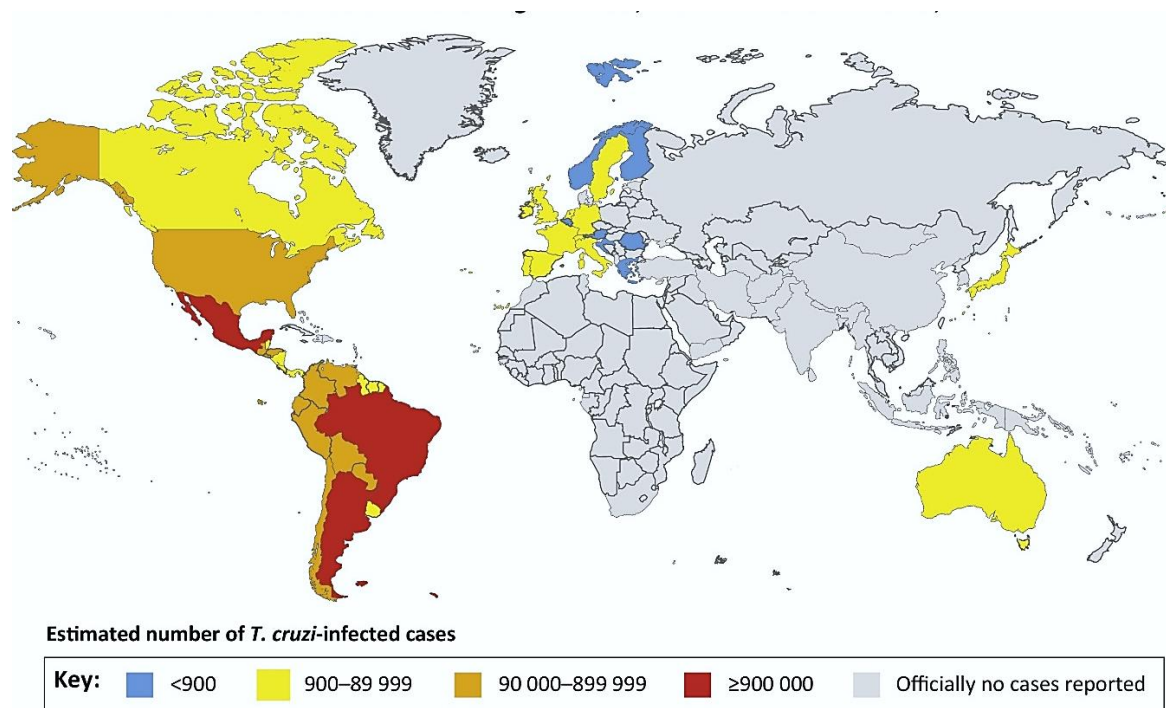


Fig. 2: The global distribution of cases of Chagas disease, based on official estimates, 2006-2010. Global migration has led to an increasing incidence of Chagas disease across the world within regions previously thought to be noendemic for infection. The spread of Chagas disease throughout these areas may be problematic due to the presence of native vectors that may support transmission of infection. Source: Perez et al., 2015 (20).

1.3.2. Chagas disease – Clinical evolution

Individuals infected with *T. cruzi* undergo a short acute phase, characterized by high numbers of parasites in the bloodstream and tissues (28). Acute-phase symptoms are generally mild, but immunosuppressed patients and children can develop a more severe form of infection, with cardiac involvement and encephalomyelitis (30). Specific therapy is successful in about 70% of the individuals diagnosed shortly after infection, but often

associated with toxic side effects. If infection is not treated, roughly 5% of individuals die of acute myocarditis, but most individuals progress to the chronic phase, which is accompanied by subpatent levels of parasitemia. Approximately 60–70% of the chronic patients develop the indeterminate form of Chagas disease and show no clinical symptoms associated with the infection, which is only identified following specific laboratory tests. After a lag period of anywhere from 10 to 30 years — known as the indeterminate form of Chagas disease— a proportion of patients may develop the symptomatic forms of Chagas disease, which can include cardiomyopathy, heart failure and digestive-tract abnormalities such as megacolon and megaesophagus. The cardiac and digestive-system involvement can vary from mild to severe, depending on the extent of tissue damage, and these symptoms generally determine the morbidity of the disease. The cardiac clinical form is characterized by conductive and/or contractile disruptions in the heart accompanied by high morbidity and mortality (Fig. 3) (28, 30).

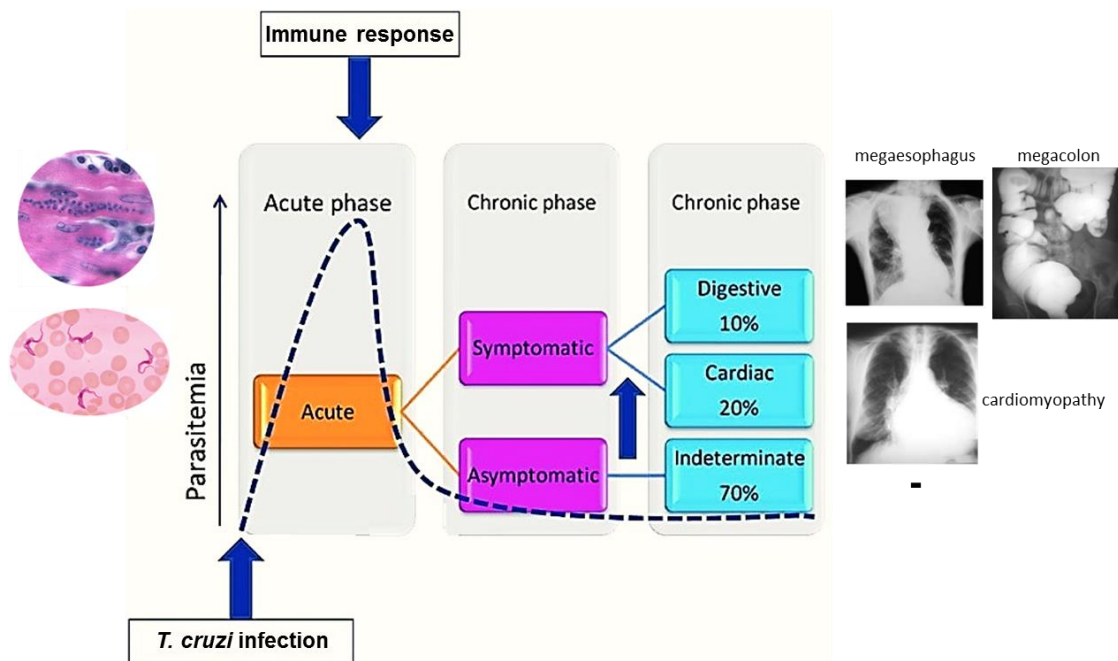


Fig. 3: Clinical evolution of human Chagas disease. Upon infection with *T. cruzi*, individuals undergo an acute phase characterized by high parasitemia. As infection is detected, treatment is offered to the patients and about 75% of the treated acute patients are cured. In the case that disease is not cured (or detected early on), patients will enter the chronic phase of disease. The transition from acute to chronic phase is accompanied by a marked decrease in parasitemia, as a result of the host's immune response. Most patients within the chronic phase are asymptomatic, classified as indeterminate. However, a significant percentage of the patients become symptomatic and develop pathology associated to cardiac or digestive tissues, which may lead to death. Graph modified from Dutra et al., 2009 (31).

1.3.3. Life cycle of *Trypanosoma cruzi*

T. cruzi is known to infect eight different mammalian orders including humans and it is transmitted by insect vectors of the Reduviidae family and the subfamily of Triatomines. Around 100 different triatomine species are susceptible to infection with the *T. cruzi* parasite but the principal vector specie has been *Triatoma infestans*. *T. cruzi* has different developmental stages in its life cycle: Epimastigotes are the form stage that proliferates by cell division in the stomach of the triatomine bugs, they migrate to the distal part of the bug's intestine, and by a process called metacyclogenesis, they transform into metacyclic trypomastigotes, the infective form for the vertebrate host (24).

In natural infection, metacyclic trypomastigotes are released in the feces or urine of infected hematophagous vectors after a blood meal and invade the host through skin lesions or intact mucosa. Once inside, the parasite rapidly infects a wide variety of nucleated mammalian cells including macrophages, smooth and striated muscle cells and fibroblast. After cell invasion, the trypomastigotes are contained within a structure known as a parasitophorous vacuole, from which they subsequently escape, differentiate into amastigotes and replicate free in the cytosol. After nine cycles of binary division, amastigotes differentiate back into the highly motile trypomastigotes which are released upon host-cell membrane rupture and infect neighboring cells or enter the bloodstream disseminates systemically infecting various cell types with a particular tropism for cardiac, skeletal and smooth muscle cells. Finally, the vector are infected by ingesting trypomastigotes in the blood from infected hosts, thus completing the *T. cruzi* life cycle (Fig. 4) (24, 25).

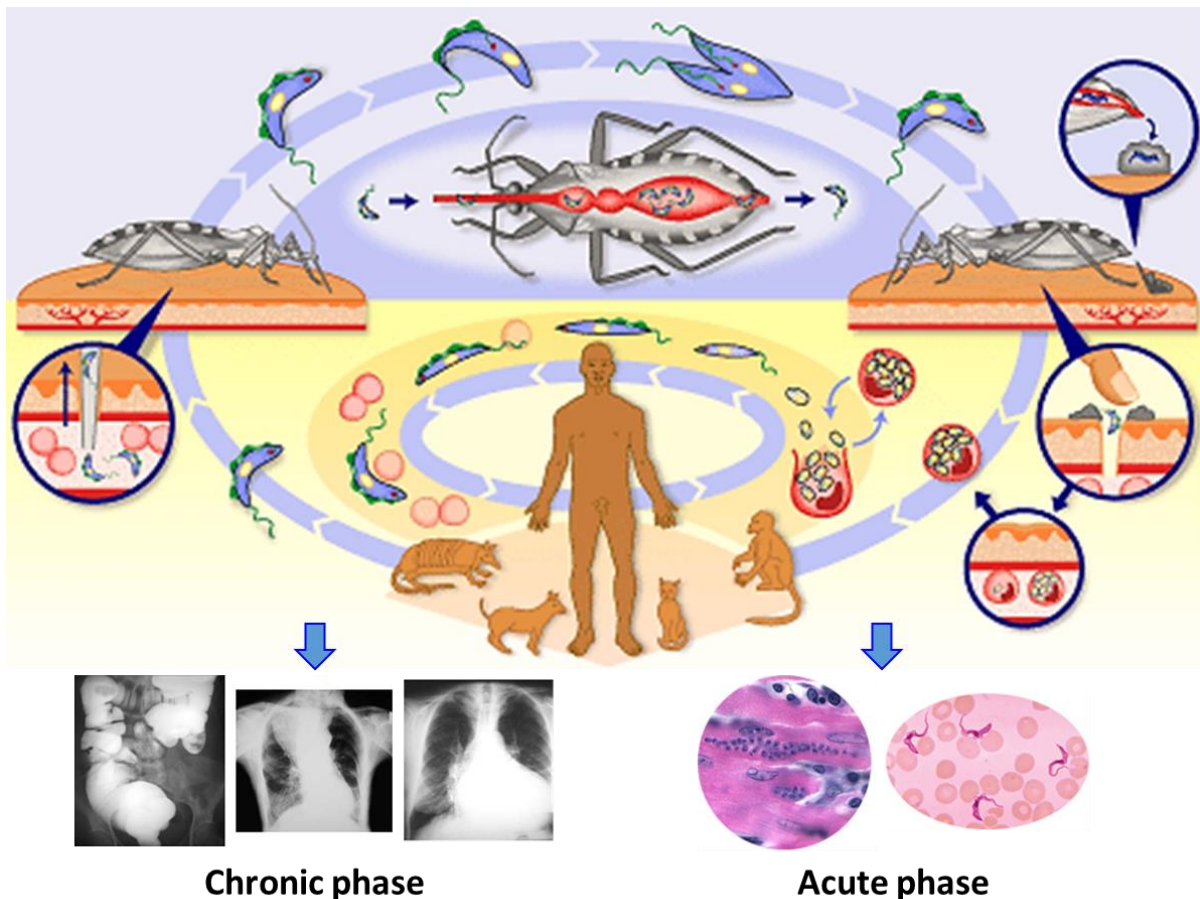


Fig. 4: Life cycle of *Trypanosoma cruzi*. Infective metacyclic trypomastigotes are deposited on human skin when the reduviid bug takes a blood meal. Trypomastigotes enter the body when the feces are either rubbed into the bite wound or the eye. Trypomastigotes invade cells, where they reproduce asexually as amastigotes. After division, amastigotes differentiate back into the highly motile trypomastigotes. The cell dies and trypomastigotes are released. Some will infect other cells and continue the amastigote reproductive cycle, while others will circulate in the blood, where they develop into non-dividing trypomastigotes. The vector ingests the circulating parasites during a blood meal. The trypomastigotes travel to the bug's gut, where they transform into epimastigotes and undergo asexual reproduction by binary fission. From here, the parasites travel to the hindgut, where they develop into metacyclic trypomastigotes and migrate to the rectum, ready to be excreted. Pictures represent the main features for acute and chronic phase. Source: <http://www.who.int/tdr/diseases/Chagas/lifecycle.htm>. (27).

1.3.4. The immune response against *Trypanosoma cruzi* and pathology

T. cruzi induces a complex immune response that involves both innate and adaptive immune responses in its control. A critical event during the infection is innate immune response, in which the macrophage's role is vital. After the infection, *T. cruzi* relies on an arsenal of polymorphic glycosylphosphatidylinositol (GPI)- anchored surface proteins to attach and invade the macrophage, leading to the formation of the parasitophorous vacuole. After lysosomes are fused to the parasitophorous vacuole, parasite survival is mediated by a complex network of antioxidant enzymes, such as peroxidases and

INTRODUCTION

superoxide dismutases (SODs), that shield it from reactive oxygen and nitrogen species and allow it to escape from phagosome into the cytoplasm, where it differentiates into the replicative amastigote forms. After several rounds of duplication, amastigotes differentiate into infective bloodstream trypomastigotes, which are released upon the rupture of the host cell membrane and infect neighboring cells or enter the bloodstream. Once the trypomastigotes reach the bloodstream, the parasite circumvents complement-mediated lysis and opsonization with aid of surface proteins that disrupt the initial attachment of mediators from classical, alternative, and lectin complement pathways and dismantle the C3 convertase, a key step in all three pathways. Thus, the parasite is allowed to disseminate towards many tissues during the acute phase. During the initial phase of infection, the parasite elicits polyclonal B cell activation and hypergammaglobulinemia based on parasite-derived B cell mitogens. The antibodies produced by these cells are not parasite specific and are inefficient in controlling infection. With the stimulation of innate receptors such as TLRs 7 and 9, followed by proinflammatory cytokine production, a T_H1 -focused immune response is established (25).

It is known that T cell-mediated immune responses, mainly T_H1 , are essential to control the parasite replication during the acute phase of the infection. The cytokines IFN- γ , IL-12, and TNF- α strengthen the activation of innate and adaptive effector immune responses, resulting in more efficient killing of the parasite and a strong inflammatory response in several tissues where parasites replicate (32). It is now appreciated that proinflammatory cytokine production is a “double-edged sword” while enhancing intracellular parasite killing it may also contribute to damage of the host tissue including the heart, resulting in acute myocarditis and chronic cardiomyopathy (33). On the other hand, the cytokines IL-10 and TGF- β counterregulate the inflammatory process, indirectly favoring parasite persistence within infected host cells because they are potent inhibitors of nitric oxide (NO) production and other IFN- α - and IL-12-mediated cell activation processes that are important for the killing of the parasite. The extent of this regulation seems to be crucial for the final outcome of the illness, since patients with both clinical forms express inflammatory and anti-inflammatory cytokines, the predominance of an inflammatory environment is observed in cardiac patients, whereas

an anti-inflammatory environment is predominantly observed in indeterminate patients (28, 32).

1.4. Aim

The chronic infection caused by some intracellular protozoa such as *Toxoplasma*, *Leishmania*, and *Plasmodium*, have been associated with an “exhaustion status” of effector T cells induced by the parasite to avoid the adaptive immune response and its clearance (34). Previous studies have demonstrated that *T. cruzi* is able to modulate the expression levels of immune checkpoints such as CTLA-4, PD-1 and PD-L2 during the experimental infection (32, 35, 36). However, many of these observations were collected from *ex vivo* trials where the infection models employed different parasite and mice strains with arbitrary results. In this work, the role of PD-1: PD-L1/PD-L2 inhibitory pathway in the resistance to the *Trypanosoma cruzi* Tulahuen infection, was evaluated. The kinetic of expression of this immune checkpoint and co-expression the others were assayed to unveil a potential strategy of the parasite that would be facilitate the chronic phase progression. Additionally, immune response was evaluated under the context of gene depletion (knockout) and blockade assays by monoclonal antibodies for these molecules in an infection model using C57BL/6J female mice to establish potential intervention points (e.g., immunosuppressive cytokines induction) for the develop a combined therapeutic vaccine against chronic infection.

2. Materials

2.1. Biological material

2.1.1. Cell lines

Tab. 1: List of utilized cell lines

Cell lines	Origin
Hg 39 (86Hg39)	BNI, Hamburg
<i>Trypanosoma cruzi</i> Tulahuen (<i>T. cruzi</i> Th)	BNI, Hamburg

2.1.2. Laboratory animals

Tab. 2: List of utilized mouse strains

Mice	Origin	Abbreviation used in the thesis
C57BL/6J	BNI, Hamburg	wt
C57BL/6J PD-L1 ^{-/-}	BNI, Hamburg	PD-L1 KO

2.2. Material for cell biology

2.2.1. Reagents for cell biology

Tab. 3: Reagents for cell biology

Reagent	Manufacturer	Information
RPMI 1640 (without L-glutamine)	PAN BIOTECH	Roswell Park Memorial Institute medium
DMEM (without L-glutamine)	PAN BIOTECH	Dulbecco's Modified Eagle Medium
FCS	PAN BIOTECH	Fetal Calf Serum
DPBS	PAN BIOTECH	Dulbecco's Phosphate Buffered Saline
L-glutamine	PAN BIOTECH	200 mM
Sodium pyruvate	GIBCO	100 mM
Gentamicin sulfate	PAA	10 mg/mL
GM-CSF	BNITM, Hamburg	Granulocyte-macrophage colony-stimulating factor
Trypsin-EDTA	Capricorn Scientific	(0.05%) in DPBS (1X)
Trypan blue solution	SIGMA	0.4% liquid
Fc-Block	BNITM, Hamburg	
PMA	SIGMA	Phorbol 12-myristate 13-acetate
Ionomycin	SIGMA	Ionomycin calcium salt form <i>S. conglobatus</i>
Monensin	BioLegend	Monensin solution 1000X
Foxp3/Transcription factor staining buffer set (Cat. N° 00-5523-00)	eBioscience	Permeabilization buffer 10X Fixation/Permeabilization (concentrate) eBioscience™ Fixation/Perm (diluent)

2.2.2. Antibodies and fluorescent dyes

MATERIALS

Tab. 4: Antibodies and fluorescent dyes

Mouse antigen	Fluorochrome	Clone	Manufacturer
CD3	AF 488 or PerCP/Cy5.5 or PEeFluor 610	145-2C11	BioLegend or Invitrogen
CD3	PE/Cy7	17A2	BioLegend
CD4	V500	RM4-5	BD Bioscience
CD8	V450	53-6.7	eBioscience
CD19	APC	6D5	BioLegend
CD19	AF700	1D3	BD Bioscience
CD11b	V450	M1/70 (RUO)	BD Bioscience
CD11c	PE	HL3 (RUO)	BD Bioscience
CD11c	PECy7	N418	BioLegend
CD44	AF700 or PECy7	IM7	BioLegend
CD160	APC or PerCP/Cy5.5	7H1	BioLegend
IFN-gamma	AF488	XMG1.2	BioLegend
TNF-alpha	APC or PE	MP6-XT22	BioLegend or eBioscience
Granzyme B	PEeFluor 610	NGZB	eBioscience
IL-10	AF700	JESS-16E3	eBioscience
Ly6C	AF488	HK1.4	BioLegend
Ly6G	PerCP/Cy5.5	1A8	BioLegend
PD-1	PE or PE/Cy7	RMP1-30	BioLegend
PD-L1	APC	10F.9G2	BioLegend
PD-L2	PE	TY25	BioLegend
LAG-3	PerCP/Cy5.5	C9B7W	BioLegend
TIM-3	APC	RMT3-23	BioLegend
2B4	PE/Cy7	m2B4 B6 458.1	BioLegend
NK1.1	FITC	PK136	BD Pharmingen

2.2.3. Buffers and cell culture media for cell biology

Tab. 5: Buffers and cell culture media for cell biology

Solutions	Ingredients
Complete RPMI 1640 medium	500 ml RPMI 1640 50 mL FCS 5 mL L-glutamine (200 mM) 2,5 mL Gentamicin (10 mg/mL)
BM-DCs medium	400 mL DMEM High Glucose with 25 mM Hepes 50 mL FCS 50 mL GM-CSF 5 mL L-glutamin (200 mM) 2,5 mL Gentamicin (10 mg/mL)
Erythrocyte lysis buffer	0,1 M Tris-HCl (pH 7,5) 0,16 M ammonium chloride (NH ₄ Cl)
FACS-Buffer	1% FCS 0,1% sodium azide (NaN ₃) in PBS1111

2.2.4. Kits for cell biology

Tab. 6: Kits for cell biology

Kit	Manufacturer
LEGENDplex™ Cat. N° 740005	BioLegend

2.3. Materials for antibody blocking

Tab. 7: Antibodies for blocking assays

Antibody	Clone	Manufacturer
LEAF™ Purified Rat IgG2a, k Isotype Ctrl	RTK2758	Biologend
Ultra-LEAFT™ Purified anti-mouse CD279 (PD-1)	RMP1-14	Biologend
LEAF™ Purified anti-mouse CD366 (TIM-3)	RMT3-23	Biologend

2.4. Materials for molecular biology

Tab. 8: Oligonucleotide primer

Primer	Sequence 5' → 3'
Tc 121F	AAATAATGTACGGGKGAGATGCATGA
Tc 121R	GGTTCGATTGGGGTTGGTGTAATATA
GAPDH-F	GTCGGTGTGAACGGATTTGG
GAPDH-R	TTCCCATCTCGGCCTTGAC

2.4.1. Kits for molecular biology

Tab. 9: Kits for molecular biology

Kit	Manufacturer
QIAamp DNA Mini Kit (Cat. N° 51306)	QIAGEN
Quantitect SYBR Green PCR Kit (Cat. N° 204143)	QIAGEN

3. Methods

3.1. Cell biology

3.1.1. Cultivation of adherent cells

In sterile conditions, Hg 39 cells were suspended in complete RPMI 1640 medium and seed in a 45 mm³ of culture flasks. Afterwards, cells were cultured for three days at 37°C and 95% CO₂ until obtain a confluent monolayer. In order to detach the cells from the flask's bottom, 500 µL of Trypsin-EDTA were given to the cells for 5 min at 37 °C. Afterwards, cells were washed twice with 5 mL of complete RPMI 1640, centrifuged at 1200 rpm, 5 min at 4 °C. Finally, cells were suspended in a 10⁵ cells to replicate in a new culture flasks. Cell counting was determined by diluting cell concentration 1:10 in Trypan blue solution and using a Neubauer chamber (0.100mm) under a microscope at low magnification.

3.1.2. Generation of bone-marrow derived dendritic cells (BM-DCs)

C57BL/6J and PD-L1 KO mice were euthanized and hind legs were removed at height of the hip. In sterile conditions, muscles were completely removed, femur bones were dissected and sterilized with 70% ethanol. With a syringe containing BM-DCs medium, the bone marrow washed out into a dish with sterile media and centrifuged at 1200 rpm for 5 min at 4°C. The supernatant was discarded and the pellet incubated with erythrocyte lysis buffer for 5 min at RT. The lysis was stopped with addition of new media and centrifuged at 1200 rpm for 5 min at 4°C. Mouse bone marrow were differentiate into dendritic cells for incubation with BM-DCs medium. 3 x 10⁶ cells were cultured in 8 mL of BM-DCs medium in a petri dish at 37°C and 9% CO₂. At day three and six after bone marrow isolation, 8 mL of BM-DCs medium were added additionally to the culture. At day seven, BM-DCs were fully differentiated and used for further experiments.

3.1.3. Isolation of spleen cells

For the isolation of murine splenic cells mice were euthanized and the spleens were dissected in sterile conditions and collected in 5 mL sterile complete RPMI 1640 medium on ice bath. The spleens were mashed through a 70- μ m-pore-size cell strainer with the stamp of a sterile 5 mL syringe and rinsed with 10 mL sterile DPBS into a 15 mL Falcon tubes and subsequently centrifuged at 1200 rpm for 5 min at 4 °C. The supernatant was discarded and the cells were suspended in 5 mL erythrocyte lysis buffer for 5 min at RT. The lysis was stopped with the addition of 5 mL complete RPMI 1640 medium. Afterwards the cells were centrifuged at 1200 rpm for 5 min at 4 °C. After discarding the supernatant the cells were suspended in 10 mL sterile complete RPMI 1640 medium and passed through a 40- μ m-pore-size cell filter. Finally, the cell number was determined and the exact cell concentration was adjusted.

3.1.4. Flow cytometry

Cells were prepared for FACS analysis by suspending 3×10^6 cells for surface and intracellular staining. For intracellular staining, cells were cultured in 96-U-shape-well plates and stimulated with 50 ng/mL PMA and 500 ng/mL Ionomycin for six hours at 37 °C and 5 % CO₂, and 2 μ M Monensin was added during the last 5 hours of culture. Cells were washed twice with cold DPBS (1500 rpm, 5 min and 4 °C), and stained with antibodies directed against surface antigens diluted in 15 μ L of Fc-block for 30 min at 4°C. In the next step, the cells were fixed and permeabilized in accordance to the manufacturer's protocol of the Foxp3 / Transcription factor staining buffer set. Briefly, after surface staining, cells were washed twice with cold DPBS and fixed with 100 μ L fixation buffer for 30 min at RT. Afterwards, cells were washed twice with permeabilization buffer and stained with fluorescently labelled anti-cytokine antibodies diluted in 15 μ L of permeabilization buffer for 30 min at RT. After incubation, cells were washed twice with permeabilization buffer and suspended in 200 μ L of FACS buffer for fluorescence measure on a BD FACSDiva™ flow cytometer (BD, Biosciences, Heidelberg). FMO controls were used for compensations and gating.

3.1.5. Cytometric beads assay-LEGENDplex™

Cytokine profile was determined using the LEGENDplex™ Mouse Th Cytokine Panel (13-plex). Serum samples were processed following the manufacturer's instructions,

afterwards the samples were measure with the Accuri C6 cytometer (Accuri Cytometer Inc., Ann Arbor).

3.2. Experimental infection model

Seven-to eight-week old C57BL/6J female mice were infected by intraperitoneal (i.p.) inoculation of 2×10^3 bloodstream trypomastigotes of *T. cruzi* Tulahuen strain diluted in 200 μL of DPBS. Parasites were obtained from C57BL/6J male mice (two-week old) in which were maintained with periodic passages every 15 days. Control mice received 200 μL of DPBS alone. In order to monitor infection progression in the infected mice, 2 μL of blood samples were taken from tale vein puncture in several time points, diluted 1:20 in erythrocyte lyse buffer to remove red blood cells, and incubated for 5 min at RT. Parasite counting was realized using a Nuebauer chamber (0.02 mm). Previously to blood collection, body weight was collected.

3.3. In vivo blocking assays

For PD-1 blockade, anti PD-1 mAb was administered in 0.2 mg doses, via i.p. puncture in 200 μL of DPBS per mouse on day 0 and day 7 post-infection. Control mice were administered the same quantities of rat IgG2a isotype control at the same time points as the blocking mAbs. Parasitemia and body weight data were collected since day 7 every 3 days until sacrifice.

For blockade of PD-1 and TIM-3, 0.2 mg of each antibody were used in 200 μL of DPBS. Control group received 0.2 mg of rat IgG2a isotype control. The treatment followed the same scheme of injection employed in single antibody blockade.

3.4. Molecular biology

3.4.1. Organ sampling

On the day 24-28 (early chronic phase) mice were sacrificed and 25 mg heart, liver, skeletal muscle and 10 mg spleen were harvested, rinsed in DPBS, to avoid contamination with blood parasites. Samples were stored in liquid nitrogen until DNA isolation.

3.4.2. Isolation of DNA

Frozen tissue samples were thawed, equilibrate to RT (15-25°C) and immediately mechanically disrupted and homogenized. The tissue suspension was incubated overnight at 56°C with lysis buffer and Proteinase K from QIAamp DNA Mini Kit and DNA isolation was performed according to manufacturer specifications.

3.4.3. Quantification of DNA

Concentrations of DNA were determined using a NanoDrop 2000 Spectrophotometer (PeqLab/Thermo Scientific).

3.4.4. Standards for qPCR

The standards were generated by spiking tissue homogenates from naive mice to which 10^5 cell cultured *T. cruzi* trypomastigotes were added. DNA was isolated as mentioned above and serially diluted with 25 µg/mL DNA isolated from unspiked naive mice tissue. The 10-fold dilution series contained DNA from 10^5 to 10^{-2} parasites, equivalents per 50 ng of total DNA. A standard curve was generated from these standards, in triplicate reactions, to determinate parasitic load in the organs from infected mice.

3.4.5. Quantitative Real Time PCR (qRT-PCR)

Real-time PCR were prepared using the QuantiTect SYBR Green PCR Kit and run on a Rotor Gene (R Corbett Research). Primers target the minicircle variable region from kDNA and amplify a 330 bp fragment. The amount of *T. cruzi* from kinetoplast DNA (kDNA) was quantified in relation to the mouse-GAPDH housekeeping gene. Samples were analyzed by duplicates. The following reaction mixture was chosen:

Master mix	Volume/reaction
QuantiTect SYBR Green (2X)	10 µL
Primer F+R (1/20), 0,25 µM	2 µL
Template DNA (50ng)	2 µL
dd H ₂ O	6 µL

The following PCR program was chosen for the performance of the kDNA specific qRT-PCR:

Steps	T [°C]	Time [sec]
Initial melting	95	900
5 repeats:	94	60

METHODS

	68	60
	72	60
40 repeats:		
Denaturation	94	45
Primer annealing	64	45
Elongation	72	45
Final denaturation	72	600
Melting curve analysis from 62°C to 95°C		

The identity of the PCR products was controlled by analysis of the melting curve at the end of the amplification. Each PCR contained two no template controls (no DNA added to the reaction), one standard sample (10^5 *T. cruzi*) in order to adjust the intra-reaction variation and each DNA was quantified in duplicate.

Duplicate values for each DNA sample were averaged (geometric mean) and parasite equivalent load was calculated automatically by plotting the Ct value against each standard of known concentration and calculation of the linear regression line of this curve. To normalize the amount of DNA, GAPDH was used to correct the initial sample amount. Murine GAPDH and Tc121F/121R amplification have the same efficiency.

3.5. Statistical analysis

Statistical significances were analyzed using GraphPad Prism 5 software. The statistical test used is described in each figure legend.

The flow cytometry analysis was made with the FlowJo Software, version 10 (BD, Biosciences).

4. Results

4.1. Evaluation of PD-L1 expression on *Trypanosoma cruzi* Tulahuen strain *in vitro* infection model

The PD-1/PD-L axis has been shown to be involved in the maintenance of peripheral tolerance (16, 37). Ligands are expressed on tumor cells and cells being infected by different pathogens as a mechanism to escape from immune response leading to sustained immunosuppression and chronic condition (9).

To evaluate whether these molecules might be involved in the establishment of chronic infection by *Trypanosoma cruzi* Tulahuen (*T. cruzi* Th) strain, PD-L1 expression was evaluated *in vitro*. Dendritic cells were differentiated from bone marrow-derived cells isolated from C57BL/6J (wt) and PD-L1-deficient (PD-L1 KO) mice and co-incubated with *T. cruzi* Th trypomastigotes for 6 hours. 72 hours after co-incubation, PD-L1 expression was evaluated by flow cytometry (Fig. 5). Dendritic cells isolated from PD-L1 KO mice were included as internal control of PD-L1 expression (data not shown).

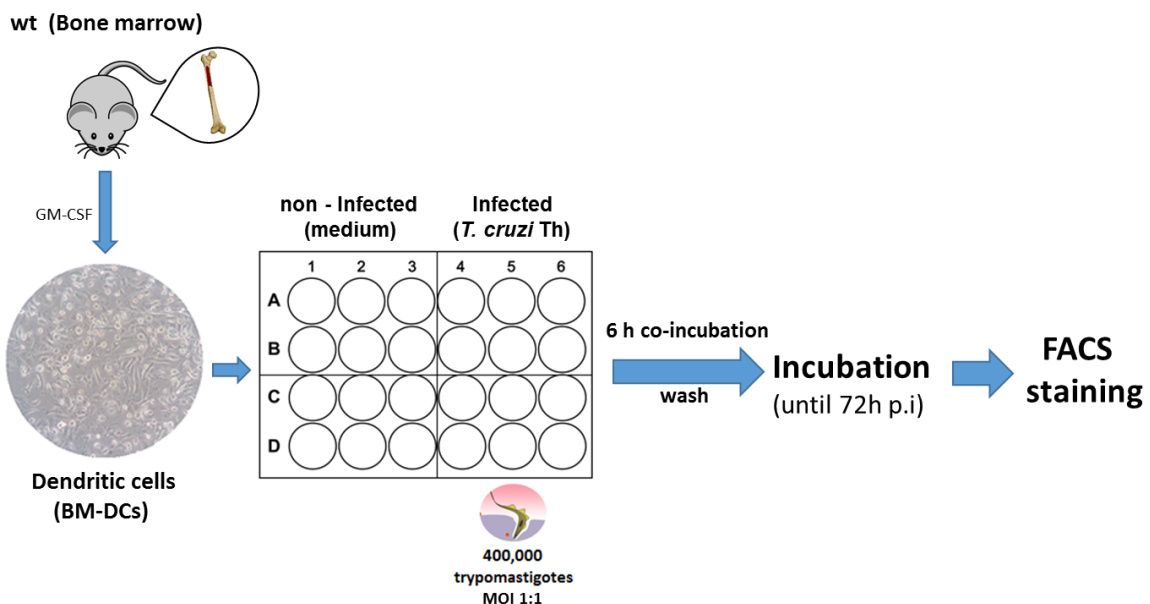


Fig. 5: Scheme of *T. cruzi* Th strain infection of mouse bone marrow-derived dendritic cells (BM-DCs). Bone marrow cells were isolated from mouse femur and cultured in presence of GM-CSF to develop into dendritic cells. BM-DCs were co-incubated with *T. cruzi* Th trypomastigotes at a MOI 1:1. Six hours later, parasites were washed away, fresh media was added and incubation was continued at 37°C. PD-L1 expression was evaluated after 72 hours by flow cytometry.

RESULTS

For the analysis of dendritic cells, anti-CD11c and anti-CD86 staining were included (Fig. 6a). Results showed increased PD-L1 expression on BM-DCs infected with *T. cruzi* Th trypomastigotes compared to non-infected cells during *in vitro* infection (Fig. 6b and 6c).

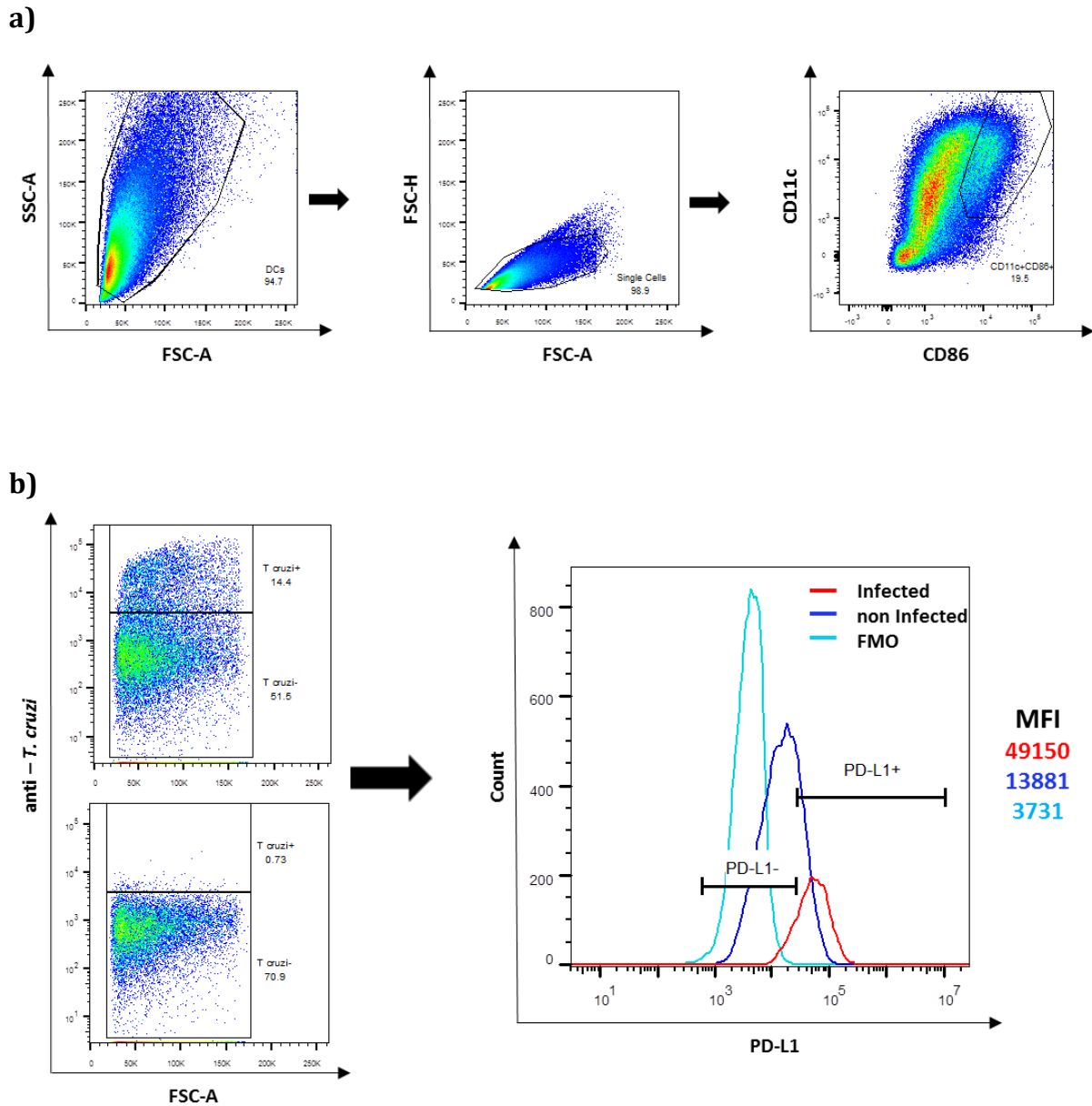


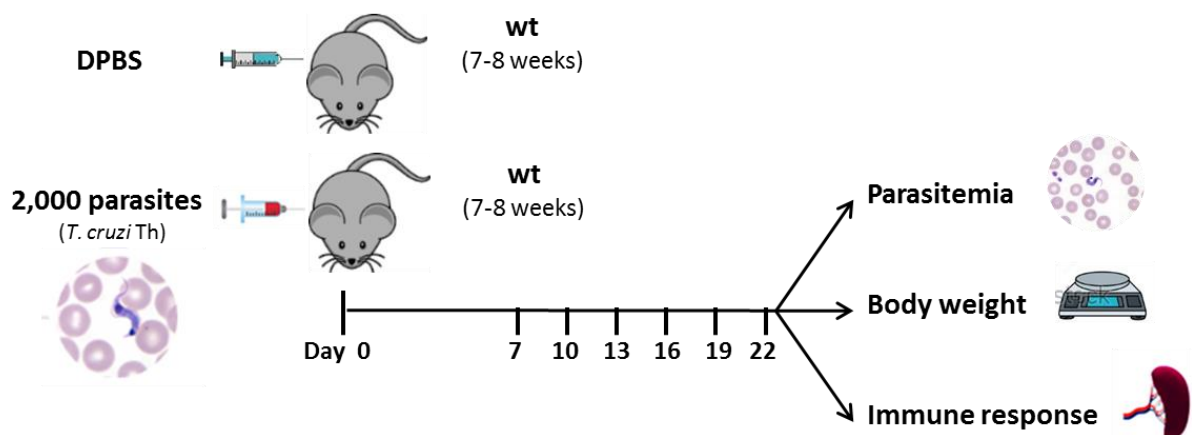
Fig. 6: Expression of PD-L1 on BM-DCs infected with *T. cruzi* Th strain *in vitro*. a) Flow cytometry gating strategy for dendritic cells. b) Gating strategy for identifying *T. cruzi* Th infected dendritic cells. Polyclonal *T. cruzi* Th antiserum was employed to define the infected dendritic cell population for FACS staining. c) Histogram shows the MFI of PD-L1 expression on infected and non-infected dendritic cells. FMO staining control is showed in light blue to identify and gate PD-L1⁻ cells population.

4.2. Development of mouse model of experimental *T. cruzi* Th strain infection

RESULTS

To evaluate *in vivo* the role of the PD-1/PD-L pathway during the infection by *T. cruzi* Th strain, an experimental model using C57BL/6J (wt) female mice, a susceptible strain, was established. Parameters as parasitemia and body weight were evaluated to establish the progress of the infection, defining the times points where the acute and early chronic phase take place and the effect of the infection on the physical condition of the mice. A final dose of infection corresponding to 2000 trypomastigotes of *T. cruzi* Th was established in basis to previous observations where higher dose resulted lethal in a short period of time. Several time points were evaluated starting with the day 7 post-infection where some mice started to exhibit trypomastigotes in peripheral blood (Fig. 7a). Results showed the *T. cruzi* Th inoculation led to an acute infection characterized by high levels of parasitemia which peaked between 13-19 days post-infection and then declined at day 22 (early of chronic phase). Moreover, a significant decrease in the body weight was observed in infected mice in comparison to naive mice (Fig. 7b).

a)



b)

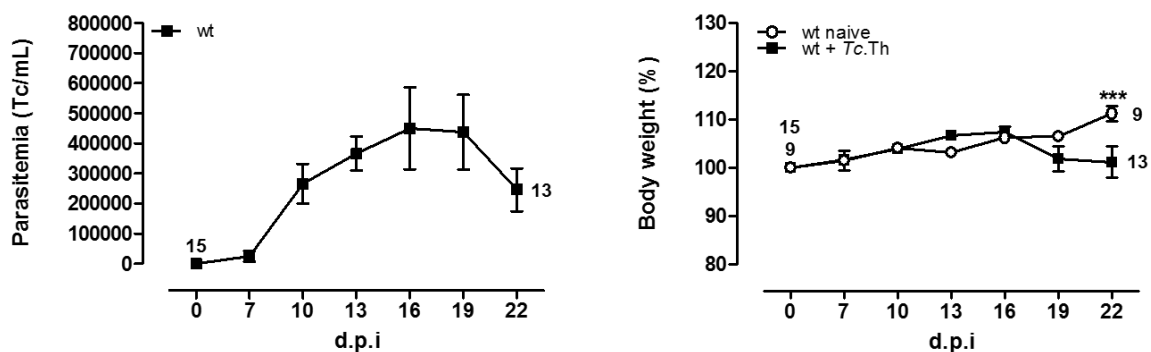


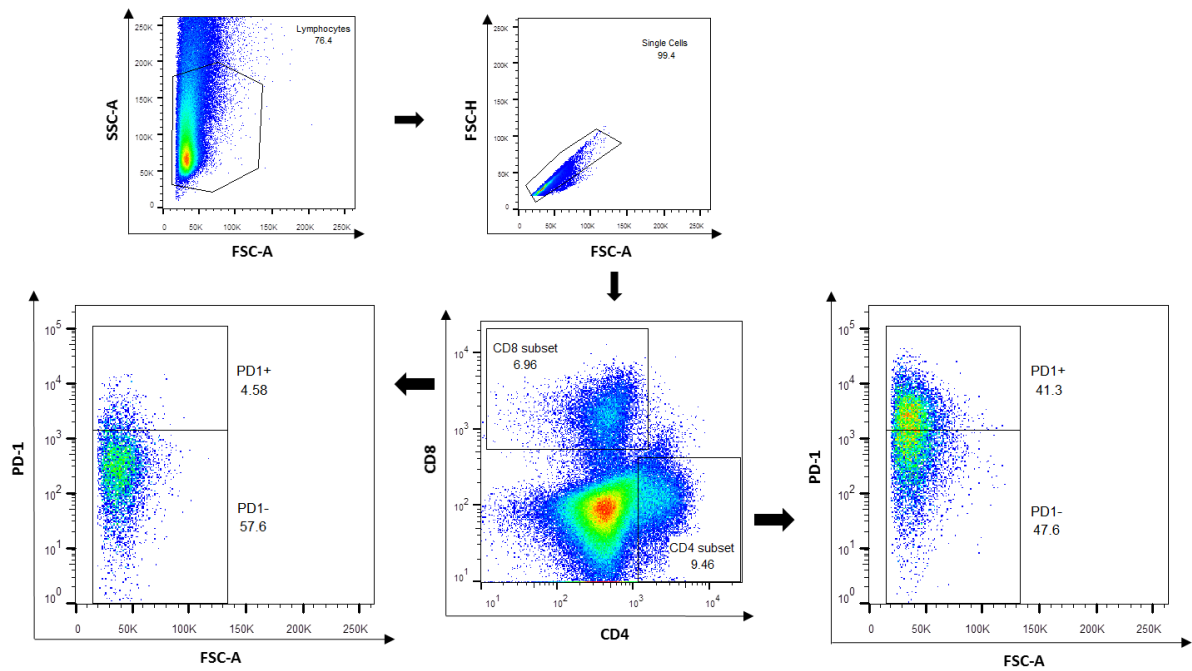
Fig. 7: *T. cruzi* Th experimental infection using an *in vivo* model. a) Scheme of infection. Two months wt female mice were inoculated with 2×10^3 *T. cruzi* Th trypomastigotes by i.p. puncture and parameters as parasitemia and body weight were evaluated in several time points. Mice injected with DPBS were employed as naive control group. Spleen and serum samples were collected for subsequent evaluations. b) Parasitemia and body weight curves following the experimental infection. Parasitemia (*T. cruzi* Th trypomastigotes/mL) was evaluated in peripheral blood by collecting 2 μ L of blood from tale vein. Data are representative of three independent experiments. Values are given as means; error bars indicate standard errors of the means (SEM). The statistical differences of the body weight are calculated with Two-way ANOVA. ($n_{naive} = 9$; $n_{Tc. Th} = 15$).

4.3. Modulation of PD-1, PD-L1 and PD-L2 expression during *T. cruzi* Th infection *in vivo*

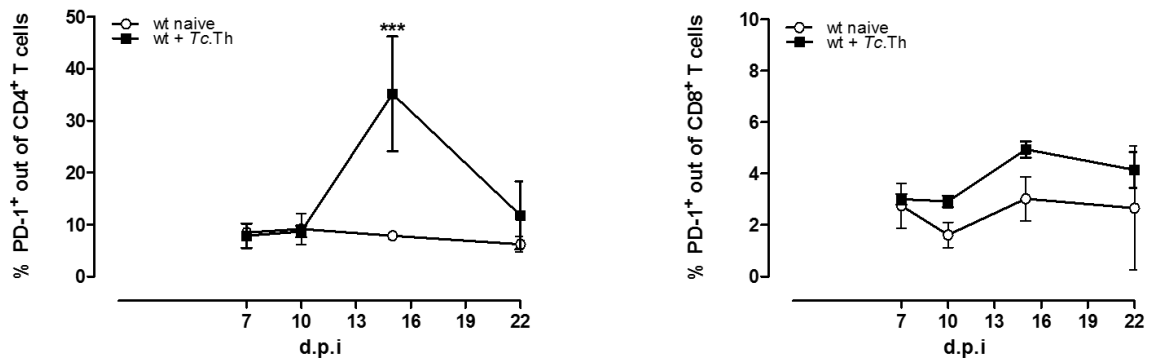
Expression of PD-1 and its ligands was evaluated *in vivo* in a mouse model of experimental *T. cruzi* Th infection previous established. Spleen cells from infected and naive mice were collected at different time points after infection (7, 10, 15 and 22 dpi). Due to the PD-L1 expression observed on DCs *in vitro*, PD-1 expression was evaluated on CD4⁺ and CD8⁺ T cells during the progress of the infection *in vivo* by flow cytometry. Results showed that PD-1 expression was strongly upregulated on CD4⁺ in contrast to CD8⁺ T cells (Fig. 8a) with a high peak at day 15 post-infection in comparison to naive mice (Fig. 8b). Although notable PD-1 expression were observed on CD8⁺ T cells, frequencies were lower than on CD4⁺ T cells, however a slight difference was observed respect to naive mice (Fig 8b).

RESULTS

a)



b)



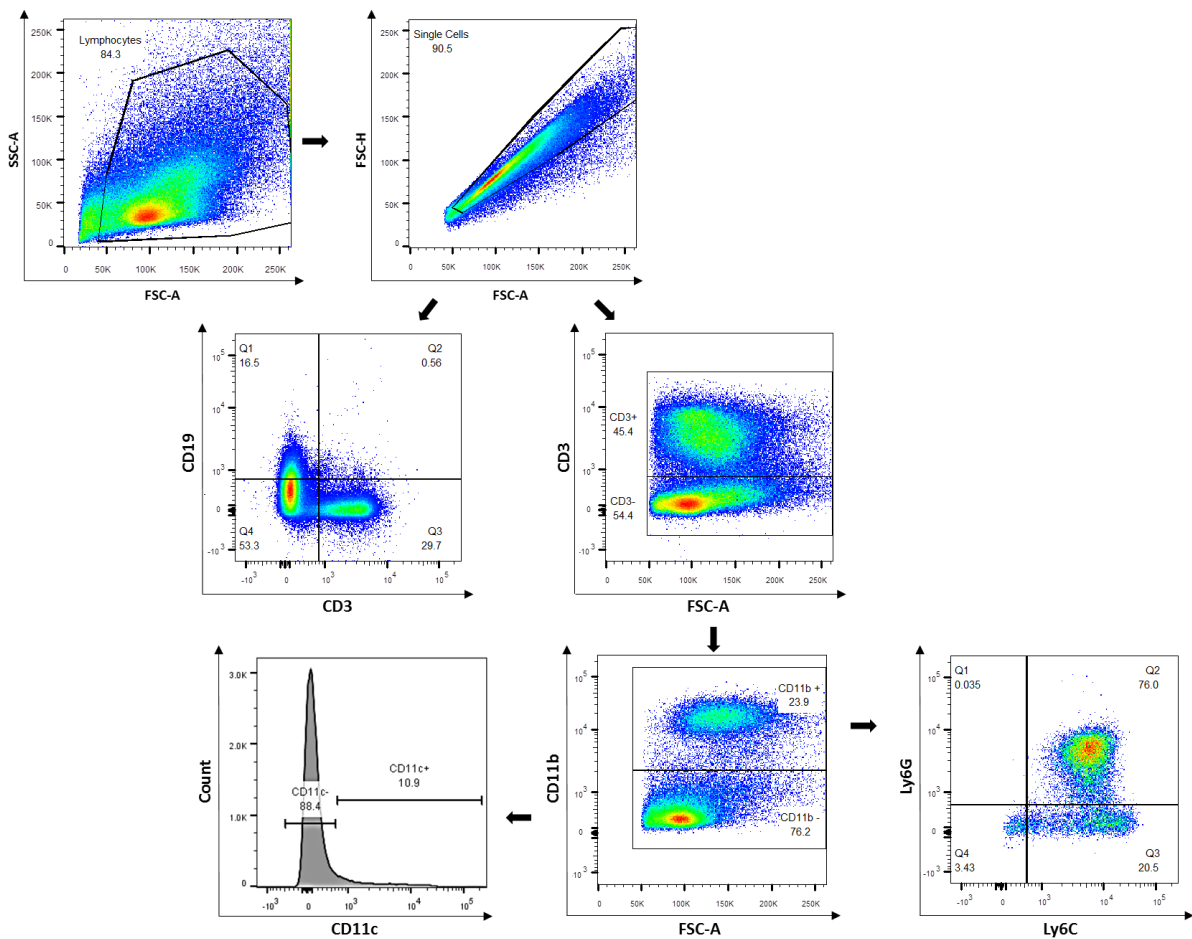
	naive	<i>Tc. Th</i> (n of samples)
7 dpi	15	24
10 dpi	3	3
15 dpi	3	11
22 dpi	9	14

Fig. 8: Time course of PD-1 expression on spleen T cells from wt mice infected with *T. cruzi* Th strain. a) Flow cytometry gating strategy for CD4⁺, CD8⁺ T cells and PD-1⁺ cells. Dot plots show PD-1 expression on CD4⁺ and CD8⁺ T cells at day 15 post-infection. b) Time course experiment showing expression of PD-1 on T cells. Square below shows the number of mice evaluated in each time point. Values are given as means; error bars indicate standard errors of the means (SEM). Asterisks denote P values of <0.05 by Two-way ANOVA compared to naive values. P<0.001***.

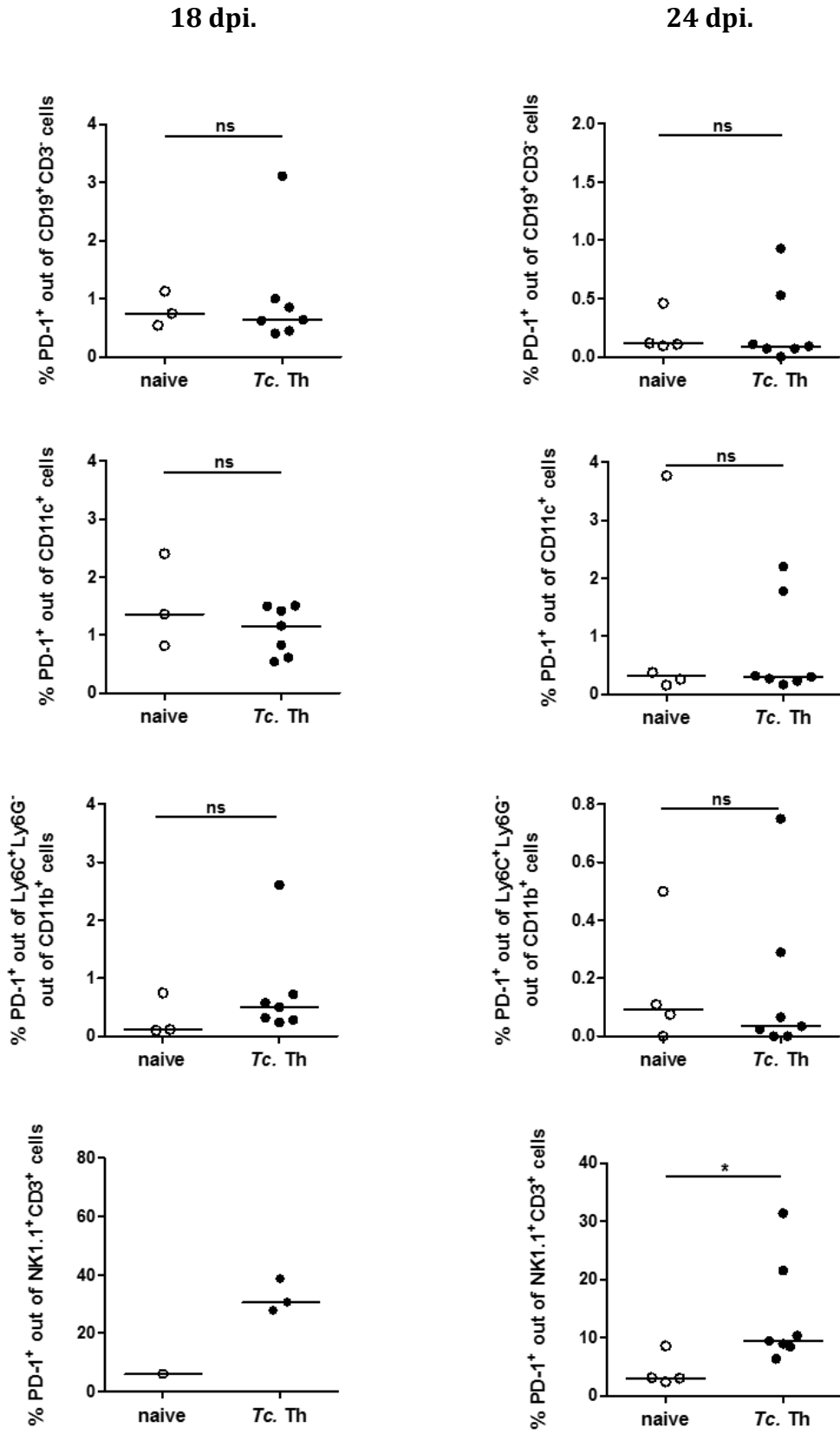
RESULTS

PD-1 expression was also evaluated on other immune cell populations involved in the innate and adaptive immune response to *T. cruzi* infection. For the analysis, anti-CD3 staining was included (Fig. 9a). Results showed that PD-1 expression at day 18 (acute phase) and 24 (early chronic phase) post-infection was not significantly increased on CD19⁺CD3⁻ (B cells), CD11c⁺CD11b⁻ (DCs), Ly6G⁺Ly6C⁺CD11b⁺ (monocytes/macrophages) and, NK1.1⁺CD3⁻ (NK cells) during the progress of the infection, however PD-1 expression was significantly upregulated on NK1.1⁺CD3⁺ (NK T cells) at day 24 post-infection (Fig. 9b).

a)



b)



RESULTS

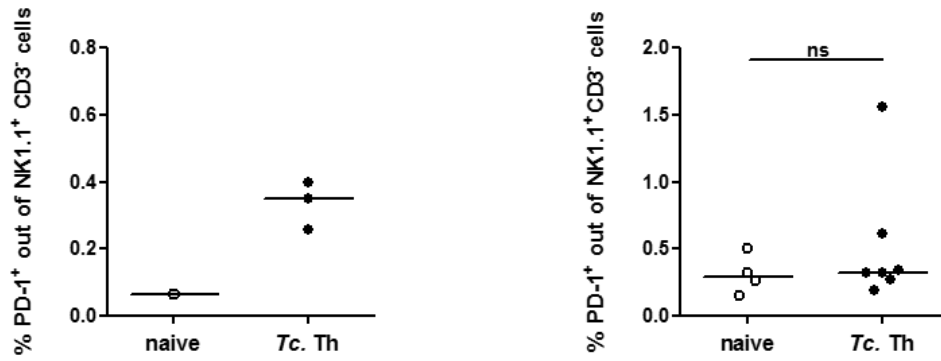
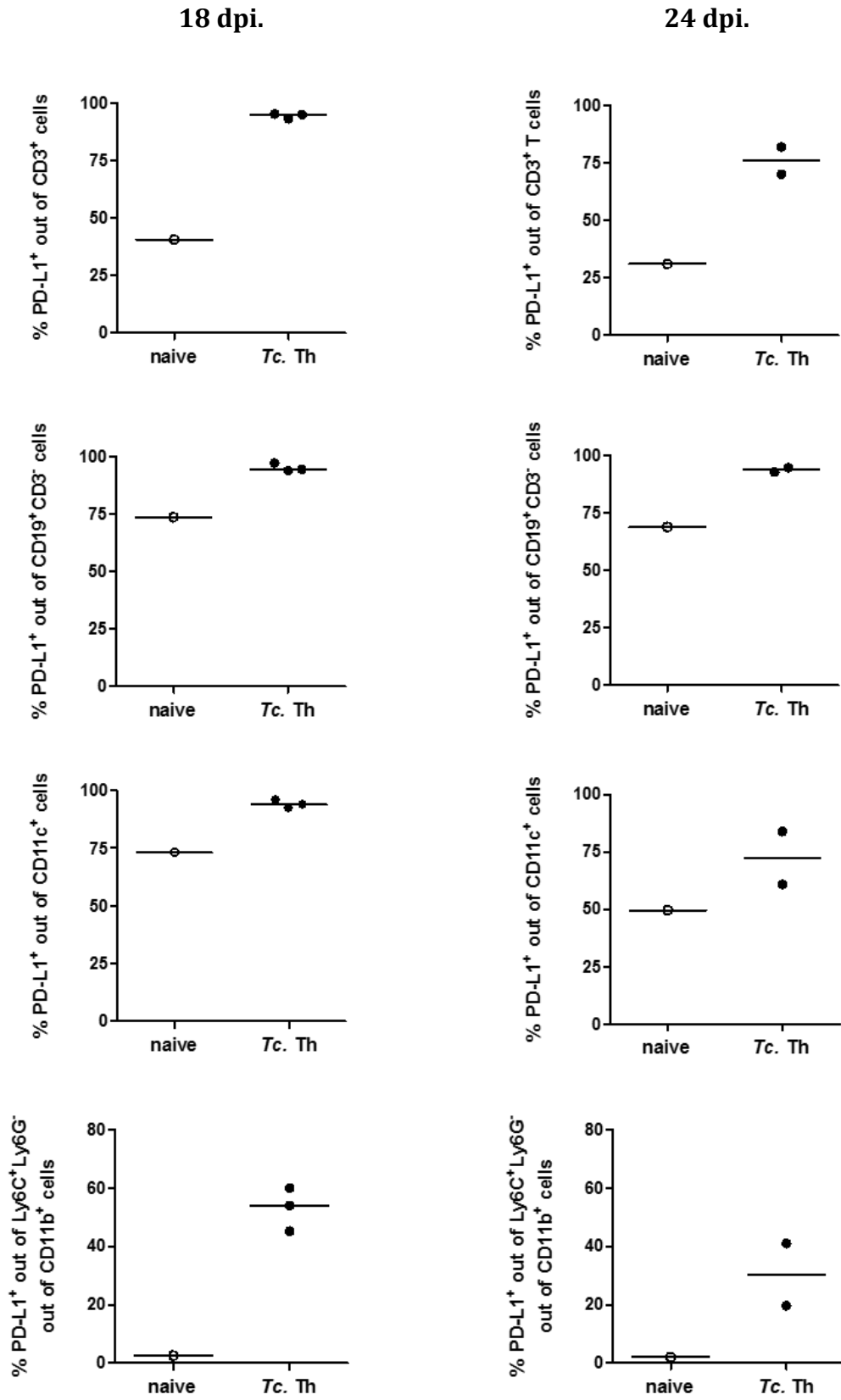


Fig. 9: Expression of PD-1 on spleen cells from wt mice infected with *T. cruzi* Th strain. Spleen cells were isolated from infected and naive mice at day 18 and 24 post-infection and the expression of PD-1 was evaluated in several subsets of cells by flow cytometry. a) Gating strategy to identify immune cells populations. b) Expression of PD-1 on CD19⁺CD3⁻ (B cells), CD11c⁺CD11b⁻ (DCs), Ly6G⁻Ly6C⁺CD11b⁺ (monocytes/macrophages), on NK1.1⁺CD3⁺ (NK T cells) and NK1.1⁺CD3⁻ (NK cells). Data are a compilation of two independent experiments ($n_{\text{naive}}=3-4$; $n_{Tc. Th}=7$). Data from expression of PD-1 on NK1.1⁺CD3⁺ (NK T cells) and NK1.1⁺CD3⁻ (NK cells) at day 18 post-infection are corresponding to one experiment ($n_{\text{naive}}=1$; $n_{Tc. Th}=3$). Median (indicated by the horizontal line) and individual values are shown. The statistical significance was calculated with the student's t-test (unpaired, two tailed). Asterisk denotes P value of <0.05. P<0.05*; ns (not significant).

The expression of the PD-1 ligands, PD-L1 and PD-L2, were also evaluated. Results showed different expression patterns at critical time points (18 and 24 dpi). PD-L1 expression was also upregulated on spleen T cells, CD19⁺CD3⁻ (B cells), CD11c⁺CD11b⁻ (DCs) and, Ly6G⁻Ly6C⁺CD11b⁺ (monocytes/macrophages) at both time points evaluated (Fig. 10a). Interestingly, results showed a trend, but not a significant increase of PD-L2 expression on CD11c⁺CD11b⁻ (DCs), however, PD-L2 expression was upregulated on Ly6G⁻Ly6C⁺CD11b⁺ (monocytes/macrophages) that was statistically significant at day 24 post-infection (Fig. 10b).

RESULTS

a)



b)

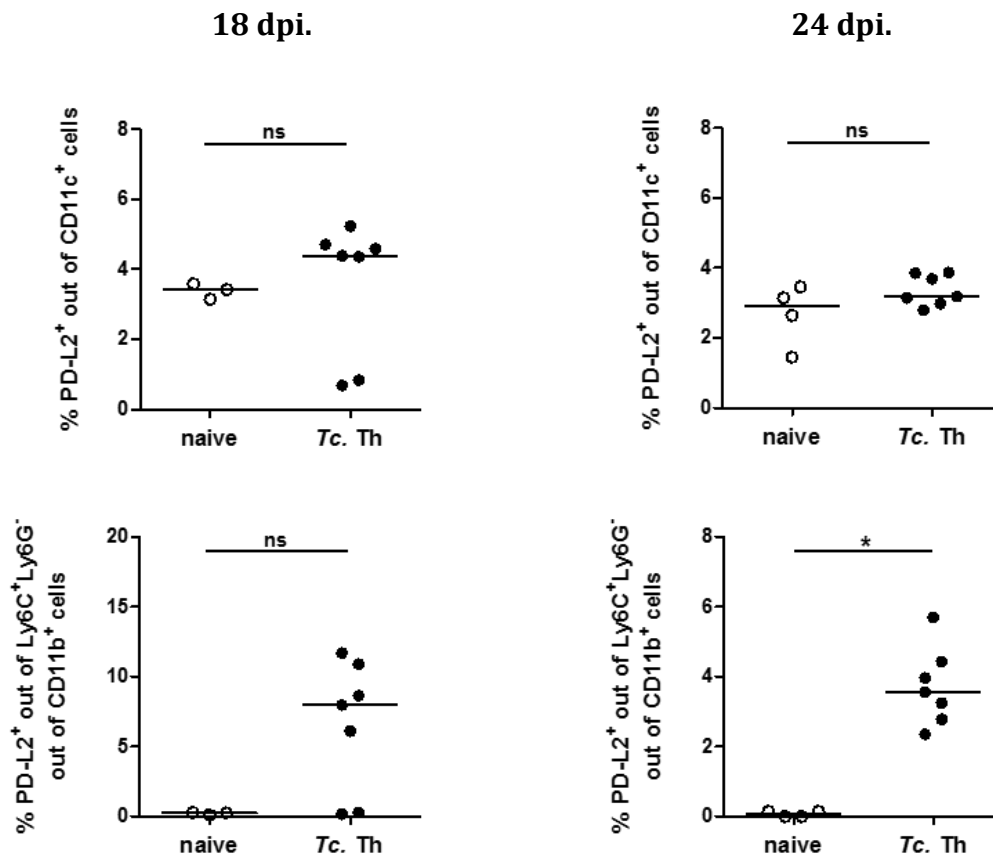


Fig. 10: Expression of PD-L1 and PD-L2 on spleen cells from wt mice infected with *T. cruzi* Th strain. Spleen cells were isolated from infected and naive mice at day 18 and 24 post-infection and the expression of PD-L1 and PD-L2 was evaluated in several subsets of cells by flow cytometry. a) Expression of PD-L1 on CD3⁺ T cells, CD19⁺CD3⁻ (B cells), CD11c⁺CD11b⁻ (DCs) and, Ly6G⁻Ly6C⁺CD11b⁺ (monocytes/macrophages). Data shown are corresponding to one experiment ($n_{\text{naive}}=1$; $n_{Tc. Th}=2-3$). b) Expression of PD-L2 on CD11c⁺CD11b⁻ (DCs) and, Ly6G⁻Ly6C⁺CD11b⁺ (monocytes/macrophages). Data are a compilation of two independent experiments ($n_{\text{naive}}=3-4$; $n_{Tc. Th}=7$). Median (indicated by the horizontal line) and individual values are shown. The statistical significance was calculated with the student's t-test (unpaired, two tailed). Asterisk denotes P value of <0.05. P<0.05*; ns (not significant).

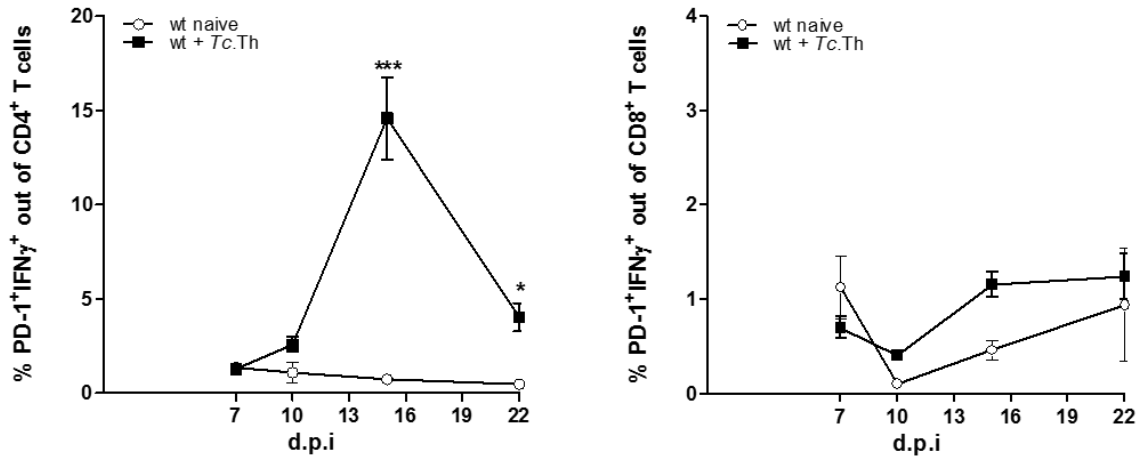
4.4. PD-1/PD-L axis and its effects in the adaptive immune response against *T. cruzi* Th infection

Due to *T. cruzi* Th infection induced an increased PD-1 expression on T cells, the next step was evaluate whether induction affects the effector function of these cells. The expression of proinflammatory cytokines (IFN- γ and TNF- α) was evaluated *ex vivo* after PMA/Ionomycin stimulation. Surprisingly, results showed that IFN- γ was upregulated on CD4⁺ and a trend to increase was observed on CD8⁺ T cells that express PD-1 (Fig.

RESULTS

11a), whereas that TNF- α was upregulated on CD4⁺ and downregulated on CD8⁺ T cells that express PD-1 during the progress of the infection (Fig. 11b).

a)



b)

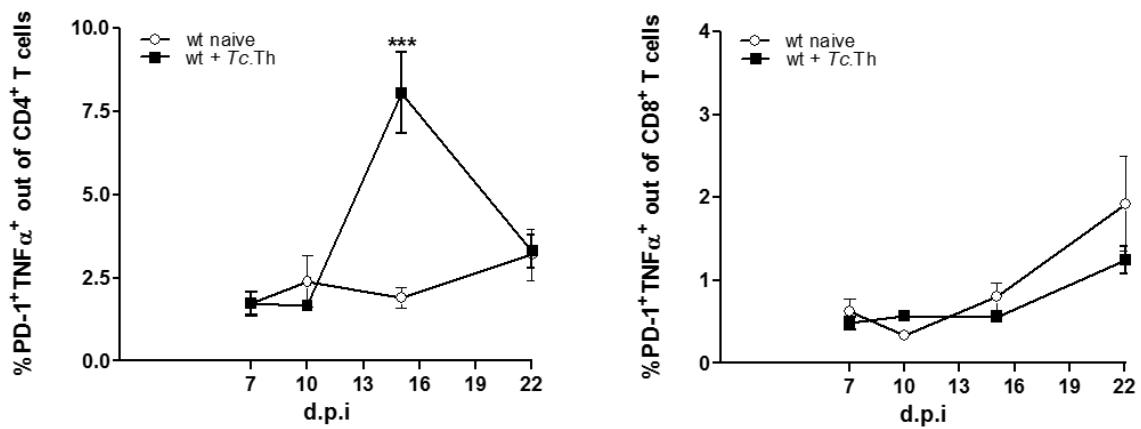


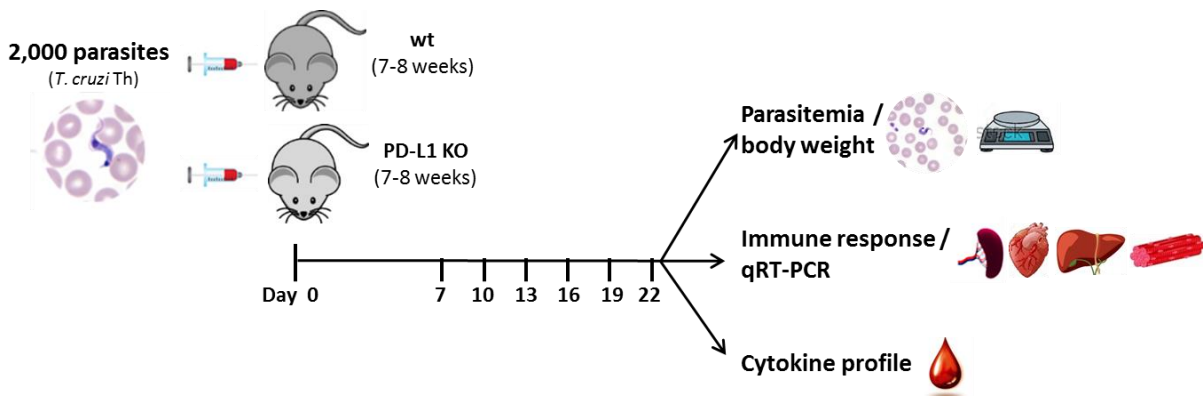
Fig. 11: Time course of cytokine production on PD-1⁺ T cells during the course of the *T. cruzi* Th infection. Spleen cells were isolated from infected and naive wt mice in different time points of the infection and analyzed by flow cytometry after a 5-hour stimulation with PMA/Ionomycin. Monensin was present throughout the stimulation. a) Expression of IFN- γ and b) TNF- α by PD-1⁺ cells in CD4⁺ and CD8⁺ T cells. Values are given as means; error bars indicate standard errors of the means (SEM). Asterisks denote P values of <0.05 by Two-way ANOVA compared to non-infected values. P<0.05*; P<0.001***.

4.5. *T. cruzi* Th infection in PD-L1 knockout mice

RESULTS

PD-L1 is the major ligand of PD-1 and upon ligation on T cells different functions such as proliferation, cytokine production and cytotoxicity are compromised. To evaluate the effect of interruption of PD-1/PD-L1 signaling during the *T. cruzi* Th infection, wt and PD-L1 KO mice were infected with 2000 *T. cruzi* Th trypomastigotes. Control groups received DPBS by i.p. puncture (Fig. 12a). Results showed that interruption of this pathway through the PD-L1 deficiency did not reduce parasitemia neither improved resistance to the infection compared to infected wt mice (Fig. 12b). It is worth noting to despite of an increased parasitemia observed in PD-L1 KO mice compared to wt mice (Fig. 12b), no physical deterioration neither significant body weight loss were observed in this group when compared to the infected wt mice. Although the increased parasitemia observed in these mice, their avidity, reflexes and motility were conserved until the sacrifice whilst infected wt mice showed more lethargic and in some cases, body weight loss could be evident.

a)



b)

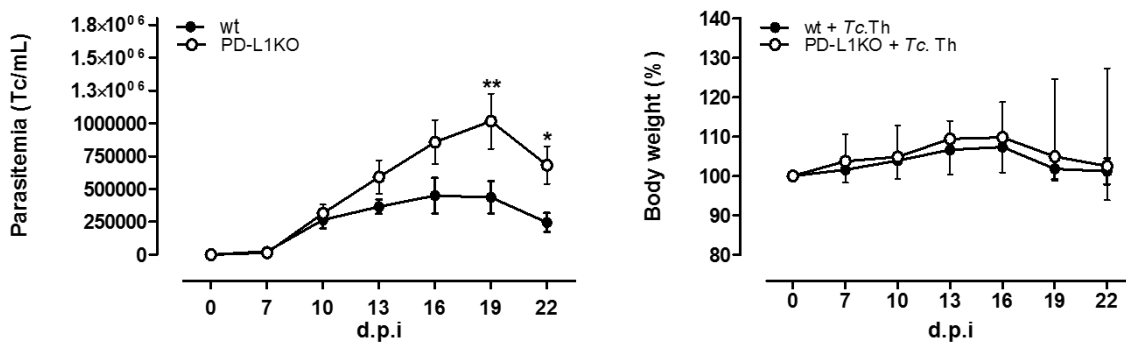


Fig. 12: Effect of PD-L1 deficiency on parasitemia and body weight during the *T. cruzi* Th infection *in vivo*. Wt and PDL1 KO mice were infected with 2×10^3 *T. cruzi* Th trypomastigotes by i.p. puncture. Parasitemia and body weight were collected in different time points. Spleen, heart, liver, skeletal muscle and sera were collected for subsequent evaluations. a) Scheme of infection and b) Parasitemia and body weight curves during the course of the infection. Data are a compilation of three independent experiments ($n_{wt}=15$; $n_{PDL1KO}=17$). Values are given as means. Error bars indicate standard errors of the means (SEM). Asterisks denote P values of <0.05 by Two-way ANOVA compared to naive values. $P<0.05^*$; $P<0.01^{**}$.

4.6. Effect of PD-L1 deficiency on immune response against *T. cruzi* Th infection *in vivo*

To evaluate an early effect of PD-L1 deficiency in the control of infection by the adaptive immune response, spleen cells were collected at day 10 post-infection (acute phase) and T lymphocyte populations were assayed by flow cytometry. For the analysis, anti-CD44 staining (activation marker) was included. Results showed PD-L1 deficiency did not induce significant differences in the frequency of activated CD4⁺CD44⁺ and CD8⁺CD44⁺ T cells in comparison to the infected wt mice, neither improved the expression of inflammatory cytokines (IFN- γ and TNF- α) (Fig. 13).

10 dpi.

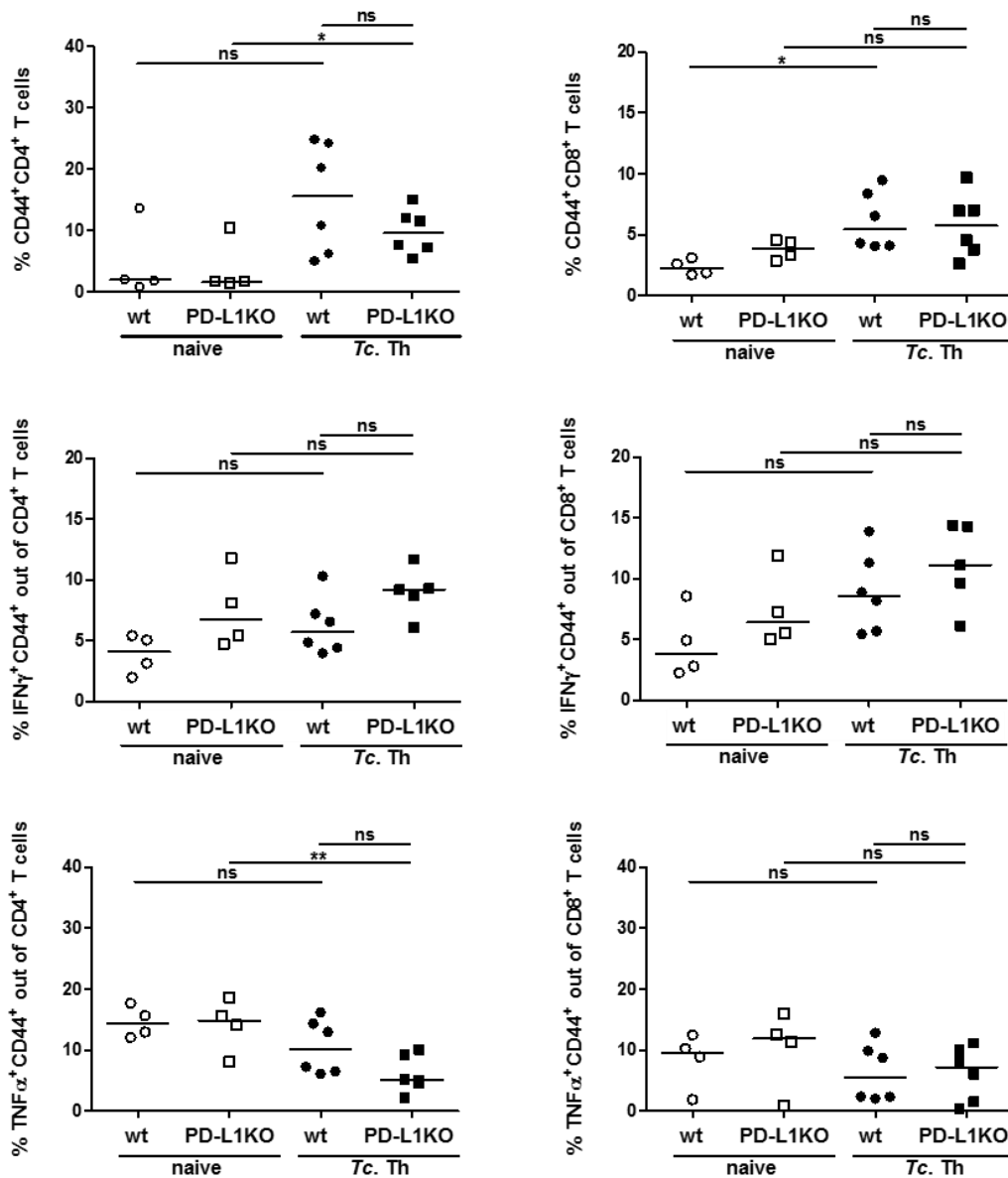


Fig. 13: Effect of PD-L1 deficiency on the activation and cytokine production by spleen T cells from mice infected with *T. cruzi* Th at day 10 post-infection. Spleen cells were isolated from infected and naive mice at day 10 post-infection, activation and cytokine expression were analyzed by flow cytometry after a 5-hour stimulation with PMA/Ionomycin. Monensin was present throughout the stimulation. Data are a compilation of two independent experiments ($n_{wt\ naive}=4$; $n_{PD-L1KO\ naive}=4$; $n_{wt + Tc. Th}=6$; $n_{PD-L1KO + Tc. Th}=6$). Median (indicated by the horizontal line) and individual values are shown. The statistical significance was calculated with the student's t-test (unpaired, two tailed). Asterisks denote P values of <0.05 . $P<0.05^*$; $P<0.01^{**}$; ns (not significant).

In the subsequent repetitions, T cell responses were evaluated at day 24 (early chronic phase). Results showed that PD-L1 deficiency did not induce significant differences in the frequency of CD4+ and CD8+ T cells in comparison to the infected wt mice neither improved the expression of inflammatory cytokines (IFN- γ and TNF- α) (Fig. 14).

RESULTS

24 dpi.

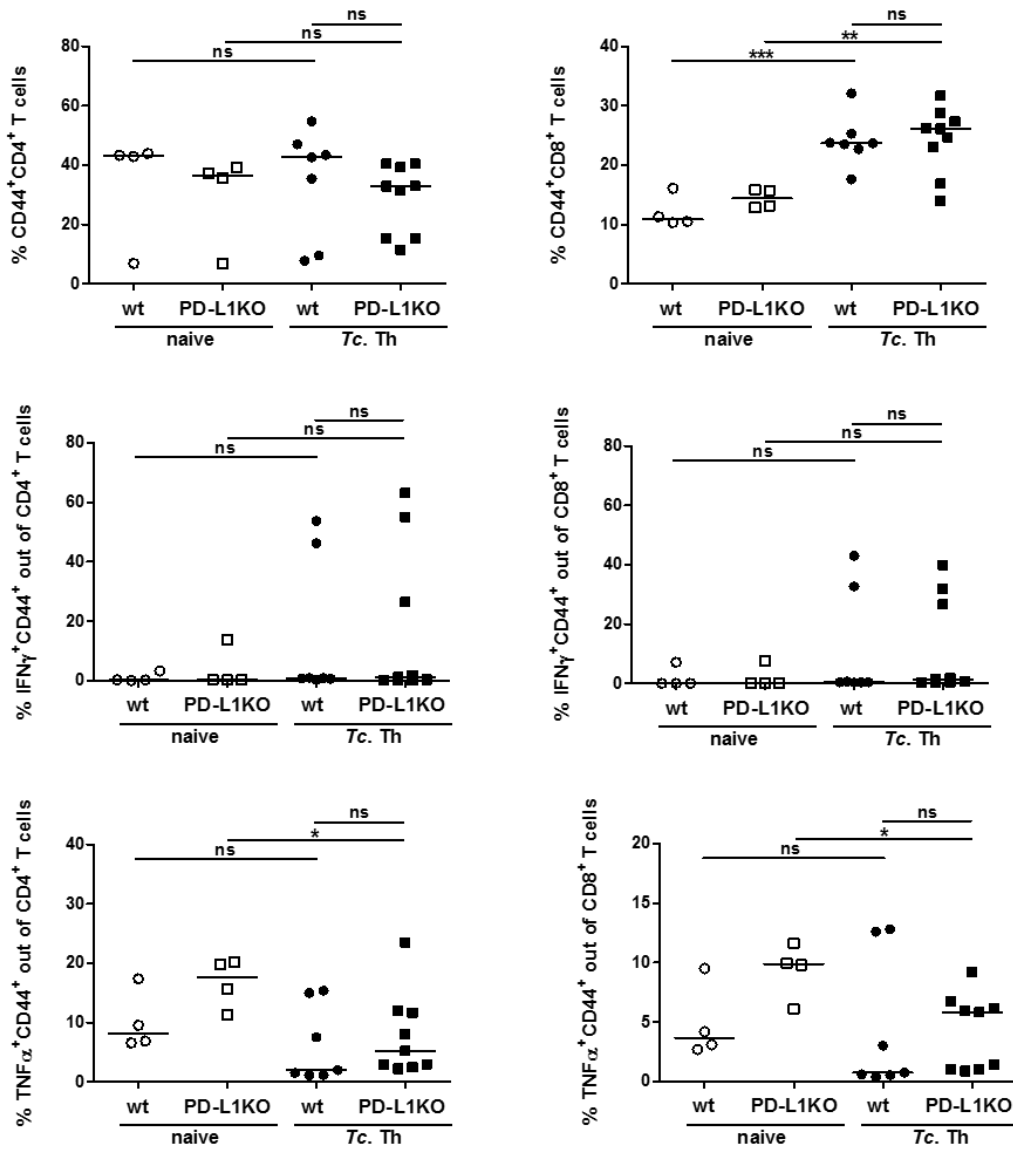


Fig. 14: Effect of PD-L1 deficiency on the activation and cytokine production by spleen T cells from mice infected with *T. cruzi* Th at day 24 post-infection. Spleen cells were isolated from infected and naive mice at day 24 post-infection, activation and cytokine expression were analyzed by flow cytometry after a 5-hour stimulation with PMA/Ionomycin. Monensin was present throughout the stimulation. Data are a compilation of two independent experiments ($n_{wt\ naive}=4$; $n_{PD-L1KO\ naive}=4$; $n_{wt + Tc. Th}=7$; $n_{PD-L1KO + Tc. Th}=9$). Median (indicated by the horizontal line) and individual values are shown. The statistical significance was calculated with the student's t-test (unpaired, two tailed). Asterisks denote P values of <0.05 . $P<0.05^*$; $P<0.01^{**}$; ns (not significant).

To evaluate the effect of PD-L1 deficiency on the effector function of cytotoxic CD8⁺ T cells, the expression of cytolytic molecules as Granzyme B was evaluated at day 10 and 24 post-infection and IL-10 (anti-inflammatory cytokine) involved in the pathogen persistence during chronic infections was also evaluated at day 24 post-infection. Results showed that PD-L1-deficiency did not induce an increase in the frequency of

RESULTS

activated CD8⁺ T cells expressing Granzyme B at both time points evaluated (Fig. 15). Interestingly, the expression of IL-10 was significant upregulated upon PD-L1 deficiency on CD8⁺ T cells from infected mice at 24 day post-infection in comparison to infected wt mice (Fig. 16).

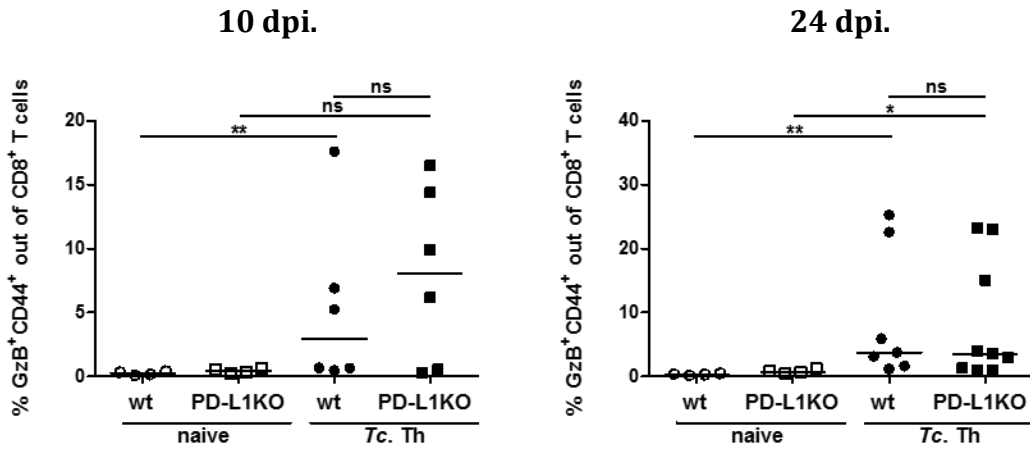


Fig. 15: Effect of PD-L1 deficiency on the expression of Granzyme B of cytotoxic T cells during *T. cruzi* Th infection. Spleen cells were isolated from infected and naive mice at day 10 ($n_{wt\ naive}=4$; $n_{PD-L1KO\ naive}=4$; $n_{wt + Tc. Th}=6$; $n_{PD-L1KO + Tc. Th}=6$) and 24 ($n_{wt\ naive}=4$; $n_{PD-L1KO\ naive}=4$; $n_{wt + Tc. Th}=7$; $n_{PD-L1KO + Tc. Th}=9$) post-infection and analyzed by flow cytometry after a 5-hour stimulation with PMA/Ionomycin. Monensin was present throughout the stimulation. Data are a compilation of two independent experiments. Median (indicated by the horizontal line) and individual values are shown. The statistical significance was calculated with the student's t-test (unpaired, two tailed). Asterisks denote P values of <0.05. P<0.05*; P<0.01**; ns (not significant).

24 dpi.

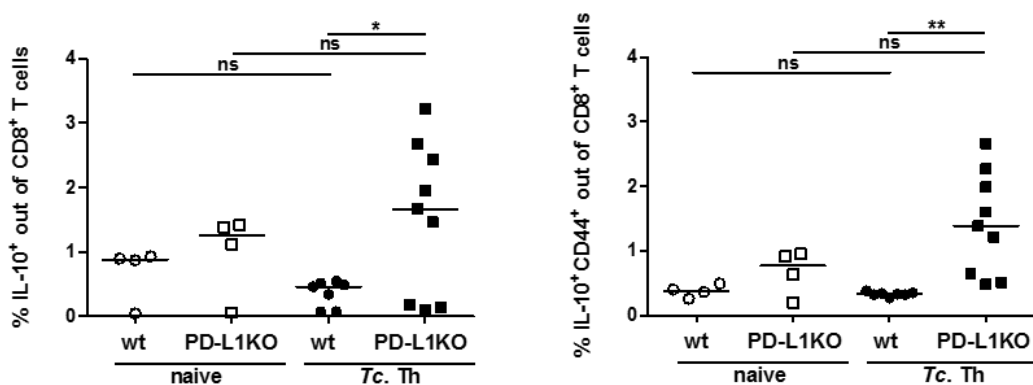


Fig. 16: Effect of PD-L1 deficiency on the expression of IL-10 of cytotoxic T cells at day 24 post-infection. Spleen cells were isolated from infected and naive mice at day 24 post-infection and analyzed by flow cytometry after a 5-hour stimulation with PMA/Ionomycin. Monensin was present throughout the stimulation. Data are a compilation of two independent experiments ($n_{wt\ naive}=4$; $n_{PD-L1KO\ naive}=4$; $n_{wt + Tc. Th}=7$; $n_{PD-L1KO + Tc. Th}=9$).

RESULTS

L1KO naive=4; $n_{wt + Tc. Th} = 7$; $n_{PD-L1KO + Tc. Th} = 9$). Median (indicated by the horizontal line) and individual values are shown. The statistical significance was calculated with the student's t-test (unpaired, two tailed). Asterisks denote P values of <0.05. P<0.05*; P<0.01**; ns (not significant).

4.7. Evaluation of the *ex vivo* cytokine profile upon interruption of PD-1/PD-L1 signaling by a cytometric beads assay

To evaluate the effect of PD-L1 deficiency on the systemic inflammatory response at the beginning of chronic phase of infection, serum samples were collected from infected wt and PD-L1 KO mice at day 24 post-infection and the cytokine profile was evaluated by a cytometric beads assay. Results showed that PD-L1-deficiency did not improve the production of cytokines that promote the proliferation and effector function of immune cells (IL-2, IL-6 and IL-9). On the other hand, a significant decreased of IFN- γ and TNF- α production were observed in infected PD-L1 KO mice in comparison to infected wt mice (Fig. 17).

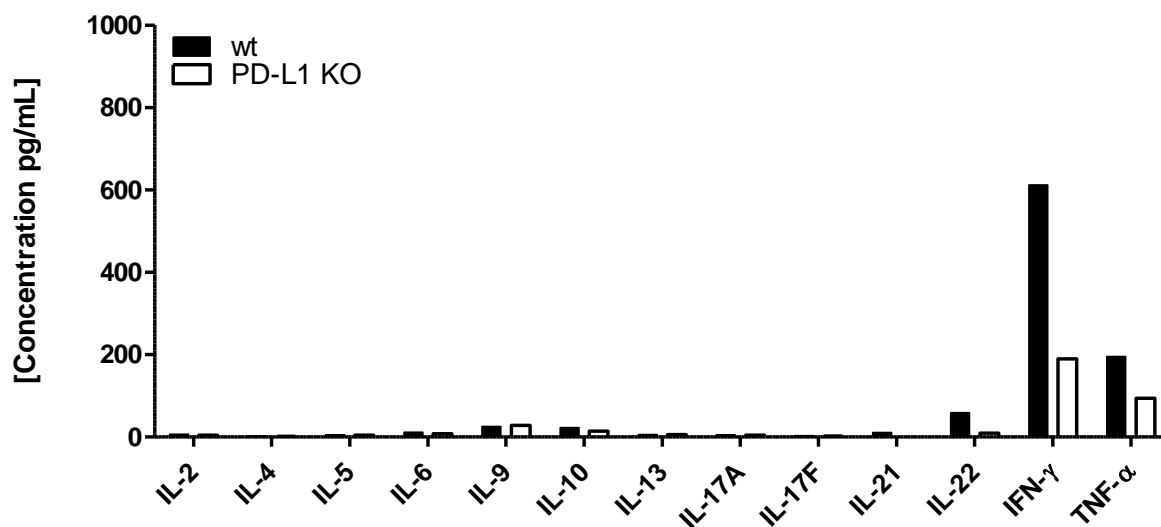


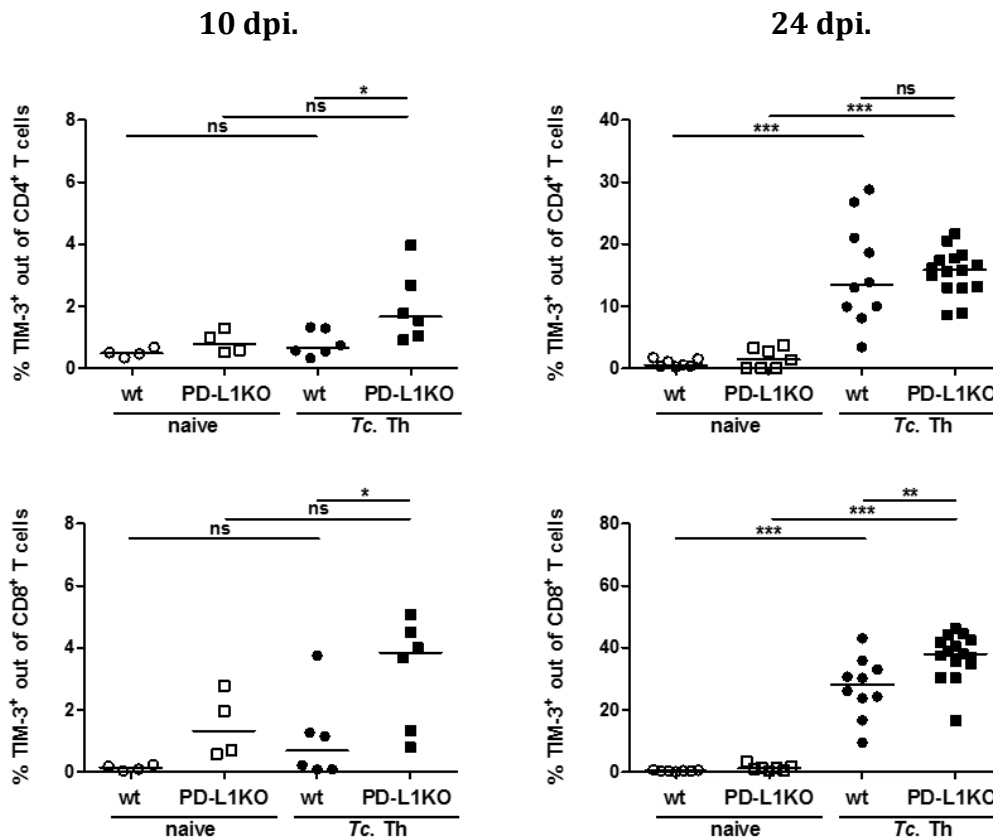
Fig. 17: Serum cytokine levels in infected wt and PD-L1 KO mice at day 24 post-infection. Whole blood samples were collected from infected mice at day 24 post-infection (early chronic phase), sera were isolated and cytokine levels were determined by a cytometric beads assay. Results are expressed as the cytokine concentration (in pictograms/milliliter) of the pooled sera samples ($n_{wt + Tc. Th} = 7$; $n_{PD-L1KO + Tc. Th} = 9$).

4.8. Evaluation of other co-inhibitory receptors upon interruption of PD-1/PD-L1 signaling

RESULTS

Since the PD-L1-efficiency did not enhance T cell activation or improve the effector function of T cells, it might be possible that other inhibitory pathway could be acting in a compensatory way upon interruption of PD1/PD-L1 signaling. The induction of TIM-3 (a co-inhibitory receptor) upon interruption of PD-1/PD-L1 signaling has been described in the context of anti-melanoma therapy. The expression of TIM-3 was evaluated on spleen T cells at day 10 and 24 post-infection in infected wt and PD-L1 KO mice by flow cytometry. Results showed a gradual and significant TIM-3 expression on CD4⁺ and CD8⁺ T cells, which was further increased on CD8⁺ T cells from infected PD-L1 KO mice compared to infected wt mice (Fig. 18a). The expression of other co-inhibitory receptors were evaluated upon infection in PD-L1 KO mice such as LAG-3 and 2B4. Results showed a significant upregulation of 2B4 on CD8⁺ T cells from infected PD-L1 KO mice at day 24 post-infection in comparison to infected wt mice (Fig. 18b).

a)



b)

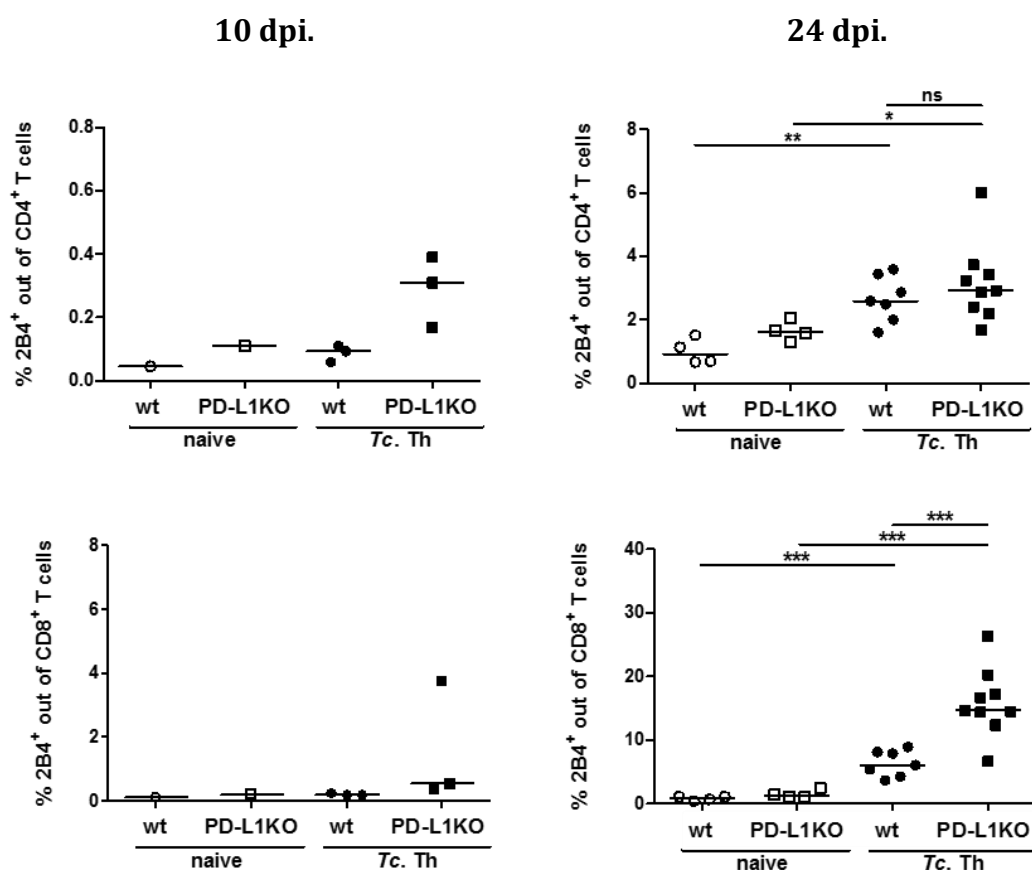


Fig. 18: TIM-3 and 2B4 expression on spleen T cells from wt and PD-L1 KO mice at day 10 and 24 post-infection. Spleen cells were isolated from infected and naive mice at day 10 and 24 post-infection and evaluated by flow cytometry. a) TIM-3 expression on CD4⁺ and CD8⁺ T cells. Data are a compilation of two (day 10) ($n_{wt \text{ naive}}=4$; $n_{PD-L1KO \text{ naive}}=4$; $n_{wt + Tc. Th}=6$; $n_{PD-L1KO + Tc. Th}=6$) and three (day 24) ($n_{wt \text{ naive}}=7$; $n_{PD-L1KO \text{ naive}}=7$; $n_{wt + Tc. Th}=10$; $n_{PD-L1KO + Tc. Th}=15$) independent experiments. b) 2B4 expression on CD4⁺ and CD8⁺ T cells. Data shown are corresponding to one experiment (day 10) ($n_{wt \text{ naive}}=1$; $n_{PD-L1KO \text{ naive}}=1$; $n_{wt + Tc. Th}=3$; $n_{PD-L1KO + Tc. Th}=3$) and a compilation of two independent experiments (day 24) ($n_{wt \text{ naive}}=4$; $n_{PD-L1KO \text{ naive}}=4$; $n_{wt + Tc. Th}=7$; $n_{PD-L1KO + Tc. Th}=9$). Median (indicated by the horizontal line) and individual values are shown. The statistical significance was calculated with the student's t-test (unpaired, two tailed). Asterisks denote P values of <0.05. P<0.05*, P<0.01**, ns (not significant).

4.9. Effect of PD-1 blockade during the *T. cruzi* Th infection *in vivo*

To analyze PD-1 function during the infection *in vivo*, wt mice received a first dose of monoclonal antibody against PD-1 and at the same time with, infection with *T. cruzi* Th strain (day 0) by i.p. puncture. Seven days later, a second dose of antibodies was administrated. Control groups received isotype control antibody following the same scheme (Fig. 19a). Results showed that PD-1 blockade had not a significant impact in the

RESULTS

control of the parasitemia neither improved the resistance to the infection. No significant difference was observed regarding the body weight loss (Fig. 19b).

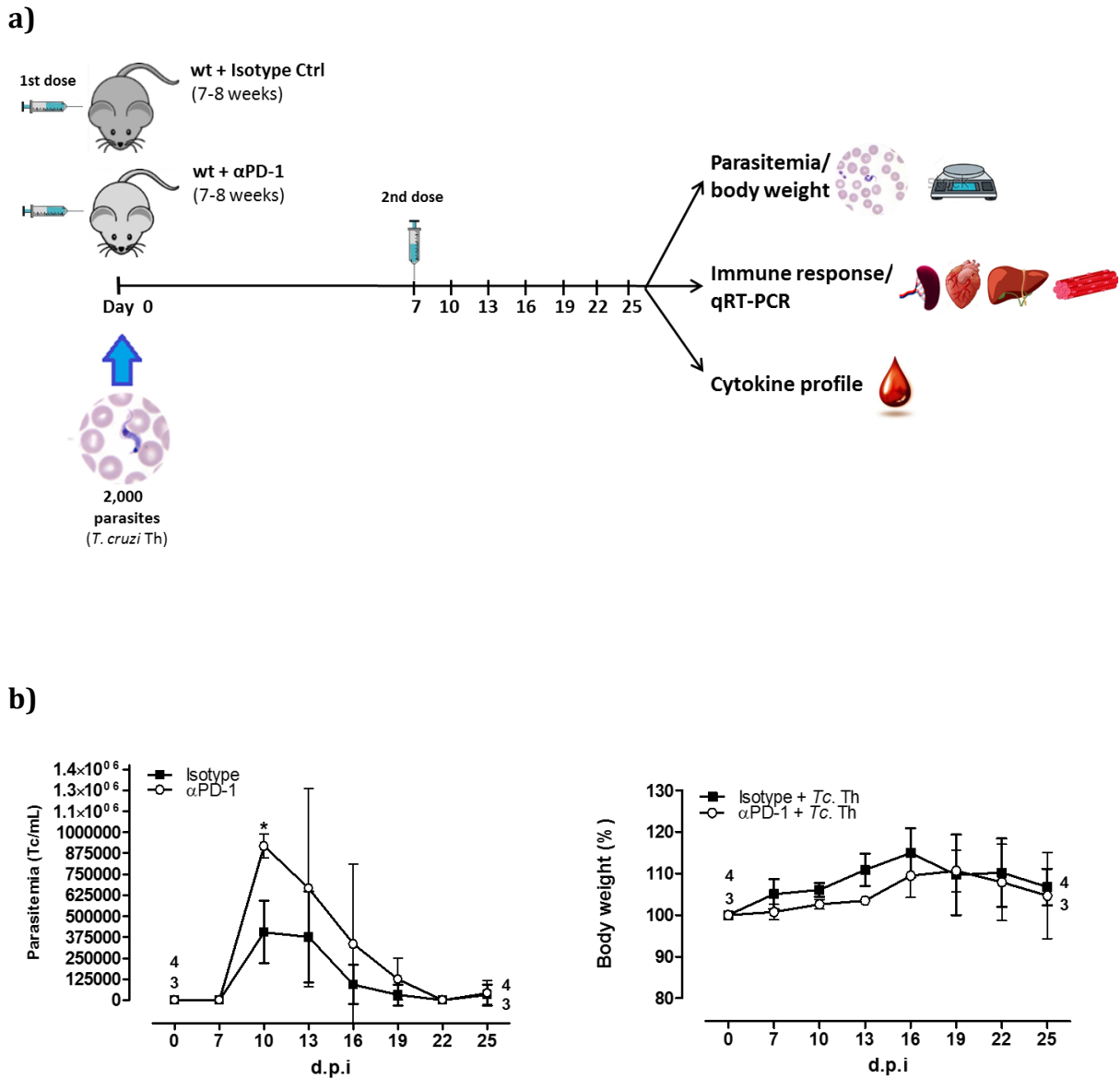
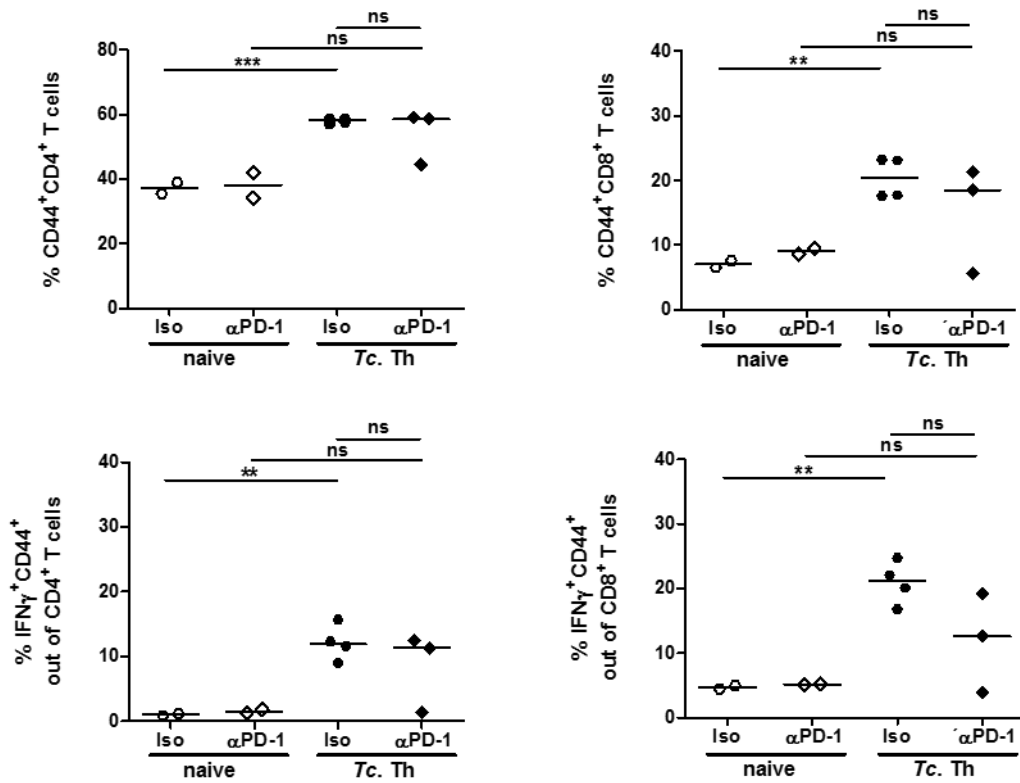


Fig. 19: Effect of PD-1 blockade on parasitemia and body weight during the *T. cruzi* Th infection *in vivo*. Wt mice were infected with 2×10^3 *T. cruzi* Th trypomastigotes (day 0) by i.p. puncture. Mice received two doses (0.2 mg/dose) of monoclonal antibody against PD-1 (day 0 and day 7) and control group, two doses (0.2 mg/dose) of isotype control antibody by i.p. puncture. Parasitemia and body weight were collected in different time points. Spleen, heart, liver, skeletal muscle and sera were collected for subsequent evaluations. a) Scheme of infection and PD-1 blockade strategy. b) Parasitemia and body weight curves during the course of the infection. Data shown are corresponding to one experiment ($n_{wt + \text{Isotype}}=4$; $n_{wt + \alpha\text{PD-1}}=3$). Values are given as means. Error bars indicate standard errors of the means (SEM). Asterisks denote P values of <0.05 by Two-way ANOVA compared to non-infected values. $P<0.05^*$.

RESULTS

T cell responses *in vivo* was evaluated at day 25 post-infection and, results showed that PD-1 blockade did not increase the T cell frequencies or improve their cytokine production in comparison to infected-isotype control mice (Fig. 20). On the other hand, the effector function of cytotoxic CD8⁺ T cells upon PD-1 blockade was also evaluated and the expression of Granzyme B was measure by flow cytometry. Results showed that PD-1 blockade did not induce an increase in the frequency of CD8⁺ T cells expressing Granzyme B (Fig. 21). IL-10 was also evaluated and results showed that IL-10 expression was not upregulated on splenic CD8⁺ T cells from infected wt mice upon PD-1 antibody blockade (Fig. 22).

25 dpi.



RESULTS

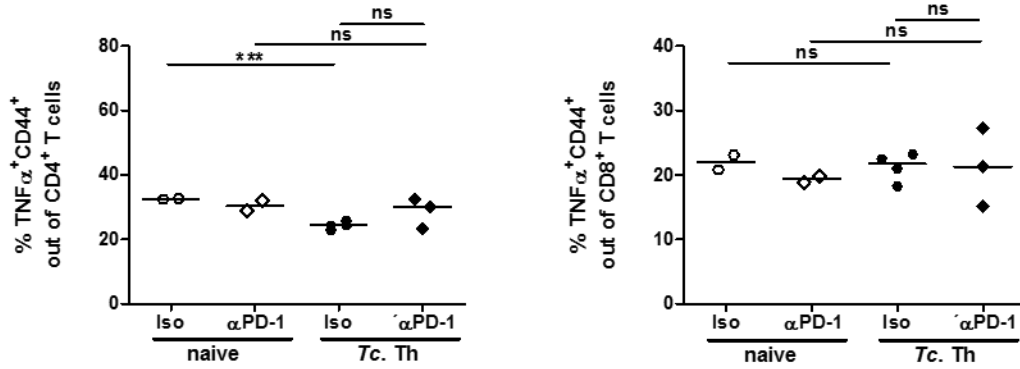


Fig. 20: Effect of PD-1 blockade on the activation and cytokine production of spleen T cells from wt mice infected with *T. cruzi* Th at day 25 post-infection. Spleen cells were isolated from infected and naive wt mice at day 25 post-infection, activation and cytokine expression were analyzed by flow cytometry after a 5-hour stimulation with PMA/Ionomycin. Monensin was present throughout the stimulation. Data shown are corresponding to one experiment ($n_{wt + \text{Isotype naive}}=2$; $n_{wt + \alpha\text{PD-1 naive}}=2$; $n_{wt + \text{Isotype} + \text{Tc. Th}}=4$; $n_{wt + \alpha\text{PD-1} + \text{Tc. Th}}=3$). Median (indicated by the horizontal line) and individual values are shown. The statistical significance was calculated with the student's t-test (unpaired, two tailed). Asterisks denote P values of <0.05. P<0.01**; P<0.001***; ns (not significant).

25 dpi.

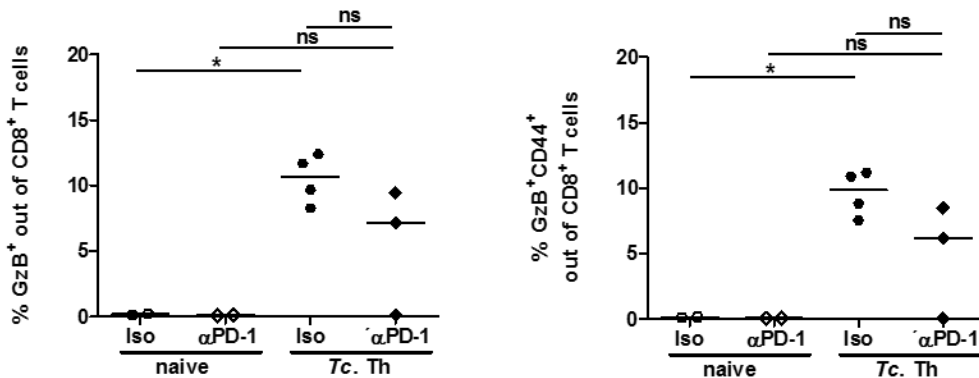


Fig. 21: Effect of PD-1 blockade on the expression of Granzyme B of cytotoxic T cells at day 25 post-infection. Spleen cells were isolated from infected and naive wt mice at day 25 post-infection and analyzed by flow cytometry after a 5-hour stimulation with PMA/Ionomycin. Monensin was present throughout the stimulation. Data shown are corresponding to one experiment ($n_{wt + \text{Isotype naive}}=2$; $n_{wt + \alpha\text{PD-1 naive}}=2$; $n_{wt + \text{Isotype} + \text{Tc. Th}}=4$; $n_{wt + \alpha\text{PD-1} + \text{Tc. Th}}=3$). Median (indicated by the horizontal line) and individual values are shown. The statistical significance was calculated with the student's t-test (unpaired, two tailed). Asterisk denotes P values of <0.05. P<0.05*; ns (not significant).

RESULTS

25 dpi.

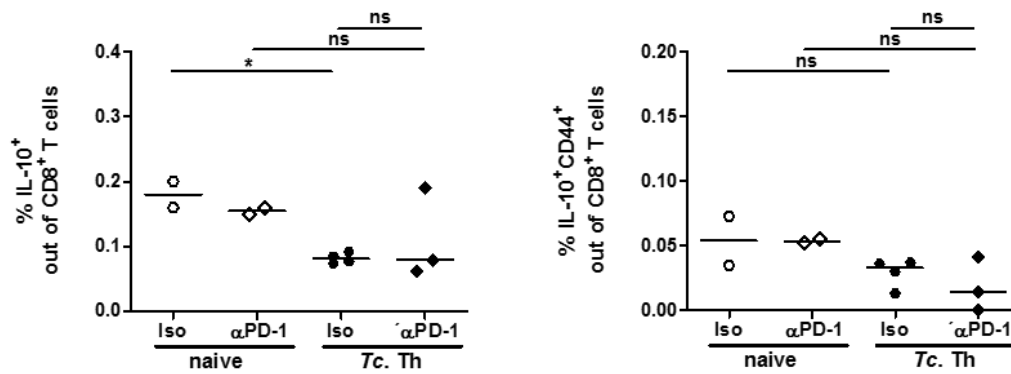


Fig. 22: Effect of PD-1 blockade on the expression of IL-10 of cytotoxic T cells at day 25 post-infection. Spleen cells were isolated from infected and naive wt mice at day 25 post-infection and analyzed by flow cytometry after a 5-hour stimulation with PMA/Ionomycin. Monensin was present throughout the stimulation. Data shown corresponding to one experiment ($n_{wt + \text{Isotype naive}}=2$; $n_{wt + \alpha PD-1 \text{ naive}}=2$; $n_{wt + \text{Isotype} + Tc. Th}=4$; $n_{wt + \alpha PD-1 + Tc. Th}=3$). Median (indicated by the horizontal line) and individual values are shown. The statistical significance was calculated with the student's t-test (unpaired, two tailed). Asterisk denotes P values of <0.05 . $P < 0.05^*$; ns (not significant).

4.10. Evaluation of the *ex vivo* cytokine profile upon PD-1 blockade by a cytometric beads assay

To evaluate the effect of PD-1 blockade on the systemic inflammatory response at the beginning of chronic phase of infection, serum samples were collected from infected PD-1 blockade mice and infected-isotype control mice at day 25 post-infection and the cytokine profile was evaluated by a cytometric beads assay. Results showed that PD-1 blockade did not improve the production of cytokines that promote the proliferation and effector function of immune cells (IL-2, IL-6 and IL-9). On the other hand, the concentration of IFN- γ and TNF- α in the serum samples of infected PD-1 blockade mice were significantly lower than those in infected-isotype control mice (Fig. 23).

RESULTS

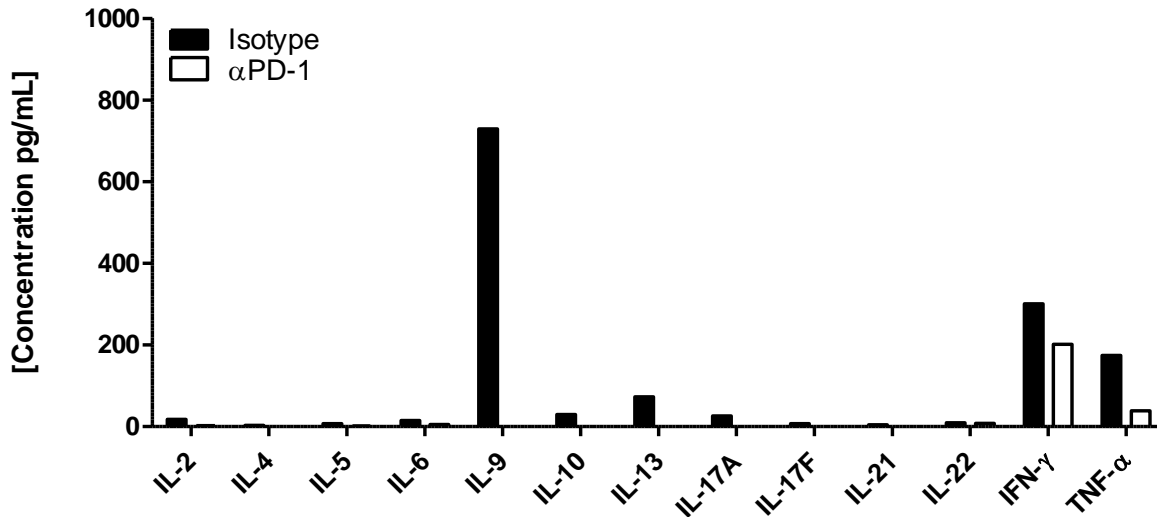


Fig. 23: Serum cytokine levels in wt mice at day 25 post-infection upon PD-1 blockade. Whole blood samples were collected from infected wt mice at day 25 post-infection (early chronic phase), sera were isolated and cytokine levels were determined by cytometric bead assay. Results are expressed as the cytokine concentration (in pictograms/milliliter) of the pooled sera samples ($n_{wt + \text{Isotype} + Tc. Th}=4$; $n_{wt + \alpha PD-1 + Tc. Th}=3$).

TIM-3 expression was also evaluated in the context of PD-1 blockade. Surprisingly, PD-1 blockade did not induce the upregulation of TIM-3 in both T cell subsets from infected wt mice (Fig. 24).

25 dpi.

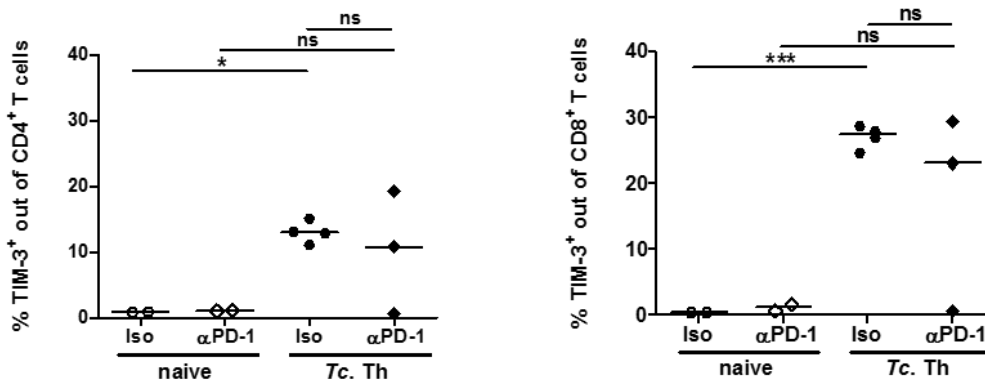
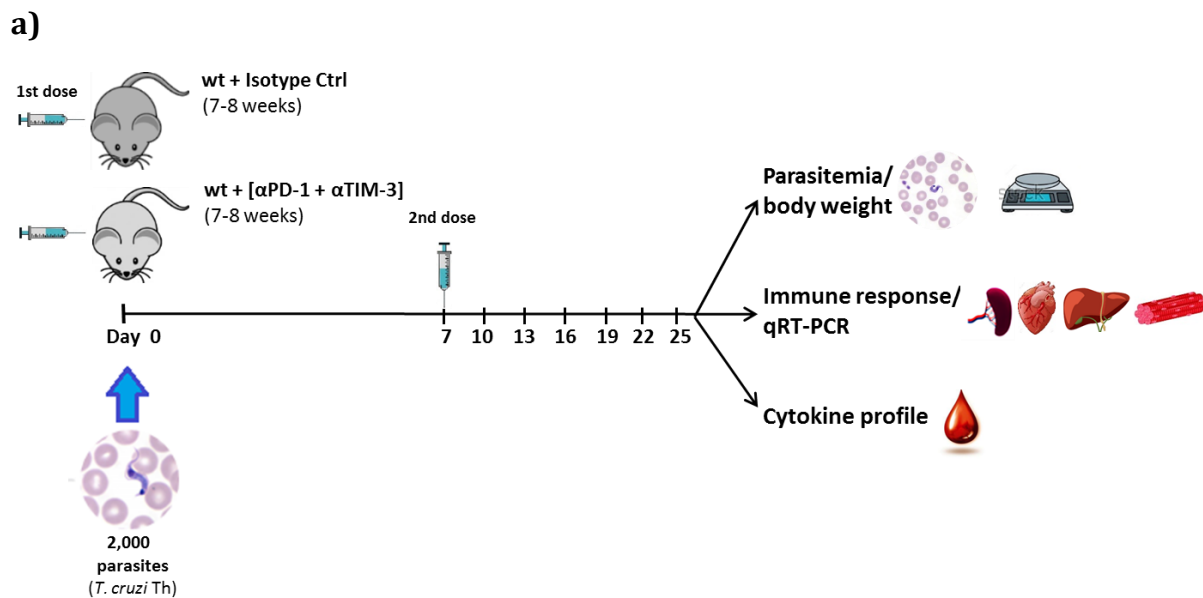


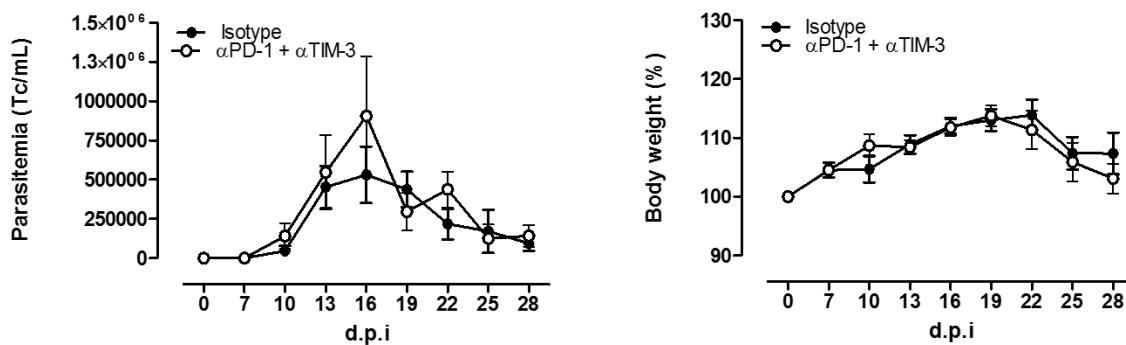
Fig. 24: TIM-3 expression on spleen T cells from wt mice at day 25 post-infection upon PD-1 blockade. Spleen cells were isolated from infected and naive wt mice at day 25 post-infection and TIM-3 expression was evaluated by flow cytometry. Data shown are corresponding to one experiment ($n_{wt + \text{Isotype naive}}=2$; $n_{wt + \alpha PD-1 naive}=2$; $n_{wt + \text{Isotype} + Tc. Th}=4$; $n_{wt + \alpha PD-1 + Tc. Th}=3$). Median (indicated by the horizontal line) and individual values are shown. The statistical significance was calculated with the student's t-test (unpaired, two tailed). Asterisks denote P values of <0.05 . $P<0.05^*$; $P<0.001^{***}$; ns (not significant).

4.11. Effect of combined blockade of PD-1 and TIM-3 by monoclonal antibodies during the *T. cruzi* Th infection *in vivo*

Based on the upregulation of PD-1 and TIM-3 on T cells observed in infected wt and PD-L1 KO mice respectively, a combined blockade of PD-1 and TIM-3 was developed to analyze the potential compensatory mechanism between these pathways during the infection. Wt mice were treated with monoclonal antibodies against PD-1 and TIM-3 following the same scheme as for the PD-1 blockade assay (Fig. 25a). Results showed that combined blockade of PD-1 and TIM-3 had not a significant impact in the control of the parasitemia neither improved the resistance to the infection. No significant difference was observed regarding the body weight loss (Fig. 25b).



b)

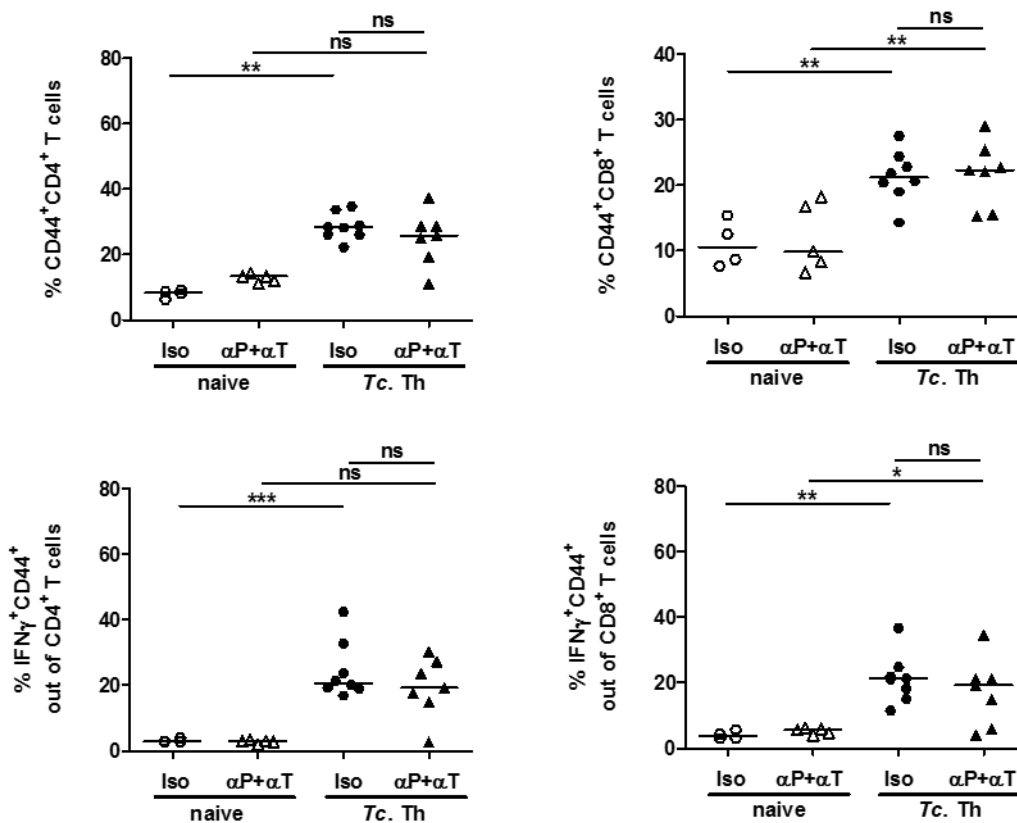


RESULTS

Fig. 25: Effect of combined blockade of PD-1 and TIM-3 by antibodies on parasitemia and body weight during the *T. cruzi* Th infection *in vivo*. Wt mice were infected with 2×10^3 *T. cruzi* Th trypomastigotes (day 0) by i.p. puncture. Mice received two doses (0.2 mg PD-1+0.2 mg TIM-3/dose) of monoclonal antibodies against PD-1 and TIM-3 (day 0 and day 7) and control group, two doses of isotype (0.2 mg/dose) control antibody by i.p. puncture. Parasitemia and body weight were collected in different time points. Spleen, heart, liver, skeletal muscle and sera were collected for subsequent evaluations. a) Scheme of infection and combined PD-1+TIM-3 blockade strategy. b) Parasitemia and body weight curves during the course of the infection. Data are a compilation of two independent experiments ($n_{wt + Iso + Tc. Th} = 8$; $n_{wt + [\alpha PD-1 + \alpha TIM-3] + Tc. Th} = 8$). Values are given as means. Error bars indicate standard errors of the means (SEM). The statistical significance was calculated with Two-way ANOVA.

T cell responses *in vivo* were evaluated at day 28. Results showed that combined blockade of PD-1 and TIM-3 did not increase the frequencies of T cells neither improved the inflammatory cytokine expression in these cells (Fig. 26).

28 dpi.



RESULTS

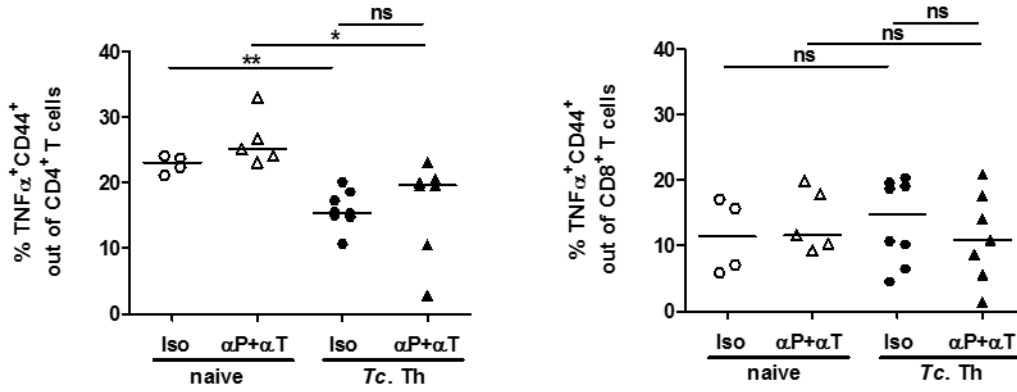


Fig. 26: Effect of combined blockade of PD-1 and TIM-3 on the activation and cytokine production of spleen T cells from wt mice infected with *T. cruzi* Th at day 28 post-infection. Spleen cells were isolated from infected and naive wt mice at day 28 post-infection, activation and cytokine expression were analyzed by flow cytometry after a 5-hour stimulation with PMA/Ionomycin. Monensin was present throughout the stimulation. Data are a compilation of two independent experiments ($n_{wt + \text{Isotype naive}}=4$; $n_{wt + [\alpha\text{PD-1} + \alpha\text{TIM-3}] \text{ naive}}=5$; $n_{wt + \text{Isotype} + \text{Tc. Th}}=8$; $n_{wt + [\alpha\text{PD-1} + \alpha\text{TIM-3}] + \text{Tc. Th}}=7$). Median (indicated by the horizontal line) and individual values are shown. The statistical significance was calculated with the student's t-test (unpaired, two tailed). Asterisks denote P values of <0.05. P<0.05*; P<0.01**; P<0.001***; ns (not significant).

The effector function of cytotoxic CD8⁺ T cells upon combined blockade of PD-1 and TIM-3 was evaluated and the Granzyme B and IL-10 expression were measured by flow cytometry. Results showed that combined blockade did not induce an increase in the frequency of CD8⁺ T cells expressing Granzyme B (Fig. 27) neither induced the IL-10 expression on infected wt mice (Fig. 28).

28 dpi.

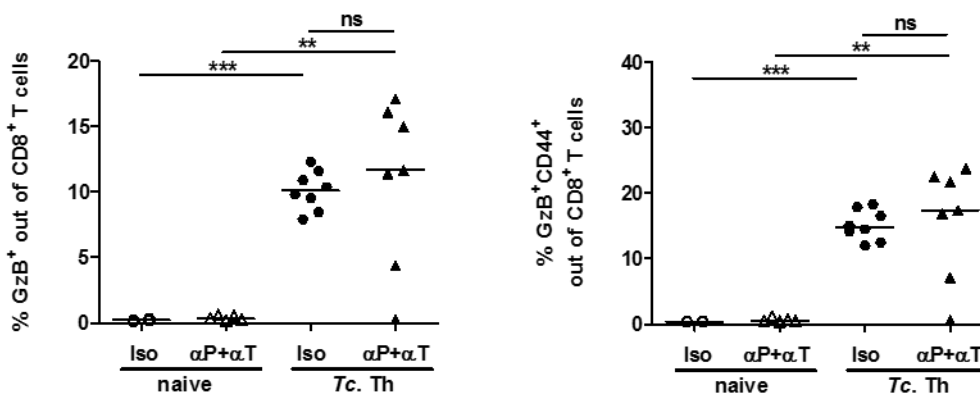


Fig. 27: Effect of combined blockade of PD-1 and TIM-3 on the expression of Granzyme B of cytotoxic T cells at day 28 post-infection. Spleen cells were isolated from infected and naive wt mice at day 28 post-infection and analyzed by flow cytometry after a 5-hour stimulation with PMA/Ionomycin. Monensin was present throughout the stimulation. Data are a compilation of two

RESULTS

independent experiments ($n_{wt + \text{Isotype naive}}=4$; $n_{wt + [\alpha\text{PD-1} + \alpha\text{TIM-3}] \text{ naive}}=5$; $n_{wt + \text{Isotype} + Tc. Th}=8$; $n_{wt + [\alpha\text{PD-1} + \alpha\text{TIM-3}] + Tc. Th}=7$). Median (indicated by the horizontal line) and individual values are shown. The statistical significance was calculated with the student's t-test (unpaired, two tailed). Asterisks denote P values of <0.05 . $P<0.01^{**}$; $P<0.001^{***}$; ns (not significant).

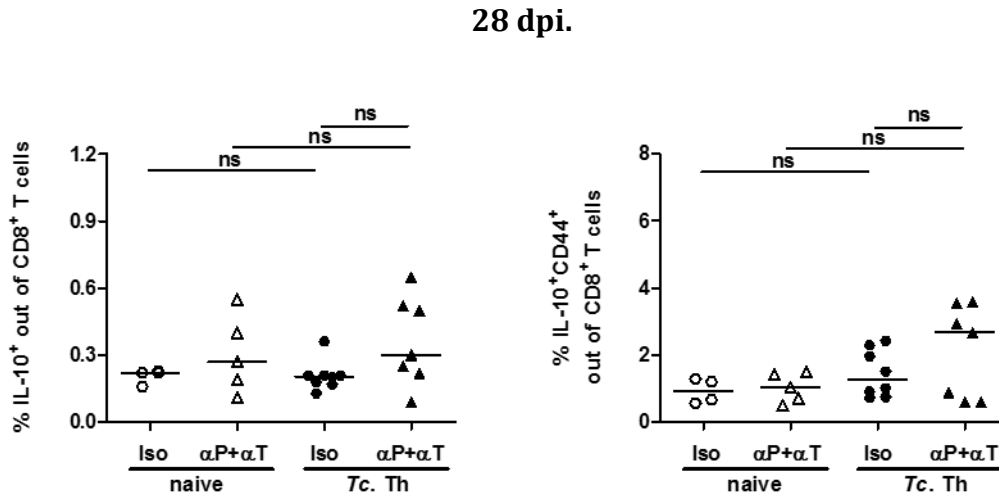


Fig. 28: Effect of combined blockade of PD-1 and TIM-3 on the expression of IL-10 of cytotoxic T cells at day 28 post-infection. Spleen cells were isolated from infected and naive wt mice at day 28 post-infection and analyzed by flow cytometry after a 5-hour stimulation with PMA/Ionomycin. Monensin was present throughout the stimulation. Data are a compilation of two independent experiments ($n_{wt + \text{Isotype naive}}=4$; $n_{wt + [\alpha\text{PD-1} + \alpha\text{TIM-3}] \text{ naive}}=5$; $n_{wt + \text{Isotype} + Tc. Th}=8$; $n_{wt + [\alpha\text{PD-1} + \alpha\text{TIM-3}] + Tc. Th}=7$). Median (indicated by the horizontal line) and individual values are shown. The statistical significance was calculated with the student's t-test (unpaired, two tailed). ns (not significant).

4.12. Evaluation of the *ex vivo* cytokine profile upon combined blockade of PD-1 and TIM-3 by a cytometric beads assay

To evaluate the effect of combined blockade of PD-1 and TIM-3 on the systemic inflammatory response at the early chronic phase of the infection, serum samples were collected from infected combined blockade mice and infected-isotype control mice at 28 dpi and cytokine profile was evaluated by a cytometric beads assay. Results showed under combined blockade of PD-1 and TIM-3, a trend to increase of cytokine levels in sera in comparison to infected-isotype control mice. Moreover, a notable increase of IFN- γ and TNF- α (compared to TNF- α levels registered upon PD-1 blockade) production were observed in mice treated with combined blockade compared to infected-isotype control mice (Fig. 29).

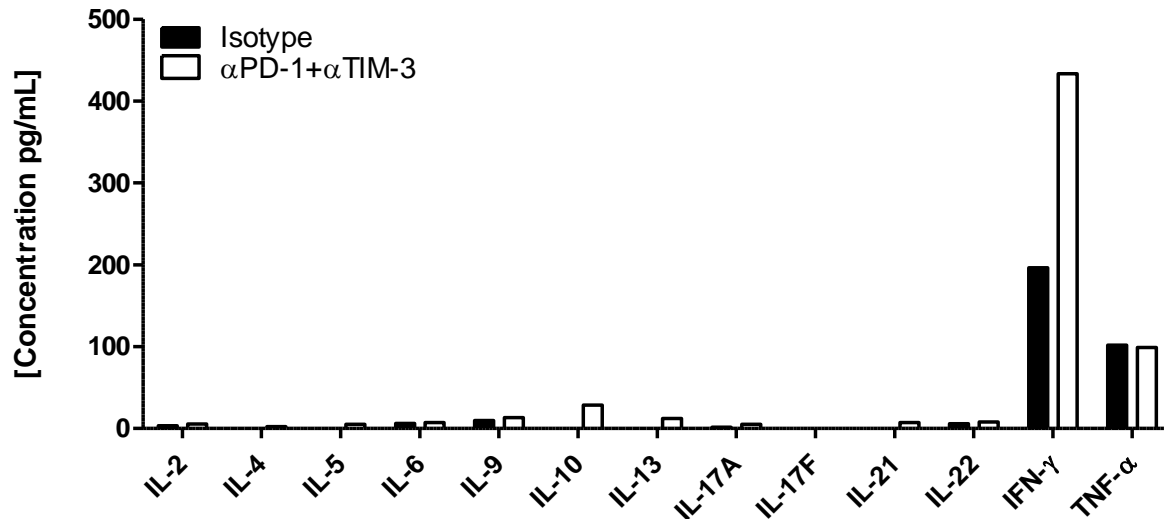


Fig. 29: Serum cytokine levels of wt mice at 28 days post-infection upon combined blockade of PD-1 and TIM-3. Whole blood samples were collected from infected wt mice at day 28 post-infection (early chronic phase), sera were isolated and cytokine levels were determined by cytometric bead assay. Results are expressed as the cytokine concentration (in pictograms/milliliter) of the pooled sera samples ($n_{wt + \text{Isotype} + Tc. Th=8}$; $n_{wt + [\alpha PD-1 + \alpha TIM-3] + Tc. Th=7}$).

4.13. Evaluation of interruption of PD-1/PD-L1 signaling on the parasite load analyzed by qRT-PCR

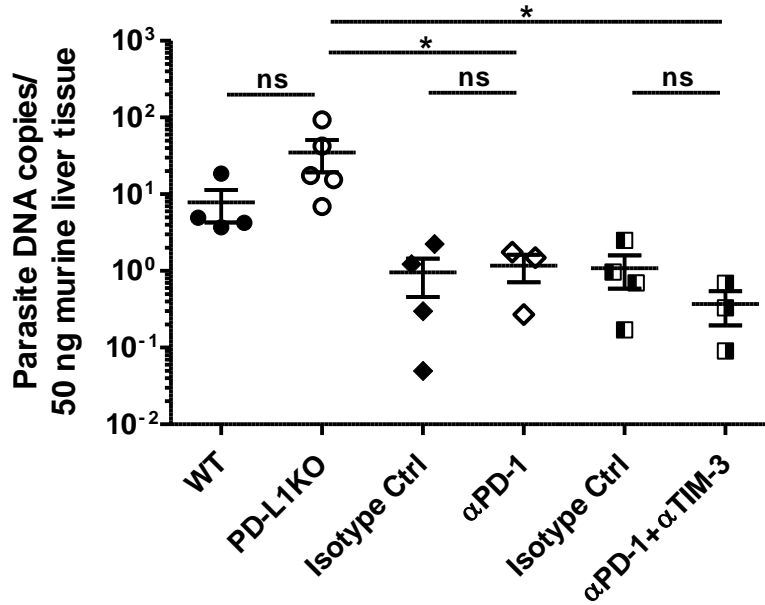
To evaluate the effect of the interruption of PD-1/PD-L1 signaling on the parasite load during the *T. cruzi* Th infection, tissues samples from spleen, liver, heart, and skeletal muscle corresponding to the infected PD-L1 KO, wt and, wt mice treated with antibodies against PD-1 and PD-1 plus TIM-3 and their respective isotype control were isolated and the parasite load was evaluated by qRT-PCR.

Liver samples were selected due to the fact that *T. cruzi* Tulahuen is a reticulotropic strain with a markedly leaning to invade spleen, liver and bone marrow cells (38, 39). Results showed no significant differences in the parasite load between the infected mice where PD-1/PD-L pathway was interrupted and their corresponding controls. Interestingly, the parasite load exhibits a trend to be higher upon PD-L1 deficiency in comparison to those observed upon blockade with antibodies (Fig. 30a). It is worth noting a slight reduction in the parasite load in the mice treated with the combined blockade of PD-1 and TIM-3 compared to isotype control group.

Finally, no significant differences in the parasite load from relevant tissues, were observed between infected mice that received combined blockade of PD-1 and TIM-3

and their respective isotype controls. However, a trend to increase of parasite load was observed in skeletal muscle in comparison to other tissues evaluated (Fig. 30b).

a)



b)

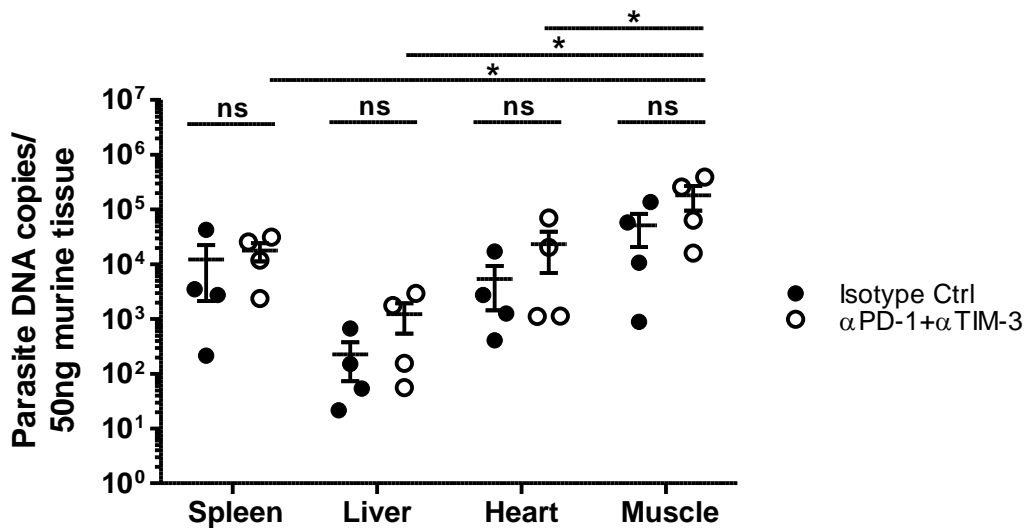


Fig. 30: Effect of interruption of PD-1/PD-L1 signaling on parasite load analyzed by qRT PCR. Tissues samples from spleen, liver, heart and skeletal muscle were collected from infected PD-L1 KO, wt and, wt mice treated with antibodies blocking (PD-1 and PD-1+TIM-3) and their respective isotype controls. *T. cruzi*-specific qRT-PCR was performed, and parasite load was calculated from a standard curve. a) Parasite load in liver samples and b) Comparative parasite load in different tissue samples after interruption of PD-1/PD-L1 signaling. Error bars indicate standard errors of the means

RESULTS

(SEM). Asterisk denotes P values of <0.05 by One-way ANOVA compared to isotype control values. P<0.05*; ns (not significant).

5. Discussion

Modulation of PD-1/PD-L pathway has been described as an escape mechanism from the immune response that several pathogens employ to establish a chronic infection. The activation of this co-inhibitory pathway inhibits T cell activation, proliferation and cytokine production (9, 40). The blockade of this pathway by antibodies or by gene deletion represents a promising alternative to improve the effector function or reverse the dysfunction on immune cells with the consequent of parasite burden decrease in different infectious disease models (9).

5.1. *T. cruzi* Tulahuen strain infection induces expression of PD-L1 on BM-DCs

To test the hypothesis that this inhibitory pathway plays a role in the resistance to the *T. cruzi* Th infection, the first step was determine if *T. cruzi* Tulahuen (*T. cruzi* Th) strain is able to modulate the expression of the PD-1 ligand, PD-L1, on immune cells. Although the PD-L1 constitutive expression has been described for dendritic cells (9, 12, 16), the co-incubation of *T. cruzi* Th trypomastigotes with BM-DCs *in vitro* showed that only infected BM-DCs exhibit an increase expression of PD-L1 in comparison to non-infected BM-DCs. This result suggests that *T. cruzi* Th infection might influence PD-L1 expression. However, it has been demonstrated that PD-L1 expression can be induced by inflammatory cytokines (e.g., IFN- α) (37, 41). Whether the cytokines produced by infected BM-DCs influence the increased PD-L1 expression might be contrasted for the absent of an increase of PD-L1 expression observed on non-infected cells in the same culture. To confirm this hypothesis, it would be necessary to infect BM-DCs knockout for these cytokines.

5.2. Mouse model of *T. cruzi* Tulahuen experimental infection

To evaluate *in vivo* the role of PD-1/PD-L pathway during the *T. cruzi* Th infection, a mouse model of *T. cruzi* Th infection was established. Mouse models are the most widely used animal models in Chagas disease research (42). C57BL/6J mice is a strain susceptible to the

T. cruzi infection (43) however, the mean survival time varies according to the parasite strain used (42). On the other hand, *T. cruzi* Tulahuen is considered a virulent strain with a relative quickly develop of acute phase followed with a high mortality that depends on the mice strain evaluated (39). Therefore, variable outcomes depending on the mouse and parasite strains used (42).

In this study, the infection of C57BL/6J female mice with 2000 *T. cruzi* Th trypomastigotes allowed to evaluate the role of PD-1/PD-L pathway on T cells responses during a period of time compromising the acute phase and the beginning of the chronic phase. The final dose of infection was established in basis to previous observations where higher dose resulted lethal in a short period of time (between 7-10 days post-infection). Parasitemia in peripheral blood was the main parameter to define the infection phases as described in other studies (38, 39) whilst female mice were used based on their less susceptibility to the infection in comparison to male mice (44). For the experimental *T. cruzi* Th infection, the intraperitoneal route was chosen, because it is the most commonly parasite inoculation route used, easy and generally successful (42). It is worth noting that this model in comparison to similar described for *T. cruzi* Th infection did not exhibited a high mortality after the resolution of the infection. The significant reduction of the body weight registered at the beginning of the chronic phase might suggest the onset of physical deterioration previous to the death. Because the aim of this study was evaluate whether PD-1/ PD-L pathway plays an important role in the resistance to the infection, the progress of the infection was studied until the day 28.

5.3. *T. cruzi* Th infection modulates the PD-1, PD-L1 and PD-L2 expression on immune cells *in vivo*

The *T. cruzi* Th infection lead to a gradual increase of PD-1 expression on immune cells. The main induction was observed on T cells and surprisingly, PD-1 expression was significant upregulated on CD4⁺ T cells whereas CD8⁺ T cells displayed a trend, but not a significant increase of PD-1 expression during the progress of the infection. Opposite to the common perception, PD-1 can also be expressed under normal physiologic conditions and can be detected on normal spleen T cells at low levels, by is strongly induced on these cells after stimulation (19). The upregulation of PD-1 on CD4⁺ T cells might be associated with an immunoregulatory mechanism activated during the infection to avoid the tissue damage cause by the exacerbated inflammatory response

mediated for these cells (45). This argument is supported by the knowledge of a cytokine milieu consisting of proinflammatory mediators augment the activation of this inhibitory pathway (46). In addition, the main trigger of PD-1 induction, the TCR engagement with the epitope-loaded MHC molecule on infected cells (46), is enhanced by the presence of the parasite (19).

The increased expression of PD-1 on T cells suggests an inhibition of their effector functions during acute phase, which might be associated with the increase parasite proliferation observed in this period of time. However, the downregulation of PD-1 expression after day16 post-infection might be associate with the control of parasite proliferation and, in consequence, the reduction of antigen concentration that is pivotal for a sustained PD-1 expression (19).

Significant PD-1 upregulation also has been observed on NK1.1⁺CD3⁺T cells (natural killer T cells; NKT cells) at the beginning of chronic phase. These cells as well as NK cells have been implicated in the control of infections and chronic inflammatory diseases (47). In the context of *T. cruzi* infection, a frequency of circulating NKT cells has been reported in late indeterminate clinical form of Chagas disease and their role might be the control of deleterious cytotoxic activity mediated by CD8⁺ T cells (48). The upregulation of PD-1 on NKT cells in this model, is in agreement with the results showed in a previous study on spleen cells where demonstrated that *T. cruzi* is able to modulate the PD-1 expression levels (32). Moreover, it has been shown that PD-1/PD-L interaction is involved in the induction and maintenance of NKT cell anergy (49) and upregulation of PD-1 might be associated with a NKT cell dysfunction during *T. cruzi* Th infection as well as been demonstrated in *Mycobacterium tuberculosis* infection (32, 49).

As it was expected, *T. cruzi* Th also modulated the ligands expression on immune cells *in vivo*. PD-L1 expression was upregulated on B, monocytes/macrophages and DCs. PD-L2 expression was upregulated on monocytes/macrophages cells and a trend towards an increase on DCs was observed. These results confirm the findings reported during the infection by *T. cruzi* Th and Y strain *in vivo* and *in vitro* (32, 35) suggesting a role of PD-1/PD-L pathway in the progress of the infection and focusing this study on its effects on T cells.

5.4. PD-1 expression might not be associated with exhausted T cell function during *T. cruzi* Th infection

Unexpected were the results obtained after the evaluation of effector functions of T cells during *T. cruzi* Th infection. Despite PD-1 upregulation observed on T cells, the expression of IFN- γ and TNF- α was not affected. These results might be explain by the existence of different levels of PD-1 expression on T cells affecting their effector functions in different intensities suggesting that PD-1, by itself, is an imperfect marker of exhaustion (46, 50) and inclusive, it might be considered an activation marker (41, 51). Recently studies demonstrated during acute viral infection, PD-1 upregulation on cytotoxic CD8⁺ T cells, do not directly affect the cytokine production (51) suggesting that the expression of the ligands for PD-1 might critically contribute to the functional involvement of PD-1 signaling in the development of viral chronicity (52). In the context of *T. cruzi* infection, PD-1 expression has been associated with the “exhausted status” of T cells exhibited during the acute myocarditis and chronic infection (32). The results observed in this study, suggest that PD-1 expression on T cells during *T. cruzi* Th infection might not be associated with an “exhausted status”, at least not in the period of time evaluated.

5.5. PD-L1 deficiency does not improve the resistance to the infection neither T cell effector functions but increases IL-10 expression by CTL at the early chronic phase

Based on the increased evidence that PD-1/PD-L1 pathway mediated T cell exhaustion in chronic infections by parasites and *in vivo* blockade of PD-L1 increase T cell effector functions, PD-L1-deficient mice (PD-L1 KO) were infected with *T. cruzi* Th and the effect of this deficiency was evaluated.

The results showed that PD-L1 deficiency had a significant impact in the resistance to *T. cruzi* Th infection that was markedly evident during the progress of the infection. The increased parasitemia exhibited in these mice in comparison to wild type suggests that this pathway, may be not complete, but partially, is involved in the resistance to the infection. On the other hand, the PD-L2 expression observed on monocytes/macrophages during the infection does not discard the possibility of a compensatory role by this ligand. The role of PD-L2 is ambiguous. In some infectious models, PD-L2 has an inhibitory effect on T cells by PD-1 ligation (9, 16) and in others, it exhibits a stimulatory effect (9, 52, 53). The results observed in this study, suggest that PD-L2 might be function as an inhibitory ligand favoring the T cell dysfunction and, in

consequence, the parasite proliferation. However, its reduced and restricted expression would make it unable to compensate the PD-L1 absence during the infection.

Interestingly, PD-L1 deficiency did not increase activation neither improve the functional capacity of T cells during the infection by *T. cruzi* Th. No differences were observed in the activation, cytokine expression neither improvement of the effector function of cytotoxic CD8⁺ T upon PD-L1 deficiency. These results suggest that regulation of cytokine production by T cells and cytotoxicity during *T. cruzi* Th infection in the context of PD-L1 deficiency might be induced by mechanisms other than PD-1/PD-L pathway. This argument might be supported by the upregulation of other inhibitory receptors such as TIM-3 and 2B4 observed on T cells, CD8⁺ T cells mainly, in infected PD-L1-deficient mice.

Surprisingly, in absent of PD-L1, IL-10 expression was significant upregulated on CD8⁺ T cells. Previous studies showed that during the infection by intracellular parasites, *T. cruzi* included, IL-10 acts by down-regulating T-cell responses favoring parasite persistence (28, 54, 55). This result suggests relationship between both pathways, and is supported by reports where PD-L1 neutralization promotes the induction of IL-10 (56). However, studies in chronic LCMV infection and *Toxoplasma* showed that PD-L1 and IL-10 are independent and act in parallel to regulate the immune response preventing immune mediated-tissue damage (57). On the other hand, a recent study in *Toxoplasma* infection revealed that the absence of PD-1 signaling promotes an increase in IL-10 production by CD4⁺ and CD8⁺ T cells, which increases susceptibility to opportunistic infection (58). Therefore, in the context of *T. cruzi* Th infection, the possibility that both pathways could synergistically act cannot be discarded.

The broad pattern of PD-L1 expression, points out the important role of this regulatory pathway in peripheral immune tolerance (16, 37, 59). The increased parasitemia and reduced physical deterioration exhibited by infected PD-L1-deficient mice in comparison to wild type mice, suggested markedly different cytokine responses between both groups. The measure of cytokine profile in serum showed a notably decrease of IFN- γ and TNF- α in infected PD-L1-deficient mice compared to wild type, which could explain the increased parasitemia and reduced physical deterioration observed in these mice. However, the limited induction of cytokines that promote the proliferation and effector function of immune cells upon interruption of PD-1/PD-L1

signaling, as showed as reported in other infectious disease models (46, 60, 61), suggests that other regulatory mechanisms might be acting behind.

Finally, the possibility of a positive or negative stimulation conducted by CD80, the other receptor for PD-L1 on T cells, upon ligation with CD28 or CTLA-4 respectively, was discarded due to the absence of upregulation of this molecule during the *T. cruzi* Th infection (data no shown).

5.6. Blockade of PD-1 by monoclonal antibodies does not improve the resistance to the infection neither T cell effector functions in the course of *T. cruzi* Th infection *in vivo*

The infection of PD-L1 deficient mice allowed to evaluate the interaction of this ligand with PD-1 receptor on T cells and its effect during the course of the infection. To evaluate the other potential interaction, PD-1/PD-L2 and its effects during the infection, wt mice infected with *T. cruzi* Th were treated with anti-PD-1 monoclonal antibodies.

Similar to the infection of PD-L1-deficient mice, PD-1 blockade did not improve the resistance to the infection, activation neither functional capacity of T cells during the infection by *T. cruzi* Th in comparison to infected-isotype control mice. Additionally, PD-1 blockade did not increase cytokine levels in sera in comparison to the infected- isotype control mice. The possibility that during PD-1 blockade, PD-L1 binds to B7.1 molecules which also inhibits T cell proliferation and cytokine regulation upon ligation (61), might explain the observation made in mice receiving the blockade however, the results obtained, similar to those reported in infected PD-L1-deficient mice, discard this argument.

On the other hand, PD-1 blockade inhibits also a possible interaction of this receptor with its other ligand, PD-L2. Again, the results obtained, similar to those reported in infected PD-L1-deficient mice, further support the limited role of this ligand during the course of infection.

Surprisingly, PD-1 blockade did not induce the upregulation of IL-10 on CD8⁺ T cells as observed in infected PD-L1-deficient mice. This result could be explained by the antibody administration. The doses and frequency of administration may not be sufficient to block PD-1/PD-L1 interactions during the infection and in consequence, the complete inhibition of PD-1 signaling could not be reached. The first dose was

administrated at the beginning of the infection (day 0) and was bolstered with a second dose at the 7 days post-infection. There is the possibility that during the period of time between the second dose and sacrifice day (18 days after), the effect of the antibodies had decrease.

In the context of cancer therapy, blockade of PD-1/PD-L1 pathway with anti-PD-1 monoclonal antibodies, has shown to be efficacious in a number of cancer types, including melanoma, renal cell carcinoma, bladder cancer, hematologic malignancies and non-small cell lung cancer (NSCLC). However, the majority of patients still fail to benefit from this treatment, identifying the upregulation of TIM-3 with adaptive resistance to PD-1 blockade (18, 62, 63). This observation in addition to the upregulation of TIM-3 on CD8⁺ T cells from infected PD-L1-deficient mice, suggest that upon *T. cruzi* Th infection, a compensatory signaling through TIM-3/Gal 9 pathway might be sustain the dysfunction of T cells in response to PD-1 blockade. Therefore, the absence of upregulation of TIM-3 upon PD-1 blockade, could be explained by the mode of antibody administration confirming the observations reported during the therapeutic PD-1 blockade in cancer: TIM-3 positivity is significantly correlated with the duration of PD-1 blocking treatment (62).

5.7. Combined blockade of PD-1 and TIM-3 does not improve the resistance to the infection neither T cell effector functions in the course of *T. cruzi* Th infection *in vivo*

Due to the upregulation of PD-1 during the course of *T. cruzi* Th infection and the upregulation of TIM-3 upon PD-L1 deficiency, a combined blockade of PD-1 and TIM-3 pathways using monoclonal antibodies was evaluated in infected wt mice with *T. cruzi* Th.

Results showed that combined blockade of PD-1 and TIM-3, did not improve the resistance to the infection, activation neither the functional capacity of T cells during the infection by *T. cruzi* Th in comparison to infected-isotype control mice. However, the combined blockade in infected mice displayed a trend, but not a significant increase of Granzyme B and IL-10 suggesting a partial improvement in the T cell responses. Moreover, a trend to an increase of cytokines levels in sera from infected combined blockade mice, suggests a partial improvement of cytokine production at systemic level. These results could be supported by previous studies in cancer and chronic viral

infections where the combined targeting of the PD-1 and TIM-3 signaling pathways was highly effective in restoring anti-tumor or anti-virus immunity in comparison to individual treatment (63-65).

It is worth noting that the cytokines measure in sera samples reflects not only the production by immune cells but also non-immune cells under normal or disease conditions. The increased cytokines observed in mice that received combined blockade might be produced by peripheral blood lymphocytes that include T cells.

Common γ -chain (γ c) cytokines, including IL-2, IL-4, IL-9 and IL-21 regulate cellular responses, such as proliferation, differentiation, and survival. Previous study during HIV infection, showed that *in vitro* stimulation of γ c cytokines mediates the induction of TIM-3 and PD-1 expression patterns on T cells and simultaneous blockade of both pathways synergistically restores T-cell secretion on IFN- γ or IL-2 (11). The slightly increased of these cytokines in sera from infected treated mice might suggests an attempt to overcome the blockade of PD-1 and TIM-3, and the increased IFN- γ levels, an effect of simultaneous blockade of PD-1 and TIM-3 induced by these cytokines on T cells.

5.8. PD-1/PD-L1 pathway plays a role in the resistance to *T. cruzi* Th infection

The increased parasitemia observed during the course of the infection upon interruption of PD-1/PD-L1 pathway (gene deletion or antibody blockade), suggests a significant role of this inhibitory pathway in the control of the parasite proliferation.

T. cruzi Th is a reticulotropic strain (38, 39) and it is expected to observe, after the immune response mounting by the host, remaining parasites in tissues as spleen, liver, and bone marrow cells. Upon PD-L1 deficiency, liver samples exhibited a trend but not significant increase of parasite load in comparison to those observed upon blockade with antibodies. These results suggest that gene deletion results to be more efficient than blockade with antibodies to evaluate the real impact of interruption of PD-1/PD-L1 signaling during *T. cruzi* Th infection. The parasite persistence could be associated with the reduced serum levels of IFN- γ and TNF- α observed upon PD-L1 deficiency. This result might be in agreement with a recent work in *T. cruzi* Sylvio X10/4 chronic infection where showed that blocking PD-1/PD-L1 interaction with monoclonal antibodies did not reduce the parasite load in heart, associating the parasite persistence with a failure of blockade treatment to increase IFN- γ and TNF- α production by

DISCUSSION

infiltrating T cells (40). However a potential role of other inhibitory pathways e.g., TIM-3 induced upon PD-L1 deficiency, might not be discarded as showed the slightly trend to parasite load reduction in mice that receive combined blockade of PD-1 and TIM-3. Furthermore, the regulatory effect of IL-10, produced upon PD-L1 deficiency, might be sustaining the dysfunction of local T cells and favoring the parasite persistence.

Unexpected were the results of parasite load in different tissues upon combined blockade of PD-1 and TIM-3. The increase serum level of IFN- γ and slightly increase of TNF- α suggested the possibility of a significant reduction of parasite load in tissues as spleen and liver especially. The results showed no differences in the parasite load between the mice that received combined blockade and isotype control antibodies. These results suggest the existence of other factors (induction of other inhibitory pathways, production of regulatory cytokines) involved to higher degree in the resistance to *T. cruzi* Th infection. These factors might also induce changes in the surface antigens of the parasite altering its tropism as a mechanism to avoid the immune response and establish the chronic infection. This assumption might explain the increase parasite load observed in skeletal muscle in comparison to other tissues evaluated.

Taking all these results together, the PD-1/PD-L1 pathway has surprisingly a protective role. The effects of blocking PD-1 might not be very pronounced but to some degree impair the control of parasite proliferation and resistance to *T. cruzi* Th infection and exert this role through the induction of other regulatory mechanism such as activation of other immune-checkpoints or production of regulatory cytokines. However the present results argue for a limited use of PD-1 blockade strategies in clinical settings.

6. Abstract

The protozoa parasite *Trypanosoma cruzi* is the etiological agent of Chagas disease or human American trypanosomiasis. Establish life-long infections which are often asymptomatic or associated with digestive or cardiac alterations that can lead to death. Preliminary studies have shown that during chronic parasitic infections, Ag-specific T cells become dysfunctional, upregulate the expression of inhibitory receptors, involving these regulatory pathways in the control of the infection. Recent studies have shown that *T. cruzi* modulates the expression of these receptors on lymphocytes after the infection. In this study we evaluate the role of PD-1/PD-L inhibitory pathway during the experimental infection by *T. cruzi* Tulahuen strain in an infection model using C57BL/6J female mice, focusing on the effects of a blockade of this pathway as a potential strategy to design future therapeutic approaches for Chagas disease. Unexpectedly, experimental infection of PD-L1 knockout mice exhibited an increased parasitemia in comparison to wild type mice suggesting that PD-L1 deficiency is not associated with a reduced parasitemia neither improve resistance to infection. No difference in the frequency of activated T cells or other immune cells populations were observed in infected PD-L1 knockout mice in comparison to infected wild type mice. Upon PD-L1 deficiency, no significant difference were observed in the T cell responses (IFN- γ production) or cytotoxic function (Granzyme B expression) in comparison to infected wild type mice.

Strikingly, PD-L1 deficiency induced the expression of IL-10 on CD8⁺ T cells and upregulation of other inhibitory receptors such as TIM-3 and 2B4. Results from blockade assay using monoclonal antibodies against the PD-1 receptor and combined blockade against PD-1 and TIM-3 confirmed the effect of the interruption of this pathway on the parasitemia and resistance to infection observed in infected PD-L1 KO mice. These results demonstrate that this inhibitory pathway might play an important role in the control of parasite proliferation and resistance of *T. cruzi* Tulahuen infection. Its interruption favors a pronounced exhaustion stage of immune cells through the induction of other regulatory mechanisms limiting its application in a clinical context.

7. Zusammenfassung

Der protozoen Parasit *Trypanosoma cruzi* ist der verantwortliche Erreger der Chagas Krankheit, auch bekannt als Amerikanische Trypanosomiasis. Diese führt zu einer lebenslangen Infektion, welche oftmals asymptomatisch verläuft oder auch zu einer Verdauungs- oder Herzstörung, bis hin zum Tode führt. Vorversuche haben gezeigt, dass während einer chronischen parasitären Infektion Ag-spezifische T Zellen dysfunktionell werden und die Expression von blockierenden Rezeptoren, welche an den regulierenden Signalwegen zur Kontrolle einer Infektion beteiligt sind, hoch reguliert wird. Neue Studien haben gezeigt, dass *T. cruzi* die Expression dieser Rezeptoren in Lymphozyten nach der Infektion moduliert. In dieser Studie untersuchen wir die Funktion von PD-1/PD-L inhibitorischen Signalwegen während einer experimentellen Infektion von weiblichen C57BL/6J Mäusen mit dem Stamm *T. cruzi* Tulahuen, mit dem Fokus auf der Blockierung dieses Signalweges als mögliche Strategie für zukünftige Therapieansätze zur Behandlung der Chagas Krankheit. Unerwarteterweise zeigten experimentell infizierte PD-L1 knockout Mäuse im Vergleich zu wildtyp Mäusen eine erhöhte Parasitenlast, was daraufhin deutet, dass das Blockieren von PD-L1 weder mit einer verringerten Parasitenlast zu assoziieren ist, noch die Resistenz gegenüber der Infektion verbessert. Es wurden keine Unterschiede in der Häufigkeit von aktivierten T-Zellen oder anderen Immunzell-Populationen in infizierten PD-L1 knockout Mäusen im Vergleich zu wildtyp Mäusen beobachtet. Das Fehlen von PD-L1 in knockout Mäusen zeigte im Vergleich zu infizierten wildtyp Mäusen keine signifikanten Unterschiede, weder in der T-Zell Antwort (IFN- γ Produktion), noch bei zytotoxischen Funktionen (Granzyme B Expression).

Auffallenderweise induzierte das Fehlen von PD-L1 eine erhöhte Expression von IL-10 auf CD8⁺ T-Zellen, sowie von anderen blockierenden Rezeptoren wie TIM-3 and 2B4. Experimentelle Ergebnisse von Blockierungs-Assays, bei welchen spezifische Antikörper gegen den PD-1 Rezeptor und kombinierte Blockierungen gegen PD-1 und TIM-3 verwendet wurden, bestätigten den Effekt der Unterbrechung dieses Signalweges auf die Parasitenlast und die Resistenz gegenüber Infektionen, welche in infizierten PD-L1 knockout Mäusen beobachtet wurden. Diese Ergebnisse zeigen, dass dieser

ZUSAMMENFASSUNG

inhibitorische Signalweg möglicherweise eine wichtige Rolle in der Kontrolle der Parasitenproliferation und gegenüber der Resistenz einer *T. cruzi* Tulahuen Infektion spielt. Seine Unterbrechung fördert einen ausgeprägten Erschöpfungszustand der Immunzellen, welcher auf die Induktion von anderen regulatorischen Mechanismen zurück zu führen ist, was somit dessen Anwendbarkeit im klinischen Bereich limitiert.

8. References

1. S A. Innate immunity to pathogens: diversity in receptors for microbial recognition. *Immunol Rev.* 2009;227(1):5-8.
2. Abbas A K LAHPS. *Cellular and Molecular Immunology*. 7th ed. Philadelphia, USA: Elsevier Saunders; 2012 2012.
3. GA D. Evasion of immune responses by *Trypanosoma cruzi*, the etiological agent of Chagas disease. *Braz J Med Biol Res.* 2011;44(2):84-90.
4. K M. *Janeway's Immunobiology*. 8th ed. New York, USA 2012 2012.
5. Joffre O NM, Spörri R, Reis e Sousa C. Inflammatory signals in dendritic cell activation and the induction of adaptive immunity. *Immunol Rev.* 2009;227(1): 234-47.
6. Gutierrez FR MT, Pavanelli WR, Guedes PM, Silva JS. The effects of nitric oxide on the immune system during *Trypanosoma cruzi* infection. *Mem Inst Oswaldo Cruz.* 2009;104(Suppl 1):236-45.
7. Ceeraz S, Nowak EC, Noelle RJ. B7 family checkpoint regulators in immune regulation and disease. *Trends Immunol.* 2013;34(11):556-63. Epub 2013/08/21.
8. del Rio ML, Lucas CL, Buhler L, Rayat G, Rodriguez-Barbosa JI. HVEM/LIGHT/BTLA/CD160 cosignaling pathways as targets for immune regulation. *J Leukoc Biol.* 2010;87(2):223-35. Epub 2009/12/17.
9. Dyck L, Mills KHG. Immune checkpoints and their inhibition in cancer and infectious diseases. *Eur J Immunol.* 2017;47(5):765-79. Epub 2017/04/11.
10. Keir ME, Butte MJ, Freeman GJ, Sharpe AH. PD-1 and Its Ligands in Tolerance and Immunity. *Annual Review of Immunology.* 2008;26(1):677-704.
11. Zhang Q, Vignali DA. Co-stimulatory and Co-inhibitory Pathways in Autoimmunity. *Immunity.* 2016;44(5):1034-51. Epub 2016/05/19.
12. Attanasio J, Wherry EJ. Co-stimulatory and Co-inhibitory Receptor Pathways in Infectious Disease. *Immunity.* 2016;44(5):1052-68. Epub 2016/05/19.
13. Mackey TK, Liang BA, Cuomo R, Hafen R, Brouwer KC, Lee DE. Emerging and reemerging neglected tropical diseases: a review of key characteristics, risk factors, and the policy and innovation environment. *Clin Microbiol Rev.* 2014; 27(4):949-79. Epub 2014/10/04.
14. Wherry EJ, Kurachi M. Molecular and cellular insights into T cell exhaustion. *Nat Rev Immunol.* 2015;15(8):486-99. Epub 2015/07/25.
15. Cai G FG. The CD160, BTLA, LIGHT/HVEM pathway: a bidirectional switch regulating T-cell activation. *Immunol Rev.* 2009;229(1):244-58.
16. Murakami N, Riella LV. Co-inhibitory pathways and their importance in immune regulation. *Transplantation.* 2014;98(1):3-14. Epub 2014/07/01.
17. Pentcheva-Hoang T CE, Allison JP. Negative regulators of T-cell activation: potential targets for therapeutic intervention in cancer, autoimmune disease, and persistent infections. *Immunol Rev.* 2009;229(1):67-87.
18. Shayan G, Srivastava R, Li J, Schmitt N, Kane LP, Ferris RL. Adaptive resistance to anti-PD1 therapy by Tim-3 upregulation is mediated by the PI3K-Akt pathway in head and neck cancer. *Oncoimmunology.* 2017;6(1):e1261779. Epub 2017/02/16.
19. Xu H, Cao D, Guo G, Ruan Z, Wu Y, Chen Y. The intrahepatic expression and

REFERENCES

- distribution of BTLA and its ligand HVEM in patients with HBV-related acute-on-chronic liver failure. *Diagn Pathol.* 2012;7:142. Epub 2012/10/17.
20. Perez CJ, Lymbery AJ, Thompson RCA. Reactivation of Chagas Disease: Implications for Global Health. *Trends Parasitol.* 2015;31(11):595-603. Epub 2015/10/16.
 21. Barber DL, Wherry EJ, Masopust D, Zhu B, Allison JP, Sharpe AH, et al. Restoring function in exhausted CD8 T cells during chronic viral infection. *Nature.* 2006; 439(7077):682-7. Epub 2005/12/31.
 22. Assarsson E, Kambayashi T, Persson CM, Chambers BJ, Ljunggren HG. 2B4/CD48-Mediated Regulation of Lymphocyte Activation and Function. *The Journal of Immunology.* 2005;175(4):2045-9.
 23. Villani FN, Rocha MO, Nunes Mdo C, Antonelli LR, Magalhaes LM, dos Santos JS, et al. Trypanosoma cruzi-induced activation of functionally distinct alphabeta and gammadelta CD4- CD8- T cells in individuals with polar forms of Chagas' disease. *Infect Immun.* 2010;78(10):4421-30. Epub 2010/08/11.
 24. Ferreira L C-NE. Understanding Chagas Disease by Genome and Transcriptome Exploration. *Transcriptomics in Health and Disease Switzerland: Springer International Publishing Switzerland;* 2014. p. 311-25.
 25. Cardoso MS, Reis-Cunha JL, Bartholomeu DC. Evasion of the Immune Response by Trypanosoma cruzi during Acute Infection. *Front Immunol.* 2015;6:659. Epub 2016/02/03.
 26. Flavia Nardy A, Freire-de-Lima CG, Morrot A. Immune Evasion Strategies of Trypanosoma cruzi. *J Immunol Res.* 2015;2015:178947. Epub 2015/08/05.
 27. Organization WH. <http://www.who.int/chagas/en/>.
 28. Dutra WO, Menezes CA, Magalhaes LM, Gollob KJ. Immunoregulatory networks in human Chagas disease. *Parasite Immunol.* 2014;36(8):377-87. Epub 2014/03/13.
 29. Mateus J, Perez-Anton E, Lasso P, Egui A, Roa N, Carrilero B, et al. Antiparasitic Treatment Induces an Improved CD8(+) T Cell Response in Chronic Chagasic Patients. *J Immunol.* 2017;198(8):3170-80. Epub 2017/03/05.
 30. Andrade LO, Andrews NW. The Trypanosoma cruzi-host-cell interplay: location, invasion, retention. *Nat Rev Microbiol.* 2005;3(10):819-23. Epub 2005/09/22.
 31. Dutra WO MC, Villani FN, et al. Cellular and genetic mechanisms involved in the generation of protective and pathogenic immune responses in human Chagas disease. *Mem Inst Oswaldo Cruz.* 2009;104(Suppl 1):208-18.
 32. Gutierrez FR, Mariano FS, Oliveira CJ, Pavanelli WR, Guedes PM, Silva GK, et al. Regulation of Trypanosoma cruzi-induced myocarditis by programmed death cell receptor 1. *Infect Immun.* 2011;79(5):1873-81. Epub 2011/03/02.
 33. Esper L, Utsch L, Soriani FM, Brant F, Esteves Arantes RM, Campos CF, et al. Regulatory effects of IL-18 on cytokine profiles and development of myocarditis during Trypanosoma cruzi infection. *Microbes Infect.* 2014;16(6):481-90. Epub 2014/04/08.
 34. Lasso P, Mateus J, Pavia P, Rosas F, Roa N, Thomas MC, et al. Inhibitory Receptor Expression on CD8+ T Cells Is Linked to Functional Responses against Trypanosoma cruzi Antigens in Chronic Chagasic Patients. *J Immunol.* 2015; 195(8):3748-58. Epub 2015/09/20.
 35. Dulgerian LR, Garrido VV, Stempin CC, Cerban FM. Programmed death ligand 2 regulates arginase induction and modifies Trypanosoma cruzi survival in macrophages during murine experimental infection. *Immunology.* 2011;133(1): 29-40. Epub 2011/02/10.

REFERENCES

36. Graefe SE1 JT, Wächter U, Bröker BM, Fleischer B. CTLA-4 regulates the murine immune response to *Trypanosoma cruzi* infection. *Parasite Immunol.* 2004; 26(1):19-28.
37. Bardhan K, Anagnostou T, Boussiotis VA. The PD1:PD-L1/2 Pathway from Discovery to Clinical Implementation. *Front Immunol.* 2016;7:550. Epub 2016/12/27.
38. Erdmann H, Behrends J, Holscher C. During acute experimental infection with the reticulotropic *Trypanosoma cruzi* strain Tulahuen IL-22 is induced IL-23-dependently but is dispensable for protection. *Sci Rep.* 2016;6:32927. Epub 2016/09/22.
39. Gorosito Serran M, Tosello Boari J, Fiocca Vernengo F, Beccaria CG, Ramello MC, Bermejo DA, et al. Unconventional Pro-inflammatory CD4(+) T Cell Response in B Cell-Deficient Mice Infected with *Trypanosoma cruzi*. *Front Immunol.* 2017;8:1548. Epub 2017/12/07.
40. Fonseca R, Salgado RM, Borges da Silva H, do Nascimento RS, D'Imperio-Lima MR, Alvarez JM. Programmed Cell Death Protein 1-PDL1 Interaction Prevents Heart Damage in Chronic *Trypanosoma cruzi* Infection. *Front Immunol.* 2018; 9:997. Epub 2018/06/06.
41. Akhmetzyanova I, Drabczyk M, Neff CP, Gibbert K, Dietze KK, Werner T, et al. PD-L1 Expression on Retrovirus-Infected Cells Mediates Immune Escape from CD8+ T Cell Killing. *PLoS Pathog.* 2015;11(10):e1005224. Epub 2015/10/21.
42. Chatelain E, Konar N. Translational challenges of animal models in Chagas disease drug development: a review. *Drug Des Devel Ther.* 2015;9:4807-23. Epub 2015/09/01.
43. Roggero E PA, Tamae-Kakazu M, et al. Differential susceptibility to acute *Trypanosoma cruzi* infection in BALB/c and C57BL/6 mice is not associated with a distinct parasite load but cytokine abnormalities. *Clin Exp Immunol.* 2002;128(3):421-8.
44. Micucci LR BP, Fauro R, Baez A, et al. Importance of host sex in the development of *trypanosoma cruzi* infection. *Rev Fac Cien Med Univ Nac Cordoba.* 2010;67 (2):73-6.
45. Engwerda CR, Ng SS, Bunn PT. The Regulation of CD4(+) T Cell Responses during Protozoan Infections. *Front Immunol.* 2014;5:498. Epub 2014/10/30.
46. Rao M, Valentini D, Doodoo E, Zumla A, Maeurer M. Anti-PD-1/PD-L1 therapy for infectious diseases: learning from the cancer paradigm. *Int J Infect Dis.* 2017; 56:221-8. Epub 2017/02/07.
47. Duthie MS, Kahn SJ. NK cell activation and protection occur independently of natural killer cells during *Trypanosoma cruzi* infection. *Int Immunol.* 2005; 17(5):607-13. Epub 2005/04/02.
48. Sathler-Avelar R V-AD, Teixeira-Carvalho A, Martins-Filho OA. Innate immunity and regulatory T-cells in human Chagas disease: what must be understood? *Mem Inst Oswaldo Cruz.* 2009;104(Suppl 1):246-51.
49. Kee SJ, Kwon YS, Park YW, Cho YN, Lee SJ, Kim TJ, et al. Dysfunction of natural killer T cells in patients with active *Mycobacterium tuberculosis* infection. *Infect Immun.* 2012;80(6):2100-8. Epub 2012/03/14.
50. Bhadra R GJ, Weiss LM, Khan IA. Control of *Toxoplasma* reactivation by rescue of dysfunctional CD8+ T-cell response via PD-1-PDL-1 blockade. *Proc Natl Acad Sci U S A.* 2011;108(22):9196-201.
51. Xu-Monette ZY, Zhang M, Li J, Young KH. PD-1/PD-L1 Blockade: Have We Found the Key to Unleash the Antitumor Immune Response? *Front Immunol.* 2017;

REFERENCES

- 8:1597. Epub 2017/12/20.
52. Wykes MN, Lewin SR. Immune checkpoint blockade in infectious diseases. *Nat Rev Immunol.* 2018;18(2):91-104. Epub 2017/10/11.
 53. Karunaratne DS, Horne-Debets JM, Huang JX, Faleiro R, Leow CY, Amante F, et al. Programmed Death-1 Ligand 2-Mediated Regulation of the PD-L1 to PD-1 Axis Is Essential for Establishing CD4(+) T Cell Immunity. *Immunity.* 2016;45(2):333-45. Epub 2016/08/18.
 54. Joshi T, Rodriguez S, Perovic V, Cockburn IA, Stager S. B7-H1 blockade increases survival of dysfunctional CD8(+) T cells and confers protection against *Leishmania donovani* infections. *PLoS Pathog.* 2009;5(5):e1000431. Epub 2009/05/14.
 55. Yi JS, Cox MA, Zajac AJ. T-cell exhaustion: characteristics, causes and conversion. *Immunology.* 2010;129(4):474-81. Epub 2010/03/06.
 56. Bodhankar S, Chen Y, Vandenbark AA, Murphy SJ, Offner H. PD-L1 enhances CNS inflammation and infarct volume following experimental stroke in mice in opposition to PD-1. *J Neuroinflammation.* 2013;10:111. Epub 2013/09/11.
 57. Charles E, Joshi S, Ash JD, Fox BA, Farris AD, Bzik DJ, et al. CD4 T-cell suppression by cells from *Toxoplasma gondii*-infected retinas is mediated by surface protein PD-L1. *Infect Immun.* 2010;78(8):3484-92. Epub 2010/05/26.
 58. McBerry C, Dias A, Shryock N, Lampe K, Gutierrez FR, Boon L, et al. PD-1 modulates steady-state and infection-induced IL-10 production in vivo. *Eur J Immunol.* 2014;44(2):469-79. Epub 2013/10/30.
 59. Chinai JM, Janakiram M, Chen F, Chen W, Kaplan M, Zang X. New immunotherapies targeting the PD-1 pathway. *Trends Pharmacol Sci.* 2015;36(9):587-95. Epub 2015/07/15.
 60. Esch KJ, Juelsgaard R, Martinez PA, Jones DE, Petersen CA. Programmed death 1-mediated T cell exhaustion during visceral leishmaniasis impairs phagocyte function. *J Immunol.* 2013;191(11):5542-50. Epub 2013/10/25.
 61. Tousif S, Singh Y, Prasad DV, Sharma P, Van Kaer L, Das G. T cells from Programmed Death-1 deficient mice respond poorly to *Mycobacterium tuberculosis* infection. *PLoS One.* 2011;6(5):e19864. Epub 2011/05/19.
 62. Koyama S, Akbay EA, Li YY, Herter-Sprie GS, Buczkowski KA, Richards WG, et al. Adaptive resistance to therapeutic PD-1 blockade is associated with upregulation of alternative immune checkpoints. *Nat Commun.* 2016;7:10501. Epub 2016/02/18.
 63. Taghiloo S, Allahmoradi E, Ebadi R, Tehrani M, Hosseini-Khah Z, Janbabaei G, et al. Upregulation of Galectin-9 and PD-L1 Immune Checkpoints Molecules in Patients with Chronic Lymphocytic Leukemia. *Asian Pac J Cancer Prev.* 2017;18(8):2269-74. Epub 2017/08/28.
 64. Takamura S, Tsuji-Kawahara S, Yagita H, Akiba H, Sakamoto M, Chikaishi T, et al. Premature terminal exhaustion of Friend virus-specific effector CD8+ T cells by rapid induction of multiple inhibitory receptors. *J Immunol.* 2010;184(9):4696-707. Epub 2010/03/31.
 65. Sakuishi K, Apetoh L, Sullivan JM, Blazar BR, Kuchroo VK, Anderson AC. Targeting Tim-3 and PD-1 pathways to reverse T cell exhaustion and restore anti-tumor immunity. *J Exp Med.* 2010;207(10):2187-94. Epub 2010/09/08.

9. Abbreviations

PRRs	Pattern recognition receptors
PAMPs	Pathogen-associated molecular patterns
DCs	Dendritic cells
TLRs	Toll-like receptors
TNF- α	Tumor necrosis factor α
IL	Interleukin
NK T lymphocytes	Natural killer T lymphocytes
APCs	Antigen-presenting cells
B cells	Bone-marrow derived lymphocytes
T cells	Thymus derived lymphocytes
BCR	B-cell receptor
TCR	T-cell receptor
CD	Cluster of differentiation
MHC	Major histocompatibility complex
T _H	Helper T cell
T _{FH}	T follicular helper
CTLs	Cytotoxic T cells
Tregs	Regulatory T cells
LCMV	Lymphocytic choriomeningitis virus
HIV	Human immunodeficiency virus
HCV	Hepatitis C virus
Ig	Immunoglobulin
IgSF	Immunoglobulin superfamily
BTLA	B- and T-cell lymphocyte attenuator
PD-1	Programmed cell death protein 1
CTLA-4	Cytotoxic T lymphocyte antigen 4
ITIM	Immunoreceptor tyrosine-based inhibitory motif
NK cell	Natural killer cell
HVEM	Human herpesvirus entry mediator
TNFSF	Tumor necrosis factor superfamily

REFERENCES

SHP	Src homology region 2 domain-containing protein tyrosine phosphate
Akt	Protein kinase B
LT α	Lymphotoxin α
LIGHT	lymphotoxin-like, exhibits inducible expression, and competes with herpes simplex virus glycoprotein D (gD) for binding to <u>HVEM</u> , a receptor expressed by <u>T</u> lymphocytes
ITSM	Immunoreceptor tyrosine-based switch motif
PD-L1	Programmed cell death ligand 1
PD-L2	Programmed cell death ligand 2
IgV	Immunoglobulin variable-like <i>domain</i>
IgC	Immunoglobulin constant- <i>like domain</i>
PI3K	Phosphatidylinositol-4,5-bisphosphate 3-kinase
IFN- γ	Interferon γ
Bcl-xL	B-cell lymphoma-extra large
HBV	<i>Hepatitis B virus</i>
LAG-3	Lymphocyte activation gene 3 protein
TIM-3	T-cell immunoglobulin-3
Gal-9	Galactin 9
ITK	Interleukin inducible T-cell kinase
CEACAM1	Carcinoembryonic antigen cell adhesion molecule 1
2B4	Natural killer cell receptor 2B4
IFN- $\alpha\beta$	Interferon $\alpha\beta$
<i>T. cruzi</i> Th	<i>Trypanosoma cruzi</i> Tulahuén
WHO	World Health Organization
GPI	Glycosylphosphatidylinositol
SODs	Superoxide dismutases
TGF- β	Transforming growth factor β
NO	Nitric oxide
mL	Milliliter
min	Minutes
°C	Degree Celsius

REFERENCES

rpm	Rounds per minute
mm	Millimeter
RT	Room temperature
mL	Milliliter
μm	Micrometer
ng	Nanogram
μM	Micromolar
μL	Microliter
mAb	Monoclonal antibody
mg	Miligram
DNA	Desoxyribonucleic acid
μg	Microgram
qRT-PCR	quantitative Real Time PCR
kDNA	Kinetoplast DNA
GAPDH	Glyceraldehyde 3-phosphate dehydrogenase
PCR	Polymerase chain reaction
MOI	Multiplicity of infection
FACS	Flow activated cell sorting
MFI	Mean fluorescence intensity
SEM	Standard error of mean

10. List of figures

Fig. 1: Molecular pathways of inhibitory receptors associated with T cell exhaustion.....	5
Fig. 2: The global distribution of cases of Chagas disease, based on official estimates, 2006-2010.....	12
Fig. 3: Clinical evolution of human Chagas disease.....	11
Fig. 4: Life cycle of <i>Trypanosoma cruzi</i>	13
Fig. 5: Scheme of <i>T. cruzi</i> Th strain infection of mouse bone marrow-derived dendritic cells (BM-DCs).....	24
Fig. 6: Expression of PD-L1 on BM-DCs infected with <i>T. cruzi</i> Th strain <i>in vitro</i>	25
Fig. 7: <i>T. cruzi</i> Th experimental infection using an <i>in vivo</i> model.....	27
Fig. 8: Time course of PD-1 expression on spleen T cells from wt mice infected with <i>T. cruzi</i> Th strain.....	28
Fig. 9: Expression of PD-1 on spleen cells from wt mice infected with <i>T. cruzi</i> Th strain.....	31
Fig. 10: Expression of PD-L1 and PD-L2 on spleen cells from wt mice infected with <i>T. cruzi</i> Th strain.....	33
Fig. 11: Time course of cytokine production on PD-1 ⁺ T cells during the course of the <i>T. cruzi</i> Th infection.....	34
Fig. 12: Effect of PD-L1 deficiency on parasitemia and body weight during the <i>T. cruzi</i> Th infection <i>in vivo</i>	36
Fig. 13: Effect of PD-L1 deficiency on the activation and cytokine production by spleen T cells from mice infected with <i>T. cruzi</i> Th at day 10 post-infection.....	37
Fig. 14: Effect of PD-L1 deficiency on the activation and cytokine production by spleen T cells from mice infected with <i>T. cruzi</i> Th at day 24 post-infection.....	38
Fig. 15: Effect of PD-L1 deficiency on the expression of Granzyme B of cytotoxic T cells during <i>T. cruzi</i> Th infection.....	39
Fig. 16: Effect of PD-L1 deficiency on the expression of IL-10 of cytotoxic T cells at day 24 post-infection.....	39

Fig. 17: Serum cytokine levels in infected wt and PD-L1 KO mice at day 24 post-infection.....	40
Fig. 18: TIM-3 and 2B4 expression on spleen T cells from wt and PD-L1 KO mice at day 10 and 24 post-infection.....	42
Fig. 19: Effect of PD-1 blockade on parasitemia and body weight during the <i>T. cruzi</i> Th infection <i>in vivo</i>	43
Fig. 20: Effect of PD-1 blockade on the activation and cytokine production of spleen T cells from wt mice infected with <i>T. cruzi</i> Th at day 25 post-infection.....	45
Fig. 21: Effect of PD-1 blockade on the expression of Granzyme B of cytotoxic T cells at day 25 post-infection.....	45
Fig. 22: Effect of PD-1 blockade on the expression of IL-10 of cytotoxic T cells at day 25 post-infection.....	46
Fig. 23: Serum cytokine levels in wt mice at day 25 post-infection upon PD-1 blockade.....	47
Fig. 24: TIM-3 expression on spleen T cells from wt mice at day 25 post-infection upon PD-1 blockade.....	47
Fig. 25: Effect of combined blockade of PD-1 and TIM-3 by antibodies on parasitemia and body weight during the <i>T. cruzi</i> Th infection <i>in vivo</i>	49
Fig. 26: Effect of combined blockade of PD-1 and TIM-3 on the activation and cytokine production of spleen T cells from wt mice infected with <i>T. cruzi</i> Th at day 28 post-infection.....	50
Fig. 27: Effect of combined blockade of PD-1 and TIM-3 on the expression of Granzyme B of cytotoxic T cells at day 28 post-infection.....	50
Fig. 28: Effect of combined blockade of PD-1 and TIM-3 on the expression of IL-10 of cytotoxic T cells at day 28 post-infection.....	51
Fig. 29: Serum cytokine levels of wt mice at 28 days post-infection upon combined blockade of PD-1 and TIM-3.....	52
Fig. 30: Effect of interruption of PD-1/PD-L1 signaling on parasite load analyzed by qRT PCR.....	53

11. List of tables

Tab. 1: List of utilized cell lines.....	16
Tab. 2: List of utilized mouse strains.....	16
Tab. 3: Reagents for cell biology.....	16
Tab. 4: Antibodies and fluorescent dyes.....	17
Tab. 5: Buffers and cell culture media for cell biology.....	17
Tab. 6: Kits for cell biology.....	17
Tab. 7: Antibodies for blocking assays.....	18
Tab. 8: Oligonucleotide primer.....	18
Tab. 9: Kits for molecular biology.....	18

12. Acknowledgments

Science is a collective enterprise and this thesis would not exist without the support and contributions of many friends and colleagues.

First, I would like to thank my supervisor PD Dr. Thomas Jacobs for providing me the interesting research PhD topic. I am very thankful for your contributions and expert advices at the lab. Thanks for have been patient and flexible throughout my work on the study and the dissertation. I learned a lot during this time, not only scientifically but also on a personal level. I also want to thank PD Dr. Minka Breloer and Prof. Dr. Eva Tolosa for their support as part of my examination committee and for evaluating the dissertation.

My gratitude belongs to Christiane Steeg who made my start at the institute smooth by sharing her expertise on helpful skills I needed for the successful completion of my project. My work has profited from the collaboration and discussions with the members of my workgroup, especially to Dr. Lydia Bosurgi and Dr. Rafeal de Freitas. I appreciate the friendship of Rosa Grote-Galvez who helped me in numerous ways anytime. It has been a joy having you on my side during encountering the world of headaches and knowing that we count on each other whenever necessary and for being my “better lab partner”.

My personal thanks go to my dear friends in Peru who through their constant contact gave me the support and love that distance could not break and my dear german friend Heike Harder, for insisting that giving up is never an option in life. My especially thanks to Dr. Vanessa Adui, I have been extremely lucky to have you here during this time. You made me feel in home every time when I needed it. I could not have done it without all of you!

Moreover, I want to express my deepest gratitude to German Academic Exchange Service-DAAD, without the financial support, the doctoral pursuits would not be possible. And also want to express my thanks to my sponsor FINCyT in Lima-Peru.

Of course, I would like to thank my beloved family. Ysabel, Chimmina y Jaime, gracias por estar alli siempre, dándome su incondicional y cariñoso apoyo en todo este tiempo, proporcionándome la fuerza y coraje cuando más lo necesitaba. Ustedes son el motor y motivo de mi vida.

ACKNOWLEDGMENTS

Finally, I want to thank to you (you know!!) for being at my side and for loving me just the way I am. Without your help throughout the last years I would never have reached my goals. I am so thankful that I have met you and that we share so many great moments. You helped me to become the person I am today.

13. Curriculum vitae

Surname: ARANA POLICARPO

Given Name: YANINA HELGA

PERSONAL DATA

DATE OF BIRTH July 26, 1973

PLACE OF BIRTH Lima, Peru

NATIONALITY Peruvian

POSITION

DOCTORAL CANDIDATE,

since October 2014

-BERNHARD-NOCHT-INSTITUT FÜR TROPENMEDIZIN (BNI)

-UNIVERSITÄTSKLINIKUM HAMBURG-EPPENDORF(UKE)

HAMBURG – GERMANY.

EDUCATION

GRADUATE: UNIVERSIDAD PERUANA CAYETANO HEREDIA

BACHELOR OF SCIENCE (BSc). – Biology

Record: **Top fifth**

PERU, 2001 – 2003. Thesis: 2005

UNIVERSIDAD PERUANA CAYETANO HEREDIA

MASTER OF SCIENCE (MSc). – Biochemistry and Molecular Biology

Record: **4.4/5.0**

PERU, 2007. Thesis: 2007

UNIVERSIDAD PERUANA CAYETANO HEREDIA

DEGREE IN BIOLOGY.

PERU, 2007. Thesis: 2007

AWARDS AND SCHOLARSHIPS

1) CONCYTEC “Ministry of Education” Scholarship

Postgraduate in Science and Technology in Peruvian Universities.

CONCYTEC (National Council of Science and Technology)

Lima - Peru

From 2001 to 2003.

2) IFS RESEARCH GRANT

Project: “Carbohydrate-lectin interactions in the adherence of *Taenia solium* larvae to host tissue”.

IFS (International Foundation for Science)

Stockholm - Sweden

June 2006.

3) CONICET / IFS SCHOLARSHIP

Training in research methodologies. Production of monoclonal antibodies
Cordoba - Argentina
March to June 2008.

4) NIH / FOGARTY INTERNATIONAL CLINICAL RESEARCH SCHOLAR

Fogarty International Center (FIC)
National Institutes of Health (NIH)
Bethesda, MD
USA
July 2008.

5) DAAD (DEUTSCHER AKADEMISCHER AUSTAUSCHDIENST)

Forschungsstipendien für Doktoranden und Nachwuchswissenschaftler
Hamburg – Germany
April 2014.

6) FINCyT (FUND FOR RESEARCH, SCIENCE AND TECHNOLOGY)

“Scholarships for doctoral studies abroad”
Lima – Peru
June 2014.

PUBLICATIONS

Author

1. Characterization of the carbohydrate components of *Taenia solium* oncosphere proteins and their role in the antigenicity. *Parasitol Research*; 112(10):3569-78. 2013 Oct.

Co-author

1. In vitro study of *Taenia solium* postoncospherical form. *PLoS Negl Trop Dis*. 2016 Feb 10;10(2):e0004396. doi: 10.1371/journal.pntd.0004396. eCollection 2016.
2. Standardization of a fluorescent-based quantitative adhesion assay to study attachment of *Taenia solium* oncosphere to epithelial cells in vitro. *Immunol Methods*; 28, 376(1-2): 89-96. 2011 Dec 9.
3. Utility of a protein fraction with cathepsin-L like activity purified from cysticercus fluid of *Taenia solium* in the diagnostics of human cysticercosis. *Am J Trop Med Hyg*; 80(6), pp. 964-970. 2009.
4. *T. solium* oncosphere adhesion to intestinal epithelial and Chinese Hamster Ovary (CHO) cells in vitro. *Infection and Immunity*; p. 5158-5166. 2007 Nov.
5. Prevalence of Antibodies to unique *Taenia solium* oncosphere antigens in taeniasis and human and porcine cysticercosis. *Am. J. Trop. Med. Hyg*; 69 (4) pp. 438-444. 2003.
6. Natural History of the eruptive phase of the Peruvian Wart and the importance of the Western blot method, preliminary report. *Folia Dermatológica Peruana*; 13 (2):36-42. 2002.
7. *Taenia solium* oncosphere antigens induce immunity in pigs against experimental cysticercosis. *Veterinary Parasitology*; 108 (1): 49-62. 2002. Aug 30.
8. Sonicated Diagnostic Immunoblot for Bartonellosis. *Clinical and Diagnostic Laboratory Immunology*; 7 (1): 1-5. 2000 Jan.

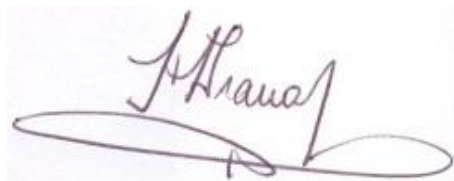
14. Eidesstattliche Versicherung

Ich versichere ausdrücklich, dass ich die Arbeit selbständig und ohne fremde Hilfe verfasst, andere als die von mir angegebenen Quellen und Hilfsmittel nicht benutzt und die aus den benutzten Werken wörtlich oder inhaltlich entnommenen Stellen einzeln nach Ausgabe (Auflage und Jahr des Erscheinens), Band und Seite des benutzten Werkes kenntlich gemacht habe.

Ferner versichere ich, dass ich die Dissertation bisher nicht einem Fachvertreter an einer anderen Hochschule zur Überprüfung vorgelegt oder mich anderweitig um Zulassung zur Promotion beworben habe.

Ich erkläre mich einverstanden, dass meine Dissertation vom Dekanat der Medizinischen Fakultät mit einer gängigen Software zur Erkennung von Plagiaten überprüft werden kann.

Hamburg, den 07.01.2019

A handwritten signature in dark ink, appearing to read 'J. Krause', with a large, sweeping flourish underneath.

Unterschrift: